DETERMINATION OF SATELLITE POSITION CO-ORDINATES AND ITS APPLICATION TO TIME & FREQUENCY BROADCASTS

FINAL REPORT

A. SEN GUPTA

TIME & FREQUENCY SECTION
NATIONAL PHYSICAL LABORATORY
NEW DELHI 110012, INDIA

MARCH 1993

RESEARCH REPORT

CLASSIFICATION UR
REPORT NO. NPL 93-0009

TITLE : DETERMINATION OF SATELLITE POSITION CO-ORDINATES AND ITS APPLICATION TO TIME & FREQUENCY BROADCASTS : FINAL REPORT

AUTHOR : A. SEN GUPTA

PROJECT : TIME AND FREQUENCY STANDARDS

PROJECT CODE : A-2

ABSTRACT

This final report is essentially a detailed and updated version of an earlier paper on the same subject [13]. It describes the method of accurately computing the position co-ordinates of a satellite using the six standard orbital elements at a specified epoch as the input data. The perturbations to the satellite orbit due to solar and lunar attractions, nonspherical part of the earth's gravitational potential and solar radiation pressure have been considered. The appproach has been to treat the satellite orbit as a Keplarian ellipse but with time varying orbital parameters. Comparisons have been made between computations and the data of INSAT and GOES standard time and frequency broadcasts at NPL and NIST(USA) respectively. A listing of the FORTRAN program for prediction of satellite co-ordinates, based on the present work is also included. Although this report deals primarily with geostationary orbits but by making the computation of the perturbation acceleration due to nonspherical gravity in a more general way than earlier [13] the present algorithm can also be applied to satellites such as GPS that are not geostationary.

DIRECTOR'S APPROVAL :

E. S. Raja Gupta
26.6.93

RESEARCH REPORT

CLASSIFICATION UR
REPORT NO. NPL 93-0009

TITLE : DETERMINATION OF SATELLITE POSITION CO-ORDINATES AND ITS APPLICATION TO TIME & FREQUENCY BROADCASTS : FINAL REPORT

AUTHOR : A. SEN GUPTA

PROJECT : TIME AND FREQUENCY STANDARDS

PROJECT CODE : A-2

ABSTRACT

This final report is essentially a detailed and updated version of an earlier paper on the same subject [13]. It describes the method of accurately computing the position co-ordinates of a satellite using the six standard orbital elements at a specified epoch as the input data. The perturbations to the satellite orbit due to solar and lunar attractions, nonspherical part of the earth's gravitational potential and solar radiation pressure have been considered. The appproach has been to treat the satellite orbit as a Keplarian ellipse but with time varying orbital parameters. Comparisons have been made between computations and the data of INSAT and GOES standard time and frequency broadcasts at NPL and NIST(USA) respectively. A listing of the FORTRAN program for prediction of satellite co-ordinates, based on the present work is also included. Although this report deals primarily with geostationary orbits but by making the computation of the perturbation acceleration due to nonspherical gravity in a more general way than earlier [13] the present algorithm can also be applied to satellites such as GPS that are not geostationary.

DIRECTOR'S APPROVAL :

26.6.93

RESEARCH REPORT

REPORT NO.NPL-93-0009

DETERMINATION OF SATELLITE POSITION CO-ORDINATES AND ITS APPLICATION TO TIME & FREQUENCY BROADCASTS

FINAL REPORT

A. SEN GUPTA

NPL-93-0009

NPL-93-0009

TIME &FREQUENCY SECTION
NATIONAL PHYSICAL LABORATORY
NEW DELHI 110012, INDIA

MARCH 1993

RESEARCH REPORT

CLASSIFICATION UR
REPORT NO. NPL

TITLE : DETERMINATION OF SATELLITE POSITION CO-ORDINATES AND ITS APPLICATION TO TIME & FREQUENCY BROADCASTS : FINAL REPORT

AUTHOR : A. SEN GUPTA

PROJECT : TIME AND FREQUENCY STANDARDS

PROJECT CODE : A-2

ABSTRACT

This final report is essentially a detailed and updated version of an earlier paper on the same subject [13]. It describes the method of accurately computing the position co-ordinates of a satellite using the six standard orbital elements at a specified epoch as the input data. The perturbations to the satellite orbit due to solar and lunar attractions, nonspherical part of the earth's gravitational potential and solar radiation pressure have been considered. The appproach has been to treat the satellite orbit as a Keplarian ellipse but with time varying orbital parameters. Comparisons have been made between computations and the data of INSAT and GOES standard time and frequency broadcasts at NPL and NIST(USA) respectively. A listing of the FORTRAN program for prediction of satellite co-ordinates, based on the present work is also included. Although this report deals primarily with geostationary orbits but by making the computation of the perturbation acceleration due to nonspherical gravity in a more general way than earlier [13] the present algorithm can also be applied to satellites such as GPS that are not geostationary.

DIRECTOR'S APPROVAL :

E. S. Raja Gupta
20.6.95

DETERMINATION OF SATELLITE POSITION CO-ORDINATES AND ITS APPLICATION TO TIME & FREQUENCY BROADCASTS : FINAL REPORT

A. SEN GUPTA

TIME AND FREQUENCY SECTION
NATIONAL PHYSICAL LABORATORY
NEW DELHI - 110012, INDIA

ABSTRACT

This final report is essentially a detailed and updated version of an earlier paper on the same subject [13]. It describes the method of accurately computing the position co-ordinates of a satellite using the six standard orbital elements at a specified epoch as the input data. The perturbations to the satellite orbit due to solar and lunar attractions, nonspherical part of the earth's gravitational potential and solar radiation pressure have been considered. The appproach has been to treat the satellite orbit as a Keplarian ellipse but with time varying orbital parameters. Comparisons have been made between computations and the data of INSAT and GOES standard time and frequency broadcasts at NPL and NIST(USA) respectively. A listing of the FORTRAN program for prediction of satellite co-ordinates, based on the present work is also included. Although this report deals primarily with geostationary orbits but by making the computation of the perturbation acceleration due to nonspherical gravity in a more general way than earlier [13] the present algorithm can also be applied to satellites such as GPS that are not geostationary.

1. INTRODUCTION

A Standard Time and Frequency Signal (STFS) broadcast system using coded transmissions on the Indian domestic satellite INSAT has been in operation since March, 1988 [1, 2]. This service is available all over the Indian subcontinent and at the present time provides a time synchronisation accuracy at about 10 μsec level relative to UTC (NPLI) and a short term jitter of better than a μsec. In order to achieve this level of accuracy the decoder performs a real time computation of the propagation delay over the Transmitter - Satellite - Receiver path using the satellite co-ordinates information that is transmitted with the signal code. The current satellite position co-ordinates used for coding with the signal are predictions, that are generated at the transmitting earth station using the orbit information received periodically from the INSAT master control facility. It has been our experience that the primary cause for inaccuracy in the INSAT broadcast is the uncertainity in the satellite position prediction. The present paper addresses this specific aspect - namely, the accurate prediction of the co-ordinates of a satellite over a period of one to two weeks.

In a similar time broadcast service operated by the NIST, USA over the GOES geostationary satellites [3] an elaborate computer program, known as the Goddard Trajectory Determination System (GTDS) [4] is being used. Also, at the Indian Space Research Organisation INSAT Master Control Facility (MCF) at Hassan, Karnataka (India) an INSAT Ephemeris generation software (by Ford Aerospace Corpn.) is used to predict satellite co-ordinates [5]. Both these software are expensive and can be run on mainframe computers only. In the present work we have sacrificed some of the elaborateness in order to make the program of manageable size so that it can run on a personal computer. At the same time all the significant perturbing forces have been taken into account to make the predictions sufficiently accurate.

The input data on satellite orbit information received from MCF, Hassan are six standard orbital elements. In the present computations we have assumed that the orbit shape is a keplarian ellipse described by these orbital elements but that the elements themselves have temporal variation due to external perturbations. This approach is known as the Variation Of Parameters (VOP) formulation [4]. Only four significant perturbation sources - namely, the solar and lunar attractions,nonspherical part of earth's gravity and solar radiation pressure have been considered.

2. KEPLARIAN ORBIT FORMULATION FOR THE SATELLITE

2.1 SYSTEM OF CO-ORDINATES

The co-ordinate system used for the geostationary satellite orbit is shown in Fig 1. This is the quasi inertial Mean Equatorial

Geocentric System of Date (MEGSD) [6]. The origin of this co-ordinate system is the mass centre of the earth. The x-y plane of this system is taken as the equatorial plane of the earth and the z-axis is along the geographical north. The earth rotates around the z-axis in a mathematically positive direction. The x direction is chosen to coincide with the intersection of the equatorial plane and the plane of the ecliptic (ecliptic is the plane of the earth's orbit around the sun). This direction is also known in astronomy as the first point of aries.

The advantage of choosing this co-ordinate system is that for all practical purposes we can consider the earth to rotate around the z-axis with a uniform angular velocity as

$$\dot{\psi} = 360^{\circ}.985647335 \ /day \qquad ..(1)$$

Positions on the earth are defined by the latitude and longitude referred to the Greenwich meridian. The Greenwich sidereal angle that is the angle ϕ between the x-axis and the Greenwich meridian can be calculated as

$$\phi = 99^{\circ}.69098 + \psi * \left(D + \frac{T}{24} \right) \qquad ..(2)$$

Where T is the time in UT and D is the epoch in days counted from 00 January, 1900 at 00 hours ephemeris time (this corresponds to midday of December 31, 1899). Value of D for a certain year (YY), month (MM) and date (DD) is given as [5]

$$D = Integr[365.25 * Y1 \ ] + Integr[30.6 * M1 + 0.41] + DD + 58.5 \qquad ..(3)$$

Where M1 = MM + (I1 * 12) - 3
Y1 = YY - I1
I1 = Integr [0.51 + 1/MM]

2.2 UNPERTURBED ORBIT OF THE SATELLITE

In this section we consider the satellite orbit that is influenced only by the gravitational attraction of a spherically symmetric earth. The equation of motion is given by

$$\frac{d^2\vec{r}}{dt^2} = -\frac{\mu}{r^3} * \vec{r} \qquad ..(4)$$

Where $\mu = G*M_e$
G = gravitational constant and
M_e = mass of the earth.

The solution of this vector differential equation is an ellipse which can be defined by the following six standard orbital parameters [7].
a = semi-major axis

e = eccentricity
i = inclination of the orbital plane with the equatorial plane
Ω = right ascension of the line of ascending node (line of ascending node is the line of intersection between the orbital plane and the equatorial plane)
ω = argument of perigee
M = mean anomaly

Fig. 2 illustrates a co-ordinate system x_p, y_p, z_p such that the satellite orbit lies in the x_p,-y_p plane. The origin lies at the focus of the elliptical orbit. x_p axis is in the direction of the perigee, y_p at right angles to it and z_p is perpendicular to the orbital plane. It is useful to define an angle known as the eccentric anomaly E, that is related to the actual angle f which the satellite-earth vector makes with the x_p axis as shown in Fig. 2. The mean anomaly M can be expressed in terms of E by the following relation [7]

$$M = E - e * \sin E = \sqrt{\frac{\mu}{a^3}}\,(t - t_p) \qquad ..(5)$$

where t_p is the time of passage of the satellite through perigee. The inverse relation for E in terms of M is given by

$$E = M + \left(e - \frac{e^3}{8} - \frac{e^5}{192}\right) * \sin M + \left(\frac{e^2}{2} - \frac{e^4}{6}\right) * \sin 2M + \left(\frac{3e^3}{8} - \frac{27e^5}{128}\right) * \sin 3M + \frac{e^4}{3} * \sin 4M + \frac{125e^5}{384} * \sin 5M + .. \qquad ..(6)$$

The other angles i, Ω and ω, which describe the orientation of the satellite orbit in MEGSD system are illustrated in Fig. 3.

It remains in this section to formulate expressions for the position and velocity co-ordinates in the MEGSD system in terms of the orbital parameters described above. For this we first consider the satellite position and velocity in the co-ordinate system x_p, y_p, z_p, given as [7]

$$\bar{r}_p = \begin{bmatrix} r_{xp} \\ r_{yp} \\ r_{zp} \end{bmatrix} = a \begin{bmatrix} \cos E - e \\ \sin E * \sqrt{1-e^2} \\ 0 \end{bmatrix} \qquad ..(7)$$

$$\bar{v}_p = \begin{bmatrix} v_{xp} \\ v_{yp} \\ v_{zp} \end{bmatrix} = \frac{\sqrt{\frac{\mu}{a}}}{1 - e * \cos E} \begin{bmatrix} -\sin E \\ \cos E * \sqrt{1-e^2} \\ 0 \end{bmatrix} \qquad ...(8)$$

Transformation from x_p, y_p, z_p system to MEGSD can be achieved by three rotations : a) about z_p-axis by ω, b) about the line of ascending node by i and c) about z-axis by Ω. We thus obtain for the position and the velocity in MEGSD as

$$\bar{r} = \begin{bmatrix} r_x \\ r_y \\ r_z \end{bmatrix} = a\,[R_{ij}] \begin{bmatrix} \cos E - e \\ \sin E * \sqrt{1-e^2} \\ 0 \end{bmatrix} \qquad ..(9)$$

$$\bar{v} = \begin{bmatrix} \dot{r}_x \\ \dot{r}_y \\ \dot{r}_z \end{bmatrix} = \frac{\sqrt{\frac{\mu}{a}}}{1 - e * \cos E}\,[R_{ij}] \begin{bmatrix} -\sin E \\ \cos E * \sqrt{1-e^2} \\ o \end{bmatrix} \qquad ..(10)$$

Where the elements of the matrix R_{ij} are given by

R_{11} = cos Ω*cos ω - sin Ω*sin ω*cos i
R_{12} = -cos Ω*sin ω - sin Ω*cos ω*cos i
R_{13} = sin Ω*sin i
R_{21} = sin Ω*cos ω + cos Ω*sin ω*cos i
R_{22} = - sin Ω*sin ω + cos Ω*cos ω*cos i
R_{23} = -cos Ω*sin i
R_{31} = sin ω*sin i
R_{32} = cos ω*sin i
R_{33} = cos i

It is necessary to formulate a further rotational transformation of $\bar{r}$ from MEGSD to a co-ordinate system x_e, y_e, z_e co-rotating with the earth. In this system, x_e-y_e is in the equatorial plane with x_e along the Greenwich meridian and y_e along 90° east. z_e and z are coincident. This is given as

$$\bar{r}_e = \begin{bmatrix} r_{xe} \\ r_{ye} \\ r_{ze} \end{bmatrix} = \begin{bmatrix} \cos\phi & \sin\phi & 0 \\ -\sin\phi & \cos\phi & 0 \\ 0 & 0 & 0 \end{bmatrix} \bar{r} \qquad ..(11)$$

where ϕ is given by equation (2). The satellite position can now be expressed in terms of latitude, longitude and height as

$$\begin{aligned} Latitude &= \sin^{-1}\left(\frac{r_{ze}}{|\bar{r}_e|}\right) \\ Longitude &= \tan^{-1}\left(\frac{r_{ye}}{r_{xe}}\right) \\ Height &= |\bar{r}_e| - R_e \end{aligned} \qquad ..(12)$$

where R_e is the equatorial radius of the earth.

3. PERTURBATIONS TO THE SATELLITE ORBIT

Perturbations to the satellite orbit arise as a result of all forces except the spherically symmetric earth's gravity. For a geostationary satellite orbit, there are several perturbing forces which are mostly of natural origin or are created by the satellite ground control in attempting to manipulate its position and orientation in space. These are listed in the following alongwith the order of magnitude of the associated acceleration in m/sec^2.

- The non-spherical part of earth's gravitational potential(10^{-6}).
- Attractions due to sun, moon (10^{-5})and other planets($\ll 10^{-9}$).
- Solar radiation pressure(10^{-7}).
- Force due to solar corpuscular wind(10^{-10}).
- Coriolis force due to precession of the MEGSD system(10^{-8}).
- Forces of reaction due to orbit manoeuvers(10^{-3}).
- Forces due to satellite attitude control manoeuvers(10^{-10}).

In the present work we have neglected the last four perturbations above and the gravitational attraction due to other planets as these are not possible to model in a simple manner. The accelerations due to the automatic attitude control manoeuvres of the satellite are small but their cumulative effect can probably be significant. The orbit manoeuvres result in large perturbations but as these are rather infrequent and isolated events they have been ignored. The large errors arising due to this will be discussed in section 6 on results.

In the remaining part of this section we shall consider the various perturbations that have been considered in detail and formulate expressions for the respective accelerations.

3.1 NON-SPHERICAL EARTH POTENTIAL

The gravitational attraction of the earth is not sufficiently symmetric to be considered as from a point mass for modelling the motions of an earth orbiting satellite. The gravity can be expressed in the form of a potential function which is a multipole expansion in the earth rotating co-ordinate system [6].

$$U = \frac{\mu}{r} + \mu \sum_{l=2}^{L} \sum_{m=0}^{l} \frac{R_e^l}{r^{l+1}} P_{lm}(\sin\theta) \left[C_{lm} \cos m\lambda + S_{lm} \sin m\lambda \right] \quad ..(13)$$

where P_{lm} are the associated Legendre functions of degree l and order m. r, θ, and λ are the geocentric distance, latitude and longitude of a point respectively. The harmonic coefficients C_{lm} and S_{lm} have been determined using accurate satellite tracking data by the Goddard Space Flight Center upto l, m = 28 [8]. Due to the term (R_e^l/r^{l+1}) in eqn 13, closer the satellite orbit is to the earth the more the number of terms we would need to take in the summation to describe the gravitational potential accurately. It can be shown

that for a geostationary orbit taking upto l, m = 4 makes the computations sufficiently accurate.

The first term μ/r in eqn.13 is the central potential and three terms with l = 1 vanish, since the co-ordinate system is centered in the mass centre of the earth. The acceleration on the satellite is the gradient of the potential function U. Thus from eqn. 13 we get the three components of the perturbation accelerations as follows.

a) The radial component, P_{rad}, is along the line joining the centre of the earth and the satellite and is given by

$$\overline{P}_{rad} = \frac{\partial U}{\partial r} = -\frac{\mu}{r^2}\sum_{l=2}^{L}\left(\frac{R_e}{r}\right)^l (l+1)\sum_{m=0}^{l} P_{lm}(\sin\theta)\left(C_{lm}\cos m\lambda + S_{lm}\sin m\lambda\right) \quad ..(14a)$$

b) The latitudinal or Northward component, P_{lat}, is perpendicular to the radial component in the direction of increasing latitude and is given by

$$\overline{P}_{lat} = \frac{1}{r}\frac{\partial U}{\partial \theta} = \frac{\mu}{r}\sum_{l=2}^{L}\left(\frac{R_e}{r}\right)^l \sum_{m=0}^{l}\left(C_{lm}\cos m\lambda + S_{lm}\sin m\lambda\right) * \left[P_{l\,m+1}(\sin\theta) - m\tan\theta\, P_{lm}(\sin\theta)\right] \quad ..(14b)$$

c) The longitudinal or eastward component, P_{lon}, is perpendicular to both P_{rad} and P_{lat} and along the direction of increasing longitude. It is given by

$$\overline{P}_{lon} = \frac{1}{r}\frac{\partial U}{\partial \lambda} = \frac{\mu}{r}\sum_{l=2}^{L}\left(\frac{R_e}{r}\right)^l \sum_{m=0}^{l} m\left(S_{lm}\cos m\lambda - C_{lm}\sin m\lambda\right) P_{lm}(\sin\theta) \quad ..(14c)$$

The associated Legendre polynomials P_{lm} can be computed using the recursion relations as follows.

$$P_{l0}(\sin\theta) = \left[(2l-1)\sin\theta\, P_{l-1\,0}(\sin\theta) - (l-1)\, P_{l-2\,0}(\sin\theta)\right] / l \quad ..(15a)$$

$$P_{ll}(\sin\theta) = (2l-1)\cos\theta\, P_{l-1\,l-1}(\sin\theta) \quad ..(15b)$$

$$P_{lm}(\sin\theta) = P_{l-2\,m}(\sin\theta) + (2l-1)\cos\theta\, P_{l-1\,m-1}(\sin\theta) \quad m\neq 0 \; m<l \quad ..(15c)$$

Where we have $P_{00}(\sin\theta) = 1$; $P_{10}(\sin\theta) = \sin\theta$; $P_{11}(\sin\theta) = \cos\theta$

and $P_{lm}(\sin\theta) = 0$ *for* $l<m$.

In the present work we have used the coefficients C_{lm} and S_{lm} only upto l=m=4 for the summations in eqns 14 a,b and c. These are listed in the following [4].

$C_{20} = -0.108265*10^{-2}$ $S_{20} = 0$
$C_{21} = -0.132673*10^{-8}$ $S_{21} = -0.1374346*10^{-7}$
$C_{22} = 0.156651*10^{-5}$ $S_{22} = -0.8869932*10^{-6}$
$C_{30} = 0.254503*10^{-5}$ $S_{30} = 0$
$C_{31} = 0.2161875*10^{-5}$ $S_{31} = 0.2571596*10^{-6}$
$C_{32} = 0.3172142*10^{-6}$ $S_{32} = -0.2078203*10^{-6}$
$C_{33} = 0.1.25055*10^{-6}$ $S_{33} = 0.1949036*10^{-6}$
$C_{40} = 0.1671500*10^{-5}$ $S_{40} = 0$
$C_{41} = -0.5052256*10^{-6}$ $S_{41} = -0.4199062*10^{-6}$
$C_{42} = 0.7739965*10^{-7}$ $S_{42} = 0.1515418*10^{-6}$
$C_{43} = 0.5901404*10^{-7}$ $S_{43} = -0.1275373*10^{-7}$
$C_{44} = -0.3608512*10^{-8}$ $S_{44} = 0.6386659*10^{-8}$

The three components P_{rad}, P_{lat}, and P_{lon} need to be further converted to a vector $\bar{P}_g$ in the MEGSD system having components P_{gx}, P_{gy}, P_{gz}. This is achieved by the following simple transformations.

$$P_{gx} = \left(P_{rad} \cos\theta + P_{lat} \sin\theta\right) \frac{r_x}{D_{sat}} - P_{lon} \frac{r_y}{D_{sat}} \qquad ..(16a)$$

$$P_{gy} = \left(P_{rad} \cos\theta + P_{lat} \sin\theta\right) \frac{r_y}{D_{sat}} + P_{lon} \frac{r_x}{D_{sat}} \qquad ..(16b)$$

$$P_{gz} = P_{rad} \sin\theta + P_{lat} \cos\theta \qquad ..(16c)$$

where $D_{sat} = \left[r_x^2 + r_y^2 + r_z^2 \right]^{1/2}$.

3.1.1 NONSPHERICAL GRAVITY ACCELERATION

In order to get some idea of the magnitude of the perturbation acceleration due to nonspherical gravity it is useful to consider the components P_{rad}, P_{lat} and P_{lon} as these are easily visualised. Figs. 4a, b and c show these components as a function of longitude at the equator and at nominal geostationary satellite height. In Fig 4a we observe that P_{rad} has a steady component of $-8.33 * 10^{-6}$ mts/sec^2 superimposed on which there is a sinusoidal variation with two peaks at 75°E and 254.5°E and two troughs at 162°E and 348.5°E. The steady component arises due to the terms with m = 0 in the summation in Eqn 14a - or the so called zonal terms. It adds on to the primary acceleration term on the right hand side in eqn 4 which has the effect of raising the effective height of a geostationary orbit. The variable component on the other hand is due to nonzero m terms - or the so called tesseral terms. The magnitude of P_{lat} or the northward component shown in Fig 14b is much smaller. The steady or the zonal component in this case is $-2.95 * 10^{-9}$ mts/sec^2 and the tesseral component has the positions of the peaks and troughs reversed as compared with those for P_{rad}.

Finally in Fig 14c P_{lon} or the eastward component has almost no steady component and a variable component which reaches a maximum of about $\pm$ 6 $*10^{-8}$ mts/sec^2. It will be shown later in section 6 (Fig 16a) that the effect of an eastward acceleration on the satellite orbit is a gradual increase of its semimajor axis and thus of the orbital period ($\tau=2\pi\{a^3/\mu\}^{1/2}$). Increase of the orbital period above the nominal geostationary value (24 Hrs) would result in the satellite gradually lagging behind the rotating earth or, in other words, drifting westwards. Conversely, a negative eastward acceleration would result in a gradual decrease of the semimajor axis and thus an eastward drift. Now in Fig 4c consider the longitudes around 75°E and 254.5°E. A satellite to the west of these points would experience negative acceleration and thus drift eastward. When it crosses over these points the direction of acceleration is reversed and it starts drifting back westwards again. If left to itself a satellite would oscillate around these two stable longitudes. The other two longitudes, 162°E and 348.5°E, where P_{lon} changes sign in opposite direction are unstable nodes. Exactly at these points a satellite is stable but slight deviation would make it drift away.

3.2 SOLAR AND LUNAR ATTRACTION

We shall first consider a general development of the perturbation model for the gravitational effect of n bodies as shown in Fig 5. If we consider an inertial coordinate system with r as the vector to the satellite we get its equation of motion as

$$\bar{F} = m \frac{d^2\bar{r}}{dt^2} \qquad ..(17)$$

The gravitational force acting on the satellite of mass m due to the attraction of a body with a point mass m_k is given by

$$\bar{F}_k = - \frac{G\, m\, m_k}{|\bar{r}_{kp}|^3} \bar{r}_{kp} \qquad ..(18)$$

In order to obtain the total contribution from all the perturbing bodies we sum over k. Thus

$$\bar{F} = \sum_{k=1}^{n} - \frac{G\, m\, m_k}{|\bar{r}_{kp}|^3} \bar{r}_{kp} \qquad ..(19)$$

Substituting in eqn 17 we get the acceleration experienced by the satellite in an inertial coordinate system due to n point masses as

$$\frac{d^2\bar{r}}{dt^2} = - \sum_{k=1}^{n} \frac{G\, m_k}{|\bar{r}_{kp}|^3} \bar{r}_{kp} \qquad ..(20)$$

It is convenient computationally to refer the motion of the satellite to one of the n bodies - say the earth. The acceleration on this reference body, j, in the inertial frame is given by

$$\frac{d^2\bar{r}_j}{dt^2} = \sum_{k=1\ k\neq j}^{n} - \frac{G\,m_k}{|\bar{r}_k|^3}\,\bar{r}_k \qquad ..(21)$$

where R_k is the vector from the body k to reference body j. Subtracting eqn 21 from eqn 20 yields

$$\frac{d^2\bar{r}}{dt^2} - \frac{d^2\bar{r}_j}{dt^2} = \sum_{k=1}^{n} - \frac{G\,m_k}{|\bar{r}_{kp}|^3}\bar{r}_{kp} - \sum_{k=1\ k\neq j}^{n} - \frac{G\,m_k}{|\bar{r}_k|^3}\bar{r}_k \qquad ..(22)$$

If we substitute $\bar{r} = \bar{r} - \bar{r}_j$; $\bar{r}_{kp} = \bar{r} - \bar{r}_k$ where $\bar{r}$ and $\bar{r}_k$ are the coordinates of the satellite and the body k with respect to the reference body j as the origin we get

$$\bar{P} = \frac{d^2\bar{r}}{dt^2} = -\frac{G\,m_j}{|\bar{r}|^3}\bar{r} + \sum_{k=1\ k\neq j}^{n} G\,m_k \left(\frac{(\bar{r}_k - \bar{r})}{|\bar{r}_k - \bar{r}|^3} - \frac{\bar{r}_k}{|\bar{r}_k|^3} \right) \qquad ..(23)$$

This is the general expression for the acceleration experienced by a satellite. The first term on the right is the primary gravitational attraction due to the reference body (the earth) which is the same as the right hand side of eqn 4 and the subsequent terms are perturbations due to other planetary bodies. All distances are now measured in the earth based coordinate system or MEGSD.

As mentioned earlier we have considered only the perturbations due to sun and moon. To evaluate these perturbation accelerations using eqn 23 we have to determine the vectors r_k which requires modelling of the solar and lunar orbits in the MEGSD system. Fig 6 illustrates the solar and lunar orbits in space. In the following sub-sections we describe the mathematical modelling of these orbits.

3.2.1 SOLAR ORBIT

The orbit of the sun around the centre of the MEGSD system can be described fairly accurately by an ellipse whose orbital parameters in the standard notation as deduced from formulae in [4] and [7] are given as

$$a_s = 149.6 * 10^6 \text{ Km}$$
$$e_s = 0.0167268$$
$$i_s = 23°.440583 \qquad ..(24)$$

$$\Omega_s = 0°$$
$$\omega_s = 281°.2208333 + 1°.719175 * T_e + 0°.452777 * 10^{-3} * T_e^2$$
$$M_s = 0°.985600267 \ (D_j - 2447529.671)$$

where D_j = Julian day number = D + 2415020
T_e = D / 36525 = centuries elapsed since 00 Jan 1900.

Using eqn. 9 we can write the expression for the co-ordinates of the sun in MEGSD as

$$\bar{r}_s = a_s \begin{bmatrix} \cos\omega_s & -\sin\omega_s & 0 \\ \sin\omega_s * \cos i_s & \cos\omega_s * \cos i_s & -\sin i_s \\ \sin\omega_s * \sin i_s & \sin i_s * \cos\omega_s & \cos i_s \end{bmatrix} \begin{bmatrix} \cos E_s - e_s \\ \sin E_s * \sqrt{1-e_s^2} \\ 0 \end{bmatrix} \quad ..(25)$$

where E_s is the eccentric anomaly which can be derived from M_s using eqn. 5. The formulation described above gives solar positions which are accurate to better than 1" of arc in right ascension and declination as verified from the Astronomical Ephemeris [9].

3.2.2 LUNAR ORBIT

The lunar orbit is somewhat more complicated than the solar orbit. This can also be described as an elliptical orbit with reference to the ecliptic plane having standard orbital parameters as deduced from formulae in [4] and [7]

$$\begin{aligned} a_m &= 384400 \text{ kms} \\ e_m &= 0.0549 \\ i_m &= 5°.145389 \\ \Omega_m &= 259°.183275 - 0°.0529539 * D \\ \omega_m &= 75°.1462806 + 0°.164358 * D \\ M_m &= 296°.104608 + 13°.064992 * D \end{aligned} \quad ..(26)$$

Similar to eqn 25 we can get the expression for the moon's coordinates in the ecliptic plane coordinate system x_e, y_e, z_e which is rotated from MEGSD by an angle i_s about the x - axis as

$$\bar{r}_{me} = a_m [R(m)_{ij}] \begin{bmatrix} \cos E_m - e_m \\ \sin E_m \sqrt{1-e_m^2} \\ 0 \end{bmatrix} \quad ..(27)$$

where the elements of the matrix $[R(m)_{ij}]$ are defined in the same way as those for $[R_{ij}]$ in eqn 9 except that the orbital parameters are taken from eqn 26. Further the lunar coordinates in MEGSD can be obtained by rotation about x - axis by i_s and thus

$$\bar{r}_m = \begin{bmatrix} 1 & 0 & 0 \\ 0 & \cos i_s & \sin i_s \\ 0 & -\sin i_s & \cos i_s \end{bmatrix} \bar{r}_{me} \qquad ..(28)$$

The eccentric anomaly E_m can be obtained from the mean anomaly M_m using eqn 5.

Formulation of the lunar orbit in terms of the standard orbital parameters in the above way is not as accurate as for the sun. There are periodic errors in right ascension and declination sometimes as large as 1°- 2°. These are caused due to libration of the lunar orbit by solar perturbation. We have adopted an alternative empirical formulation which gives the lunar positions in the standard astronomical format - namely, in terms of the latitude (β), longitude (λ) and horizontal parallax (π) of the moon in the ecliptic plane[9]. The horizontal parallax, π is an indirect measure of the lunar distance. We thus have

$$\begin{aligned}\beta = {} & 5°.13 \sin(93°.3 + 483202°.03 * T_{e1}) \\ & + 0°.28 \sin(228°.2 + 960400°.87 * T_{e1}) \\ & - 0°.28 \sin(318°.3 + 6003°.18 * T_{e1}) \\ & - 0°.17 \sin(217°.6 - 407332°.20 * T_{e1}) \end{aligned} \qquad ...(29a)$$

$$\begin{aligned}\lambda = {} & 218°.32 + 481267°.883 * T_{e1} \\ & + 6°.29 \sin(134°.9 + 477198°.85 * T_{e1}) \\ & - 1°.27 \sin(259°.2 - 413335°.38 * T_{e1}) \\ & + 0°.66 \sin(235°.7 + 890534°.23 * T_{e1}) \\ & + 0°.21 \sin(269°.9 + 954397°.70 * T_{e1}) \\ & - 0°.19 \sin(357°.5 + 35999°.05 * T_{e1}) \\ & - 0°.11 \sin(186°.6 + 966404°.05 * T_{e1}) \end{aligned} \qquad ...(29b)$$

$$\begin{aligned}\pi = {} & 0°.9508 \\ & + 0°.0519 \cos(134°.9 + 477198°.85 * T_{e1}) \\ & + 0°.0095 \cos(259°.2 - 413335°.38 * T_{e1}) \\ & + 0°.0078 \cos(235°.7 + 890534°.23 * T_{e1}) \\ & + 0°.0028 \cos(269°.9 + 954397°.70 * T_{e1}) \end{aligned} \qquad ...(29c)$$

where, $T_{e1} = T_e - 1$. The position co-ordinates of the moon in the ecliptic plane are given in terms of β, λ and π as

$$\bar{r}_{me} = \frac{R_e}{\sin \pi} \begin{bmatrix} \cos\beta * \cos\lambda \\ \cos\beta * \sin\lambda \\ \sin\beta \end{bmatrix} \qquad ..(30)$$

The lunar co-ordinates in MEGSD can then be obtained from the position in the ecliptic plane $\vec{r}_{me}$ by rotation about x-axis through an angle i_s using eqn 28. Using this formulation we get lunar coordinates accurate to better than 0.2° in right ascension and declination which is fairly acceptable in our computations.

3.2.3 SOLAR & LUNAR ACCELERATIONS

In order to get an idea of the magnitudes of the solar and lunar perturbation accelerations it is again useful to consider the components in the radial, eastward and northward directions as in subsection 3.1.1. For this purpose we use the inverse of the transformation similar to that shown in eqns 16a, b and c.

Fig 7a shows the radial component of the solar perturbation acceleration computed for a geostationary orbit at 74°E. The start of the computation is January 29 and it runs for 29 days. We observe in Fig 7a a clear semidiurnal oscillation superimposed on a steady component of about $0.5*10^{-6}$ mts /sec^2. The peak values reached are $+3 *10^{-6}$ and $-1.8*10^{-6}$ mts/sec^2. The corresponding eastward component of the solar acceleration, shown in Fig 7b, also exhibits semidiurnal variation with a $\pm 2.3*10^{-6}$ mts/sec^2 amplitude. The radial and the eastward components form the in-plane acceleration. In Fig 7c is shown the the variation of the northward or the out-of-plane component of solar perturbation. This variation is diurnal with an amplitude which is gradually decreasing as we approach the spring equinox on March 21. In can be shown that the northward component has largest values during summer and winter solstices and almost zero during the two eqinoxes.

In Figs 8a, b and c are shown the lunar perturbation acceleration components for the same period as in Fig 7. We notice that the magnitude of these are in general twice or more than those for the solar perturbation. For the in-plane (radial and eastward) components in Figs 8a and b we observe a predominantly semidiurnal variation but having a noticeable diurnal component. This diurnal component arises due to the closer proximity of the moon to the satellite. The out of plane or northward component shown in Fig 8c has again a diurnal variation and goes through maxima and minima twice during the lunar orbital period of about 28 days.

It must be noted that since the lengths of the solar and lunar days are not equal the combined effect of the solar and lunar perturbation would show constructive and destructive interference patterns. This is illustrated in Figs 9a and b which show the radial and northward components of the vector sum of the solar and lunar perturbations. The strongest perturbation peaks in Fig 9a occur twice a month and coincide with the new moon and full moon when the sun, earth and moon are approximately aligned. The weakest perturbations occur on the other hand when the the sun and moon are at right angles to each other relative to the earth. The net northward component in Fig 9b is very similar to that in Fig 8c due to the moon alone but the position of the peaks are shifted due to solar interference.

3.3 SOLAR RADIATION PRESSURE

The electromagnetic radiation from the sun in the visible, ultraviolet and infrared light exerts a pressure ξ on a satellite.

This pressure, having an inverse square dependence on the distance to the sun, stays constant within about 0.04% over the entire satellite orbit around the earth and has a magnitude about $4.5*10^{-6}$ N/m^2. This causes acceleration on the satellite given by

$$\vec{P}_r = \frac{\xi * C}{m}(1 + \epsilon) = \xi * \sigma \qquad ..(31)$$

where C, m and ϵ are the cross-section, mass and the surface reflectivity coefficient of the satellite respectively. This acceleration is always directed away from the sun along the earth-sun line.

In order to compute the acceleration due to solar radiation pressure one would need to determine C and ϵ. Accurate preflight modelling of these parameters is very difficult since different surfaces of the satellite with varying reflectivity and cross section face the sun at different times. Moreover the surface reflectivity in orbit deviates from measurements in the laboratory because of outgassing and ageing due to radiation damage. It is normally sufficient for most missions to deal with only one parameter σ, the effective cross section to mass ratio. This is usually determined indirectly from the tracking measurements for the satellite in orbit.

For the INSAT satellites, we have adopted a value of $4.22*10^{-2}$ m^2/Kg for σ [5], which gives $|P_r| = 1.9*10^{-7}$ m/sec^2. The INSAT satellites are three axis stabilised and are oriented such that they present the maximum cross section normal to the equatorial plane. This results in a seasonal variation in P_r that follows cosine of the solar declination angle. This has also been taken into account.

4. TEMPORAL VARIATION OF ORBITAL PARAMETERS

In presence of perturbations described in section 3, the six orbital elements undergo temporal variations. The elements a, e, i, Ω and ω which describe the shape and the attitude of the elliptical orbit, change slowly with time. The position of the satellite in orbit which is described by M, is the only parameter which changes rapidly with time. This fact is utilised by the Gaussian Variation of parameters (VOP) formulation [4] to describe the time derivatives in two forms. For slow varying parameters, α, we have

$$\frac{\partial \alpha}{\partial t} = \frac{\partial \alpha}{\partial \vec{v}} * \vec{P} \qquad ...(32a)$$

where P is the perturbation acceleration. For a rapidly varying parameter β, we have

$$\frac{\partial \beta}{\partial t} = \beta' + \frac{\partial \beta}{\partial \vec{v}} * \vec{P} \qquad ..(32b)$$

where β' is the time derivative of β for the unperturbed orbit. Using eqns. 9, 10 and 32a,b we can write the Gaussian VOP equations of motion for the orbital elements as

$$\frac{\partial a}{\partial t} = \frac{2}{n^2 a} \left(\vec{v} . \vec{P} \right) \qquad ..(33)$$

$$\frac{\partial e}{\partial t} = \frac{\sqrt{1 - e^2}}{n a^2 e} \left[r_{yp} \hat{x}_p - r_{xp} \hat{y}_p + \frac{\sqrt{1-e^2}}{n} \vec{v} \right] . \vec{P} \qquad ..(34)$$

$$\frac{\partial i}{\partial t} = - \frac{\left[\left(r_{yp} \hat{x}_p - r_{xp} \hat{y}_p \right) \cos i + \frac{\partial \vec{r}}{\partial \Omega} \right] . \vec{P}}{n a^2 \sqrt{1 - e^2} \sin i} \qquad ..(35)$$

$$\frac{\partial \Omega}{\partial t} = \frac{1}{n a^2 \sqrt{1 - e^2} \sin i} \left(\frac{\partial \vec{r}}{\partial i} . \vec{P} \right) \qquad ..(36)$$

$$\frac{\partial \omega}{\partial t} = - \frac{1}{n a^2} \left[- \frac{\sqrt{1 - e^2}}{e} \left(L \hat{x}_p + N \hat{y}_p \right) + \frac{\cot i}{\sqrt{1 - e^2}} \frac{\partial \vec{r}}{\partial i} \right] . \vec{P} \qquad ..(37)$$

$$\frac{\partial M}{\partial t} = n + \frac{1}{n a^2} \left[- 2 \vec{r} - \frac{1 - e^2}{e} \left(L \hat{x}_p + N \hat{y}_p \right) \right] . \vec{P} \qquad ..(38)$$

where $n = \sqrt{\frac{\mu}{a^3}}$

$$L = \frac{a^2}{r} \left(e \cos E - \sin^2 E - 1 \right)$$

$$N = \frac{a^2 \sin E}{r \sqrt{1 - e^2}} \left(\cos E - e \right)$$

$$\frac{\partial \vec{r}}{\partial \Omega} = \begin{bmatrix} -r_y \\ r_x \\ 0 \end{bmatrix}$$

$$\frac{\partial \vec{r}}{\partial i} = \begin{bmatrix} r_z \sin \Omega \\ -r_z \cos \Omega \\ \cos i \left(r_{xp} \sin \omega + r_{yp} \cos \omega \right) \end{bmatrix}$$

In the above eqns 33 - 38 the perturbation accelaration $\vec{P}$ is a vectorial sum of all the individual accelarations due to nonspherical gravity, the sun, moon and solar radiation pressure as discussed in section 3.

5. THE ORBIT PREDICTION PROGRAM

Based on the mathematical formulations described in the earlier sections, a program has been developed in fortran for the prediction of the satellite position at every one hour interval over a period of several days. The computations have been done in double precision. The program outputs both the cartesian co-ordinates of the satellite in the earth rotating system, x_e, y_e and z_e as well as its latitude, longitude and height. The flow chart for this program, shown in fig.10, is quite descriptive and we shall elaborate only the following two points:

i) The numerical integration process adopted here involves simply incrementing the six orbital elements by an amount $\Delta\alpha$ corresponding to a time increment Δt given as

$$\Delta\alpha = \frac{\partial \alpha}{\partial t} * \Delta t \qquad ..(39)$$

This method can lead to errors which are proportional to Δt. In the present computations we have tested the program using Δt values of 0.25, 0.5 and 1.0 minutes and observed no significant variation in the output. Hence, Δt = 1 min has been adopted.

ii) Input data of the satellite orbital parameters is in general given for an epoch which has non-zero seconds. For convenience the data is first converted to correspond to the previous full minute. For this conversion we assume that values of all parameters except M remain unchanged over this duration. The change in M can be approximated by the formula for the unperturbed orbit as

$$\Delta M = \frac{\partial M}{\partial t} * \Delta t = \sqrt{\frac{\mu}{a^3}} * \Delta t \qquad ..(40)$$

The complete listing of the orbit prediction program is given in Appendix - 1. The program can run on a PC-XT and takes typically less than 10 min to do computations for 10 days.

6. RESULTS AND DISCUSSIONS

To illustrate typical results of the satellite position prediction and the variation of orbital parameters we choose a set of orbital elements for INSAT 1B, received from MCF, Hassan as follows :

Epoch date and time = Jan 28 1990 ; 21h 57m 35.38sec UT
a = 42167.1246 km.
e = 0.0005692
i = 0°.43619595
Ω = 84°.924561
ω = 169°.719357
M = 276°.624348

A small modification of the program enables it to output the orbital elements every hour in addition to the satellite position. Running the program with the above input data, the temporal variation of the orbital elements over a 24 hour period on February 3 are obtained as illustrated in Figs 11a - 11e. One clearly observes a semidiurnal variation in a while e and ω (omega) show predominantly diurnal pattern. The parameters i and Ω (OMEGA) show a gradual increase with a superimposed semidiurnal variation. The variation of M have not been shown as it is very rapid and covers 360° over a full day. In order to get a clearer understanding of the contributions of the individual perturbations acceleration the prediction program has been run with the above input but only one source of perturbation at a time. The individual effects of solar and lunar perturbations are illustrated in Figs 12a - 12e and Figs 13a - 13e respectively. The general nature of the variations for solar and lunar perturbation are same except for minor differences in detail - such as, the magnitude of variation in a; the trend in the variation in Ω etc. This is indeed to be expected since the solar and lunar perturbations are essentially of the same nature except for their slightly different periodicities. All the general observations made earlier in Figs 11a - 11e also seem to hold for the individual solar and lunar cases thus clearly indicating that these two are the dominant sources of perturbation.

As additional interesting observations we have shown in Fig 14a - 14c long term variations of the parameters a, i and Ω due to combined effects of sun and moon starting on Jan 29 for 29 days. If we compare the variation of semimajor axis in Fig 14a with the net luni-solar radial acceleration in Fig 9a for the same period we observe almost perfect correlation. Again we observe direct relationship between the variations of i and Ω in Figs 14b and c with the northward component of the net luni-solar acceleration in Fig 9b.

With only the solar radiation pressure as the perturbation there is found to be negligible variations in a, i and Ω. The only significant variation is obtained for the parameters e and ω which, as illustrated in Figs 15a, b, are linear drifts.

To illustrate the effects of nonspherical gravity acceleration we have run the prediction program with a different set of input orbital elements valid for INSAT 1D at 83°E on Sep 23, 1992. This is because INSAT 1B at 74°E is very close to the stable longitude node of 75°E where P_{lon} and its effects would be very small. There is found to be negligible effect on the parameters i and Ω due to nonspherical gravity. The variation of the remaining parameters a, e and ω are shown in Figs 16a - 16c. In Fig 16a we observe a linear increase of the semimajor axis with time which, as explained in section 3.1.1, would mean a westward drift. It can be shown that for a satellite to west of 75°E the semimajor axis would decrease linearly and thus drift eastward. The effects on the parameters e and ω, shown in Figs 16b, c are sinusoidal diurnal variations.

To get an idea of the way the satellite wobbles in space about its nominal position we have plotted in Figs 17a, b and c the projections of the motion in three orthogonal planes. Each point in the plots represents an hourly value of the position of INSAT 1D at 83°E and the total duration of the plots is 60 hours. Fig 17a shows the motion in the local horizontal plane, a view that we would get if we were to watch the satellite from its subsatellite point directly overhead. Fig 17b is the motion in the equatorial plane, or a view from the North or z-axis and finally Fig 17c is the motion in the meridian plane or a view from the local eastward direction. These plots clearly indicate the typical extent of diurnal excursion of the satellite in latitude longitude and height. Another feature which is brought out very clearly is Figs 17a and c is the slow drift of about 0°.004/day in longitude which occurs due to the P_{lon} component of the nonspherical gravity.

There are two ways in which the accuracy of the results of position prediction have been examined. Firstly, a comparison has been made between the present results and those obtained using the elaborate Ford Aerospace software at MCF [5]. This is shown in the Table 1 which gives the results of position predictions of INSAT 1B using the MCF software and the present program for the same set of input orbital elements. We observe a difference of 0°.001 or less in latitude and longitude and 50 mts in height after three days of prediction.

Secondly, a more direct test involves monitoring the INSAT broadcast at NPL and comparing the received and propagation delay corrected signal with UTC(NPLI). Departures from zero of this comparison or the residuals would indicate the inaccuracy in the satellite position prediction. This is based on the experimental finding that the delays in the receiver and transmitter setups are constant at about 0.2 μsec level. Fig 18 shows a small segment of data obtained during 12 - 19 Dec 1989. We observe that the residuals have a clear sinusoidal form and the peak departure is

±5 μsec. This indirectly indicates a maximum position uncertainity of about 1 km. The situation is not always as good as in Fig 18. An examination of longer period of monitoring of INSAT 1B, in Fig 19, shows that sometimes the residuals can be as large as ±10 μsec. Monitoring data of INSAT 1D, in Fig 20, also reveals the same general picture as in Fig 19. The residuals are mostly about ±10μsec or less. Fig 20 shows, in addition, two periods of about a week each in early November and January when the satellite orbit was being manoeuvred. During these periods the present orbit prediction fails completely as it does not take into account the perturbation accelarations due to on board thruster firings. It has been generally observed that with a fresh set of orbital elements and predicting for 2-3 days in future the residuals are generally within ± 5μsec and for a week they seldom exceed ± 8μsec . For longer periods of prediction, however, they can sometimes grow to ± 15 μsec. This is clearly observable in Fig 20 where one can almost make out when fresh sets of orbital data were received. There are sometimes exceptions to this general behaviour, as during late Jan- early Feb 1992 period when the residuals did not grow with time.

It is appropriate to discuss limitations in the present work and plans for future improvements. It is clear that for short term prediction of 2 - 3 days the present program gives residuals that are only a few μsecs. This indicates that the quality of the orbital elements supplied by MCF are generally good. To investigate the reason for the gradual increase in inaccuracy of prediction with time we must therefore look for either a) inaccurate modelling of some of the perturbing forces considered or b) effect of some unaccounted perturbations. On detailed examination of uncertainities associated with each perturbation that has been accounted for it is felt that it is probably the latter factor. A very likely candidate for being significant unaccounted perturbations is the automatic on board attitude correction manoeuvre. Individual attitude control manoeuvres cause small perturbations but the cumulative effect over several days can probably be quite significant. It is not possible to take these perturbations into account and this will remain as a limitation of the present program.

The other major limitation of the present program is its failure during orbit manoeuvres. Unlike the attitude corrections the orbit manoeuvres involve large perturbing accelarations for short durations at predetermined times. It is possible for us to know from MCF in advance the times, durations and the accelaration vectors for the orbit manoeuvres. Utilising these informations we can then predict in advance the satellite position during and after the manoeuvres. This prediction will probably not be so accurate as there is always some discrepancy between planned and actually executed manoeuvre accelerations.

In conclusion, the satellite position prediction program described in this paper, is relatively simple and convenient to implement. It has been successfully used in the one way INSAT time

broadcast providing a synchronisation accuracy of about ± 10μsec.

The present program has been tried for short durations on the GOES satellite broadcast at NIST . The performance comparisons with the presently used GTDS software for GOES is shown in Appendix 2 [10]. We observe that the transitions from GTDS to GOESTRAK (a name used at NIST for the present prediction program) and back produce very little changes in the received time residuals. This is an indication of good agreement between the two programs.

The present program is also being used in NPL for INSAT position prediction in the time synchronisation experiments using the satellite common view passive TV technique [11]. In the passive TV technique using a geostationary satellite it is found that assumption of a nominal stationary satellite position can lead to diurnal variations of the differential delay exceeding 1 μsec over two widely separated sites. A knowledge of the satellite position variations can bring down this error by an order of magnitude.

One other situation where this program can be very useful is in the proposed plans by NIST to provide 1 μsec level one way geostationary satellite time broadcast with the help of real time satellite position determination by trilateration [12]. In between the actual position determinations the present program can provide short term predictions which we expect to be sufficiently accurate for the purpose.

In its present form the prediction program is not only strictly applicable to geostationary satellites but can be applied to satellites in other orbits also. The only restriction is that the satellite should not be in a low altitude orbit since that would necessitate (i) the use of more terms in the nonspherical gravity acceleration and (ii) inclusion of the perturbation due to atmospheric drag. One very interesting possibility is the application of the present program to GPS satellites which are in about 20,000 km orbits. It is expected that for the GPS satellites, for which the transmitted ephemeris is degraded due to introduction of Selective Availability (SA), the accurate orbital elements will be available post facto to the time and frequency community. Using these orbital elements as the input data with the present prediction program one can then compute accurate satellite position coordinates for time transfer links.

7. ACKNOWLEDGEMENT

Major part of this work was carried out while the author was visiting the Time and Frequency Division of NIST under an Indo-US collaboration program. The author is thankful to D. W. Hanson of NIST and Dr. B. S. Mathur of NPL for their keen interest in the work and encouragement. The author would like to express sincere thanks to Dr. A. K. Hanjura for help at various stages of the work. Helpful information received from Drs. S. Rangarajan and S. G.

Patil of INSAT Master Control Facility at Hassan is acknowledged.

8. REFERENCES

[1] A. Sen Gupta, A. K. Hanjura, P. Banerjee and B. S. Mathur, "Standard time and frequency dissemination service via Indian domestic satellite INSAT-1B", in Proc. 19th Annual PTTI Meet., Washington,DC, Dec. 1987, pp. 381-398

[2] A. Sen Gupta, Ashok K. Hanjura, Bhupendra S. Mathur,"Satellite broadcasting of time and frequency signals",in Proc. IEEE, 79, No.7, July 1991, pp. 973-982

[3] R. E. Beehler, D. D. Davis, J. V. Cateora, A. J. Clements, J. A. Barnes and E. Mendez Quinones, "Time recovery measurements using operational GOES and TRANSIT satellites", Proc 11th Ann PTTI Meet., Dec 1979, pp 283-312.

[4] "Mathematical theory of Goddard Trajectory Determination System", Published by Goddard Space Flight Centre, USA, April 1976

[5] S. Rangarajan, Private communication, 1989.

[6] E. Mattias Soop,"Introduction to geostationary orbits", European Space Agency publication, esa SP-1053, Paris, 1983

[7] P. R. Escobal,"Methods of Astrodynamics", John Wiley publications, 1968

[8] F. J. Lerch, S. M. Klosko, R. E. Laubscher and C. A. Wagner, "Gravity model improvements using GEOS-3", Published by Goddard Space Flight Centre, USA, 1977

[9] "The Astronomical Ephemeris" issued by Her Majesty's Stationery Office, London, 1989

[10] R. E. Beehler, Private communication, 1993.

[11] P. Banerjee, M. Saxena and A. K. Suri, "A study on time link between NPL and Sikandarabad earth station via INSAt-TV network", to be published.

[12] D. W. Hanson and D. A. Howe, "Industrial Time Service Study," NBSIR 86-3042, Feb.1986.

[13] A. Sen Gupta, "A program to compute the co-ordinates of a geostationary satellite for time and frequency broadcast", IEEE Trans I & M, In press.

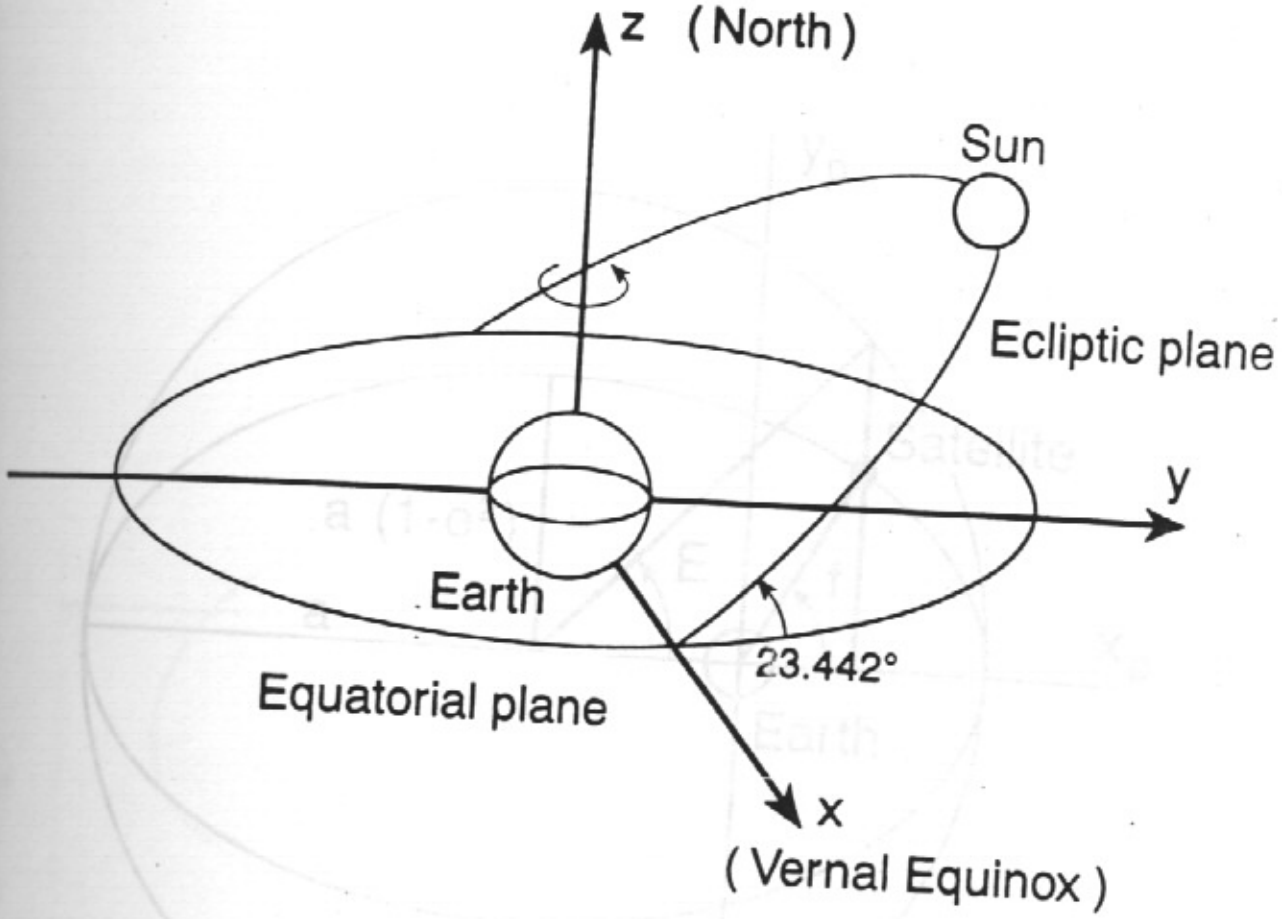

Fig. 1 Illustrating the MEGSD co-ordinate system.

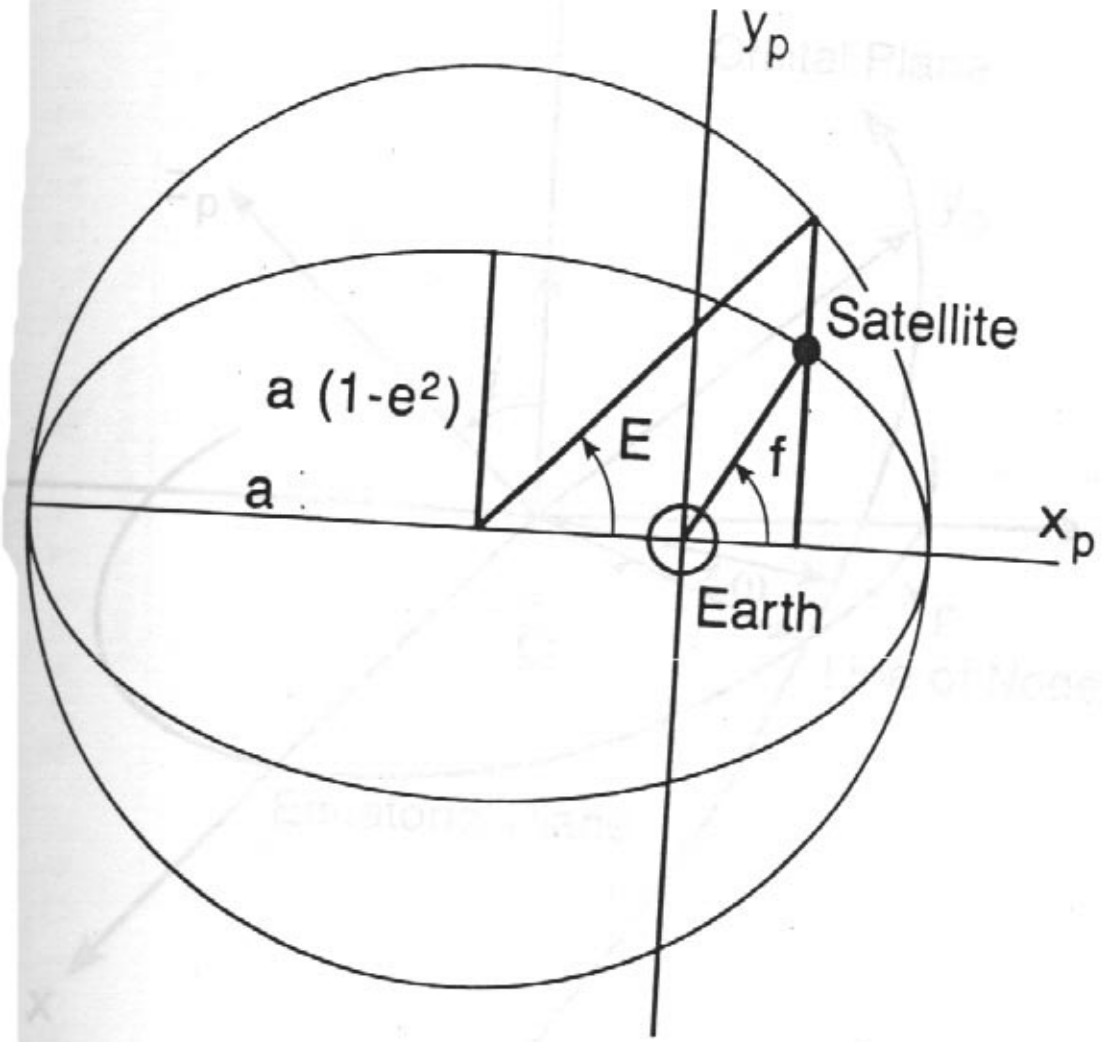

Fig. 2 Illustrating the satellite orbit in the orbital plane

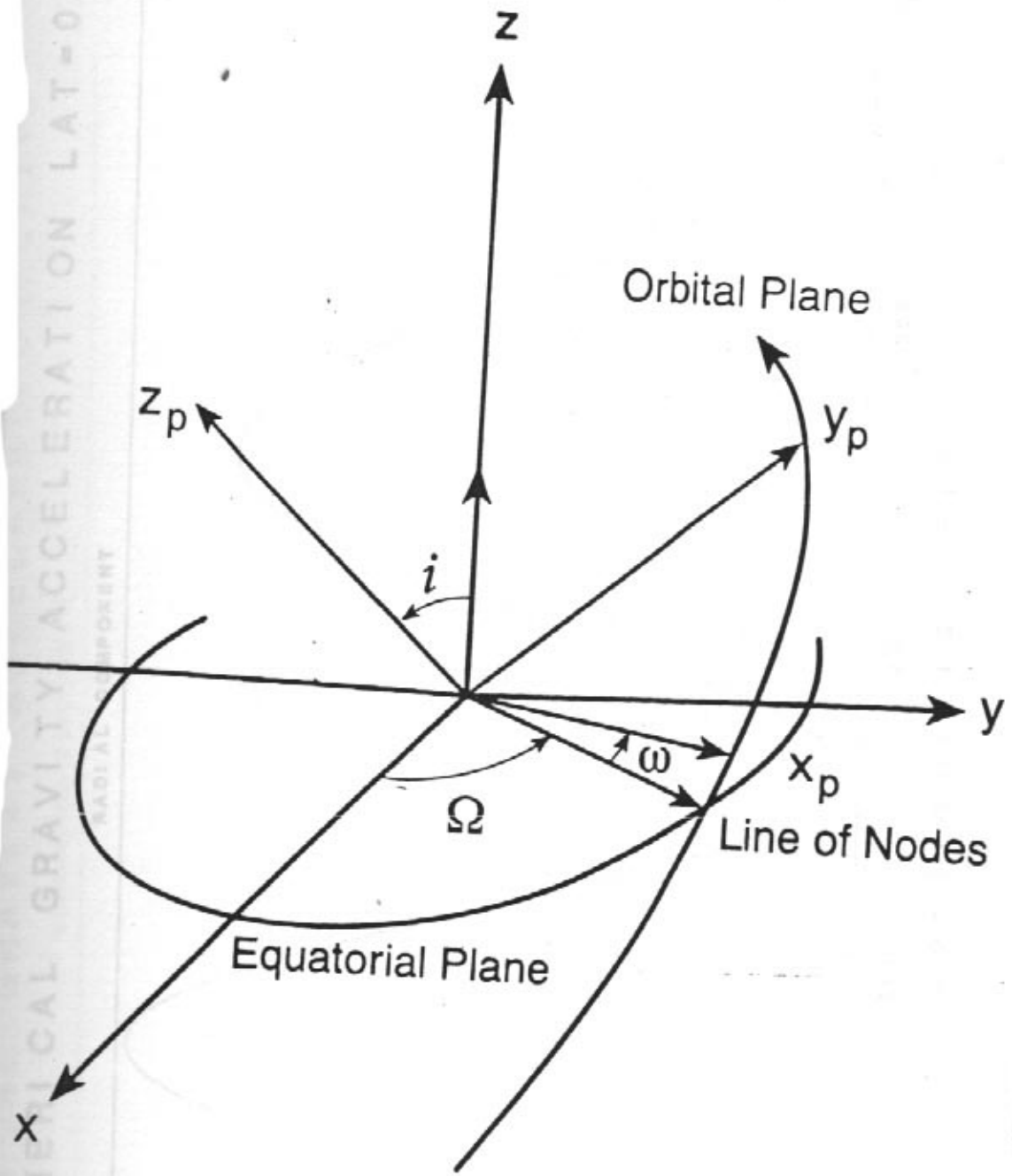

Fig. 3 Illustrating the angles i, Ω and ω in MEGSD.

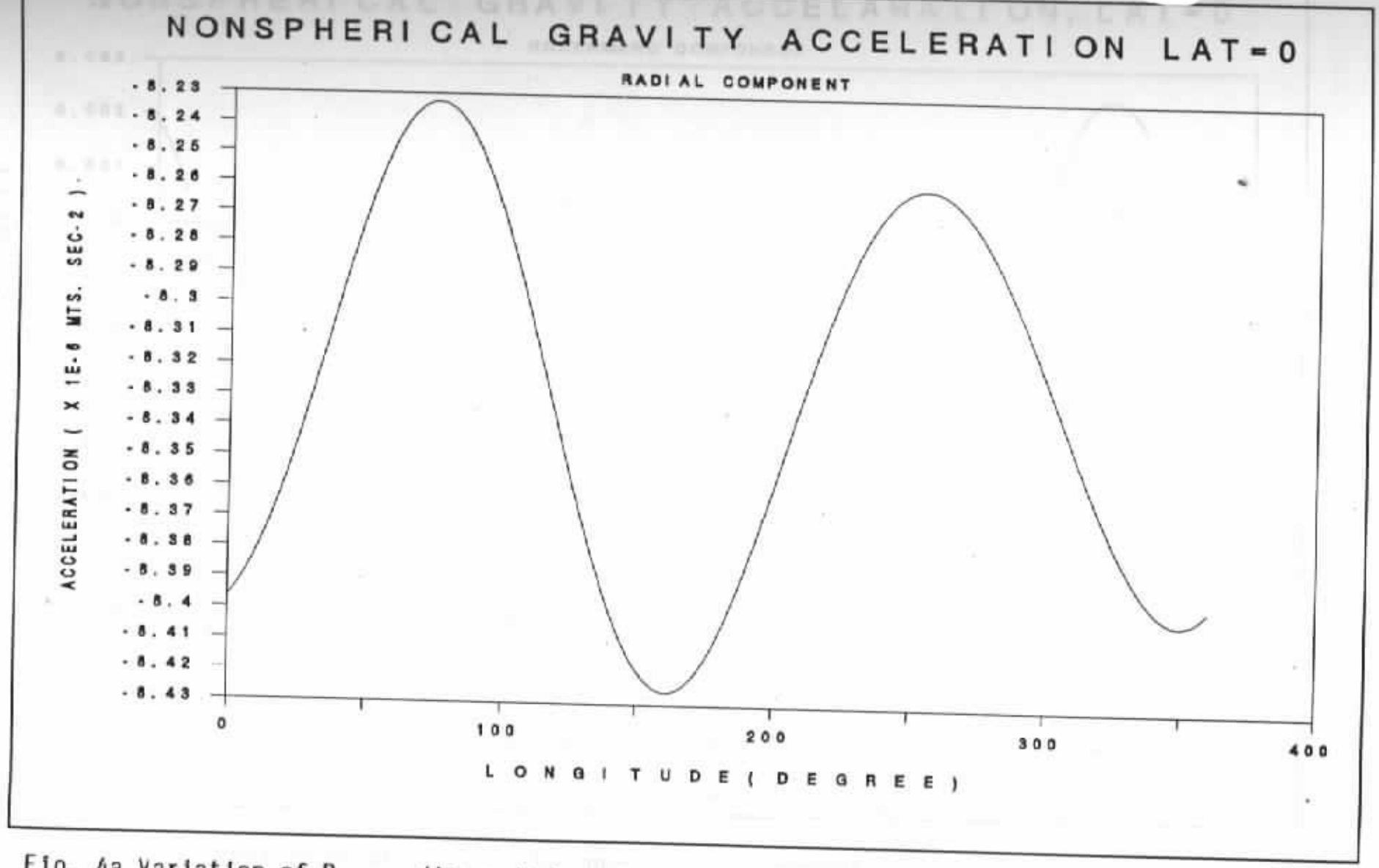

Fig. 4a Variation of P_{rad}, the radial component of the nonspherical gravity

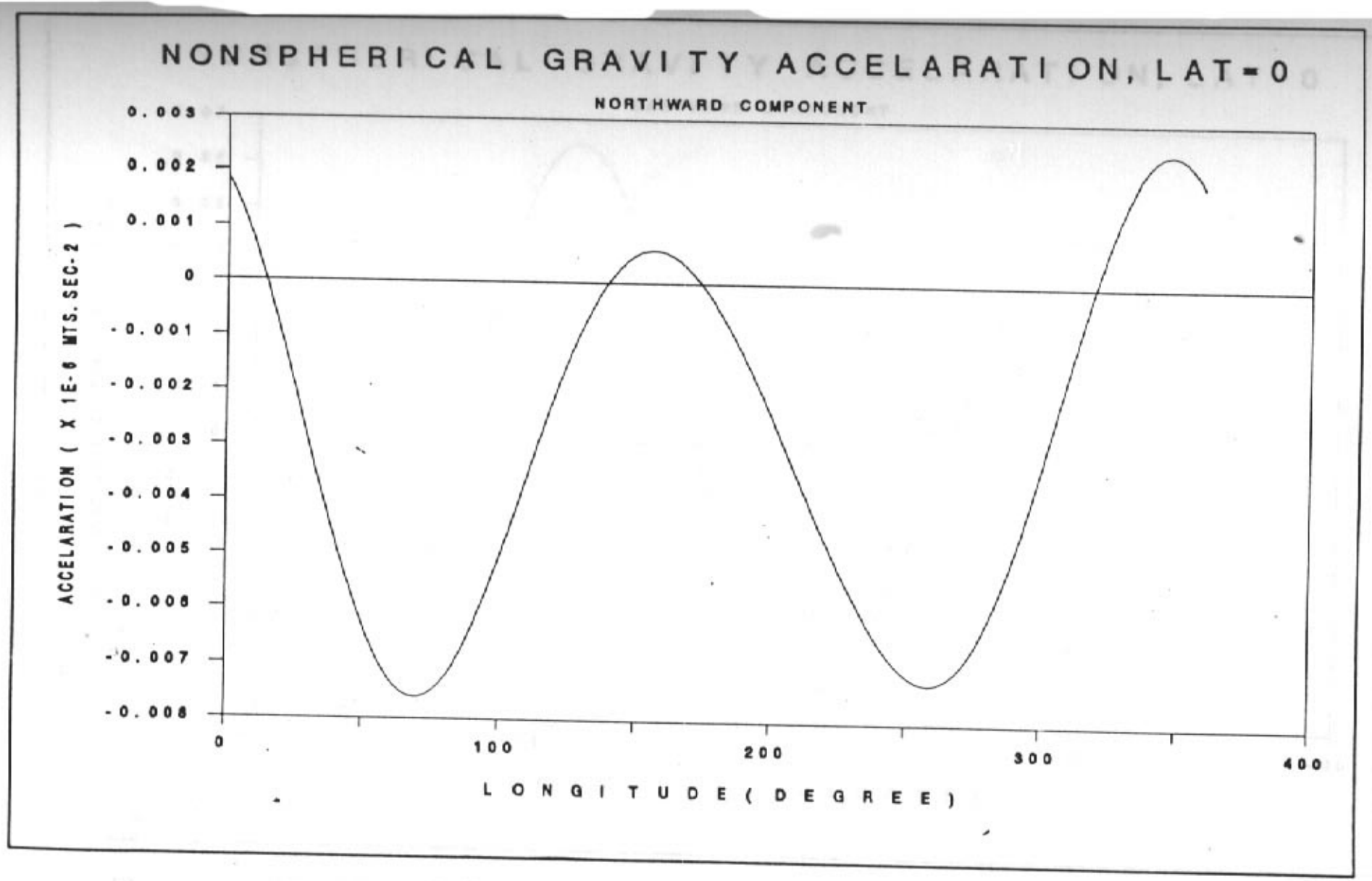

Fig. 4 : Variation of P_{lat}, the northward component of nonspherical gravity acceleration with longitude.

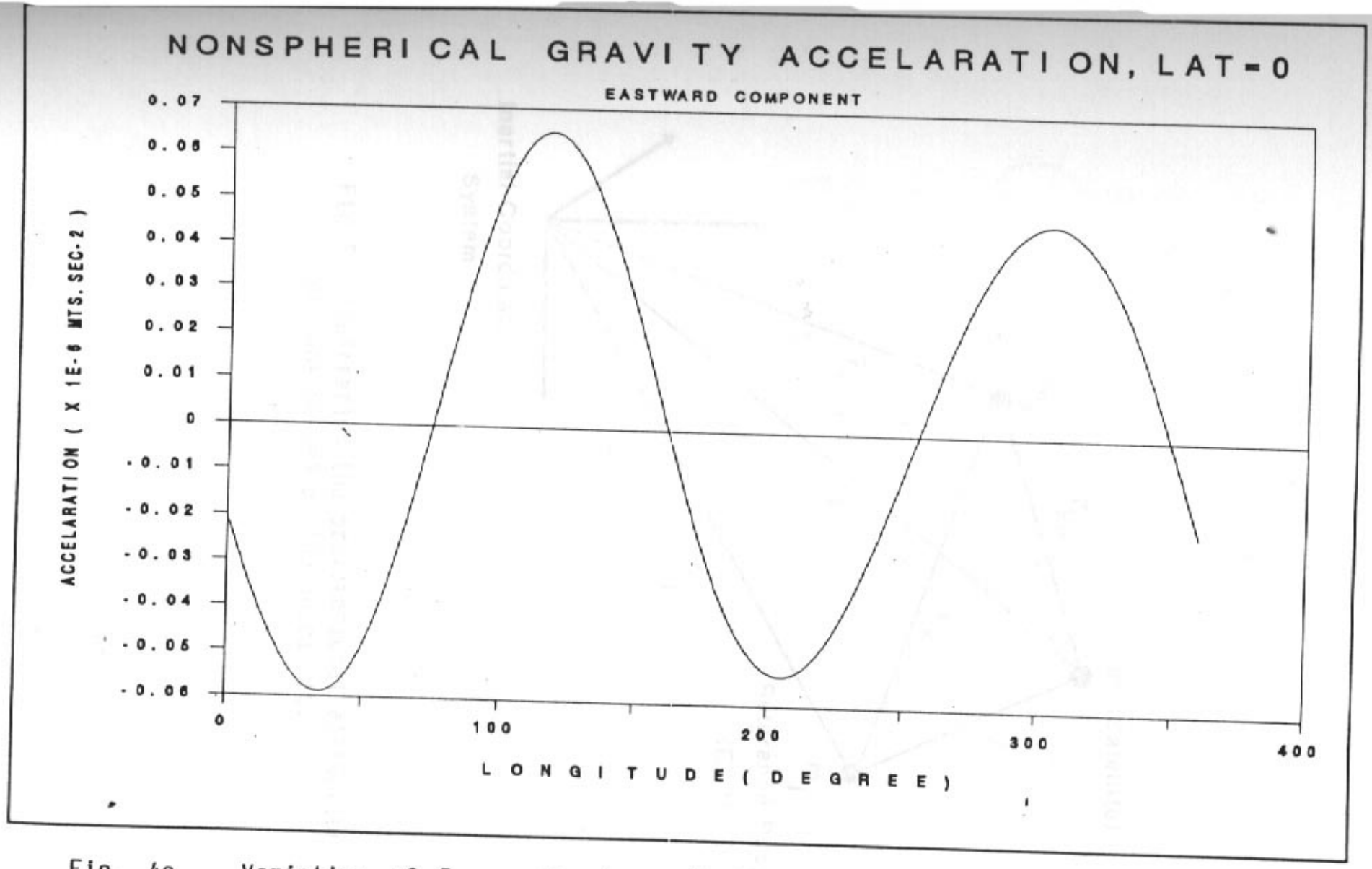

Fig. 4c Variation of P_{lon}, the tangential component of nonspherical gravity with longitude.

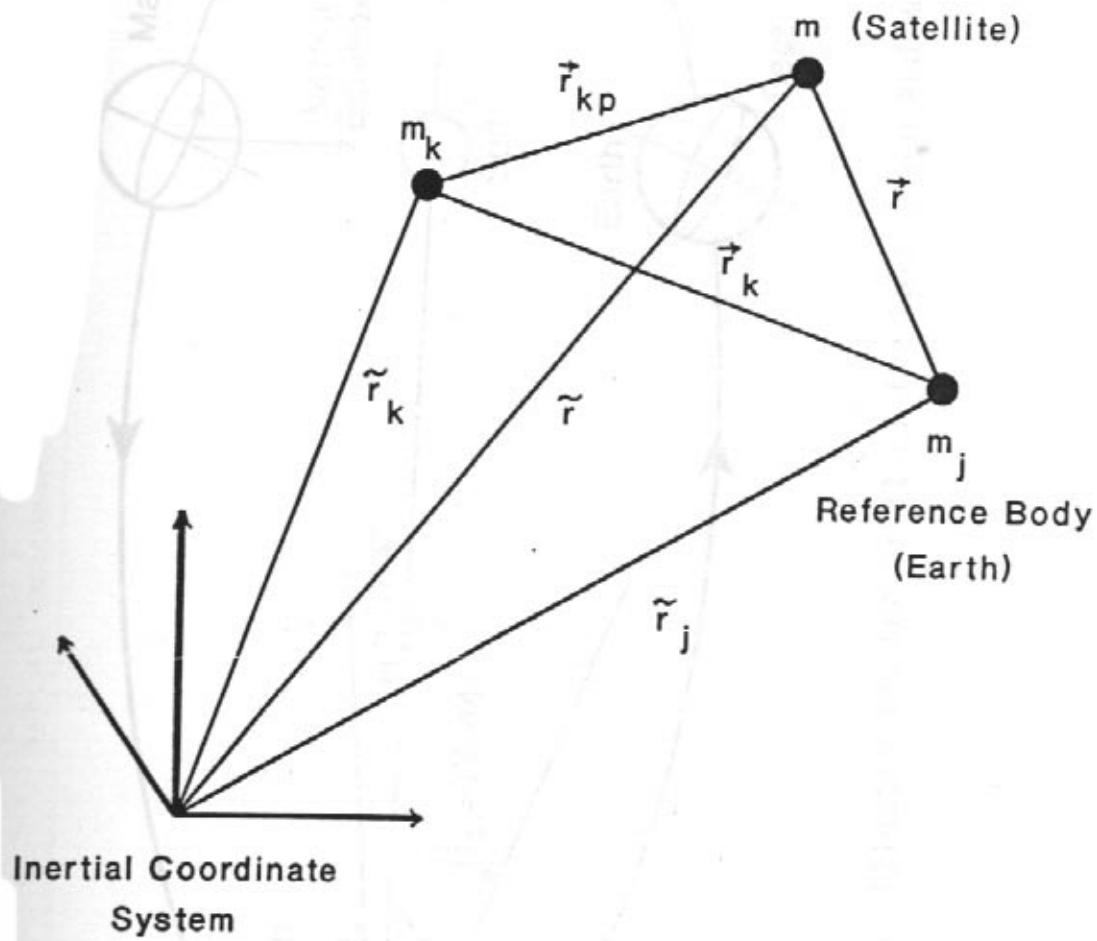

Fig.5 Illustrating the gravitational attraction of many bodies on the satellite.

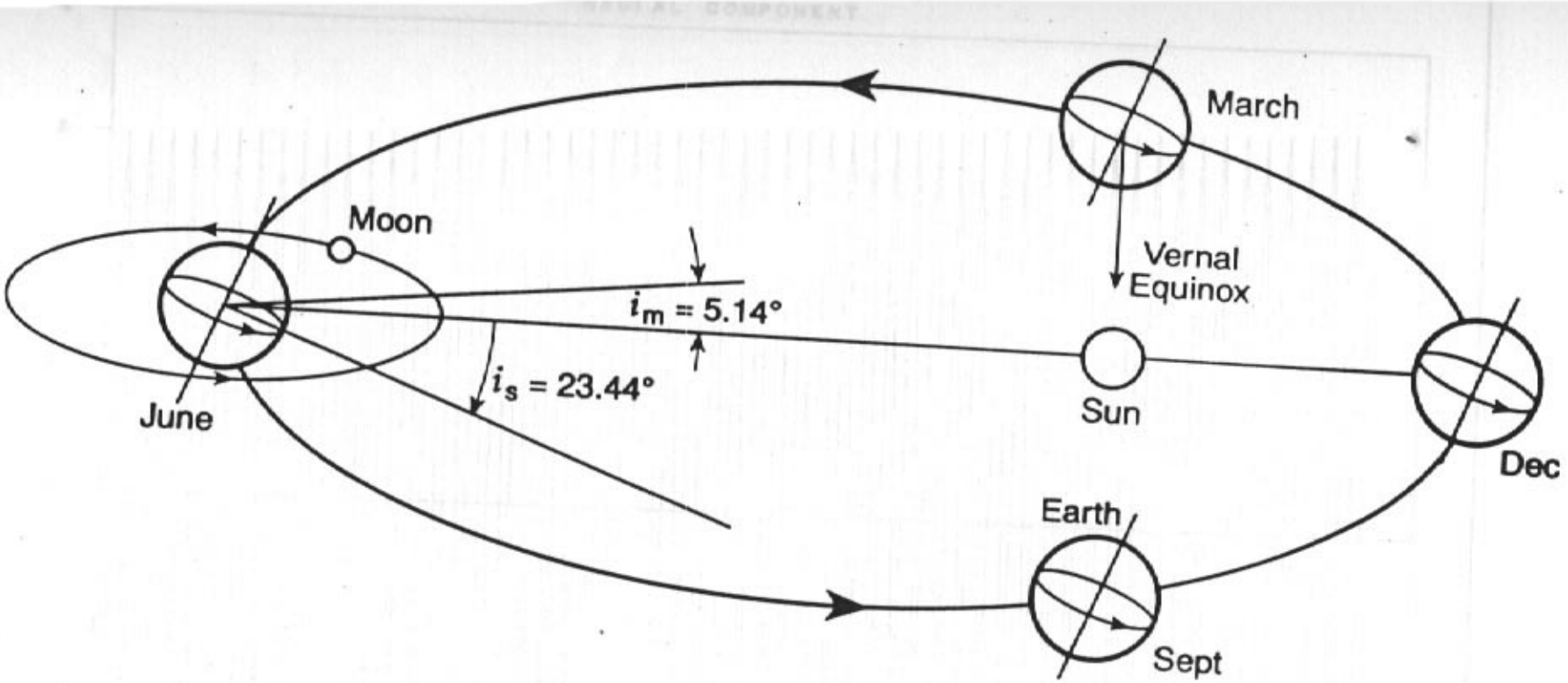

Fig. 6 Illustrating the orbit of the Earth, Sun and Moon.

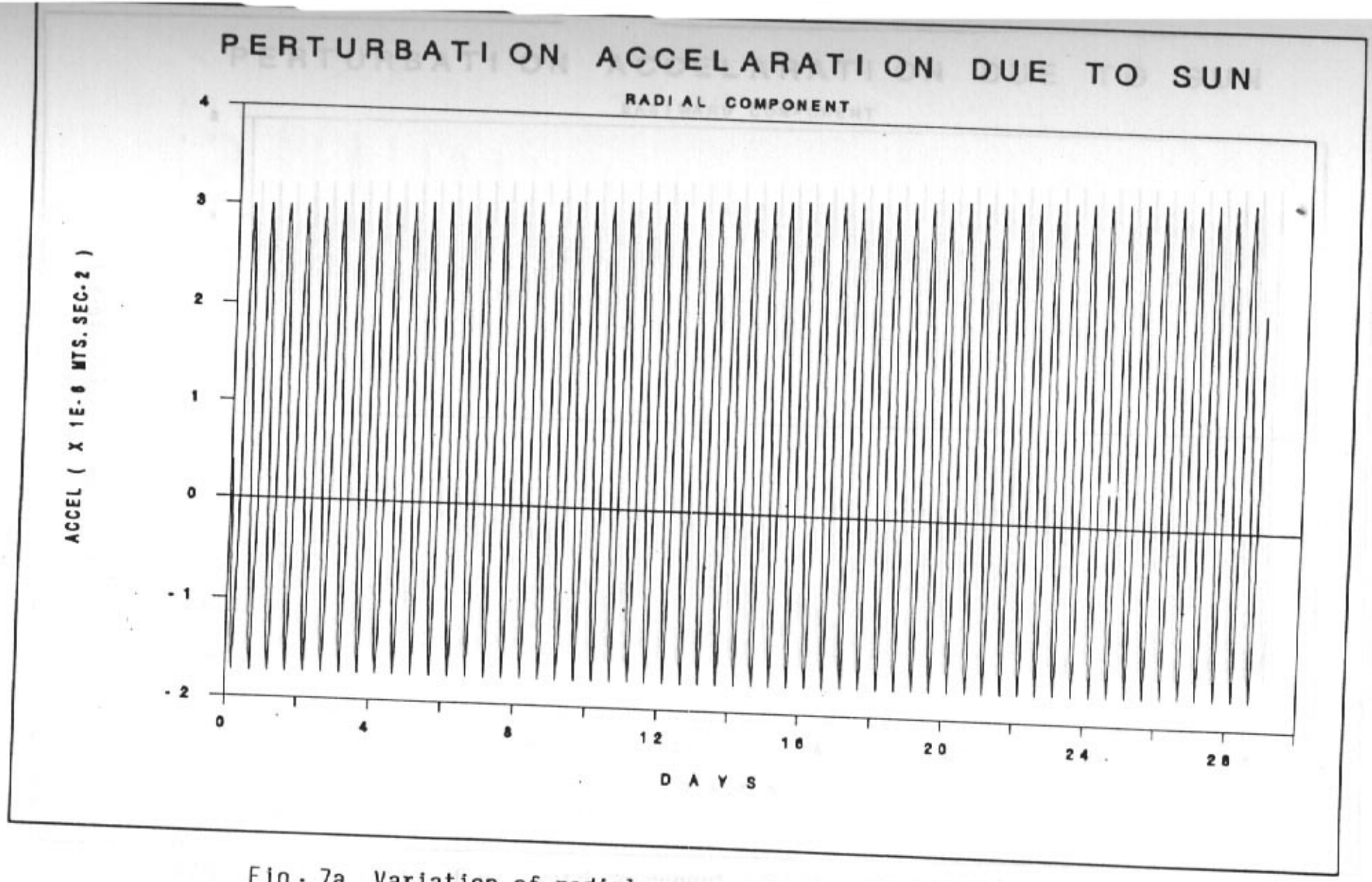

Fig.- 7a Variation of radial component of solar perturbation acceleration for the period Jan 28 through Feb

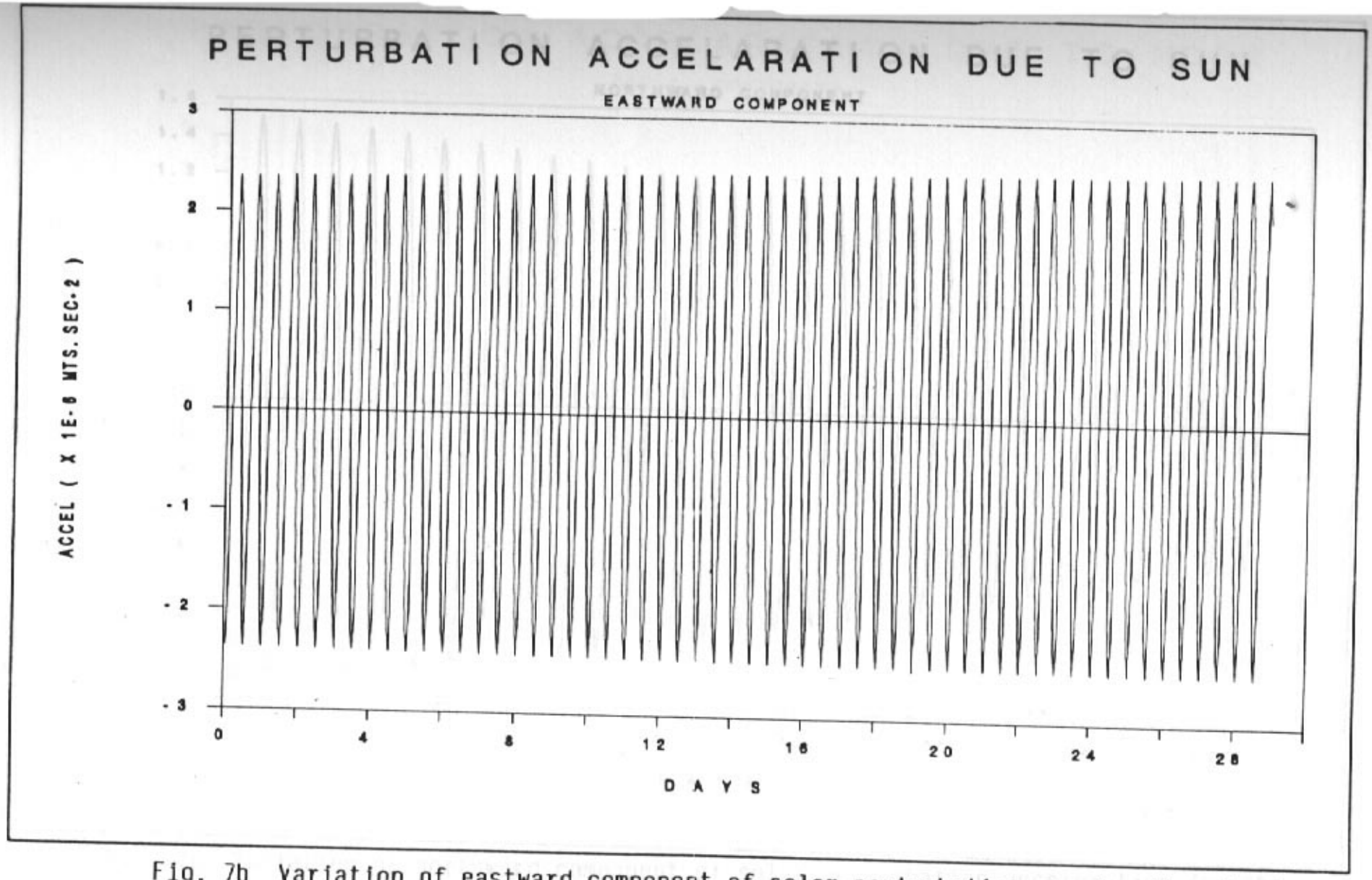

Fig. 7b Variation of eastward component of solar perturbation acceleration for the period Jan 29 through Feb 26.

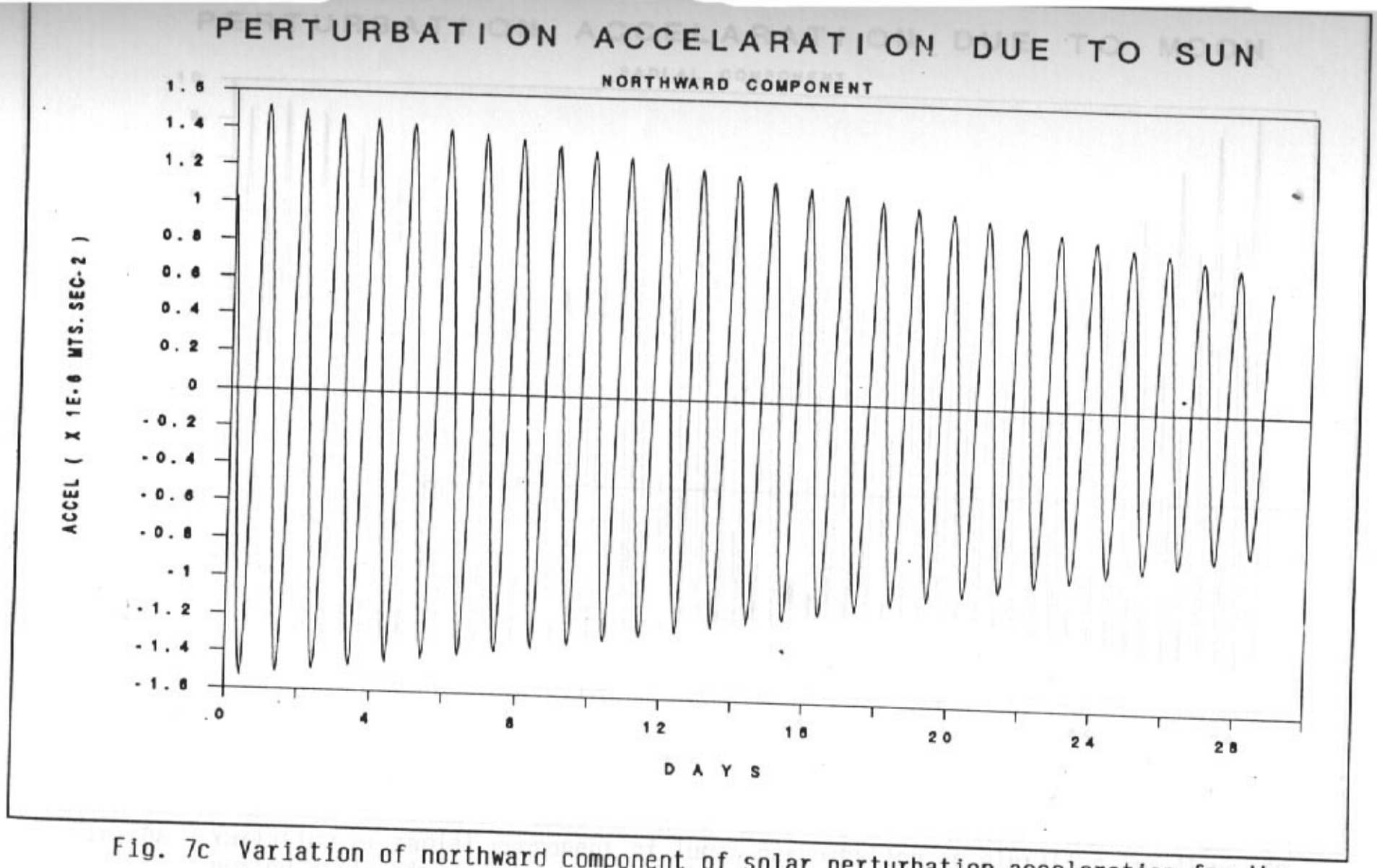

Fig. 7c Variation of northward component of solar perturbation acceleration for the period Jan 29 through Feb 26.

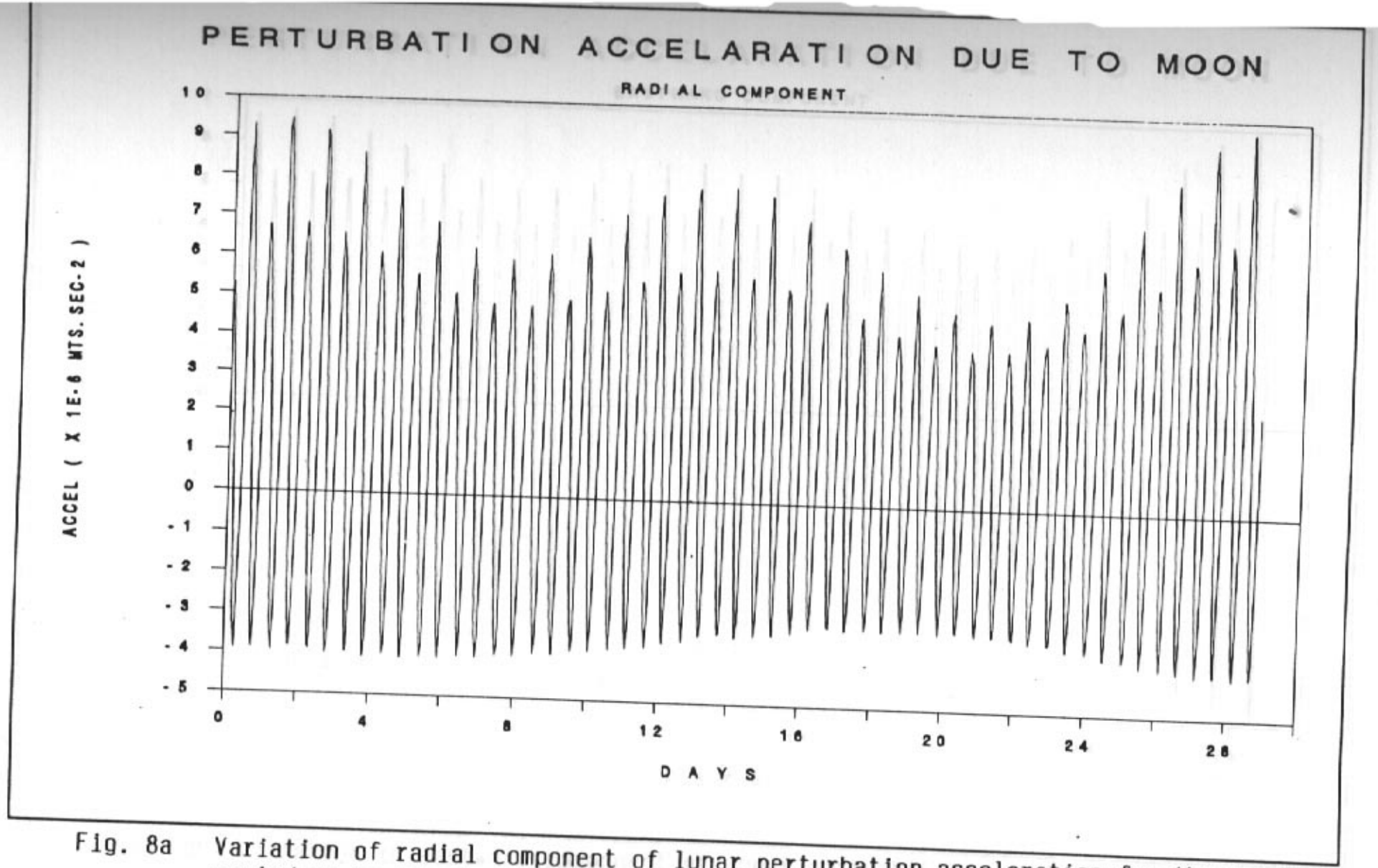

Fig. 8a Variation of radial component of lunar perturbation acceleration for the same period as in Fig.7.

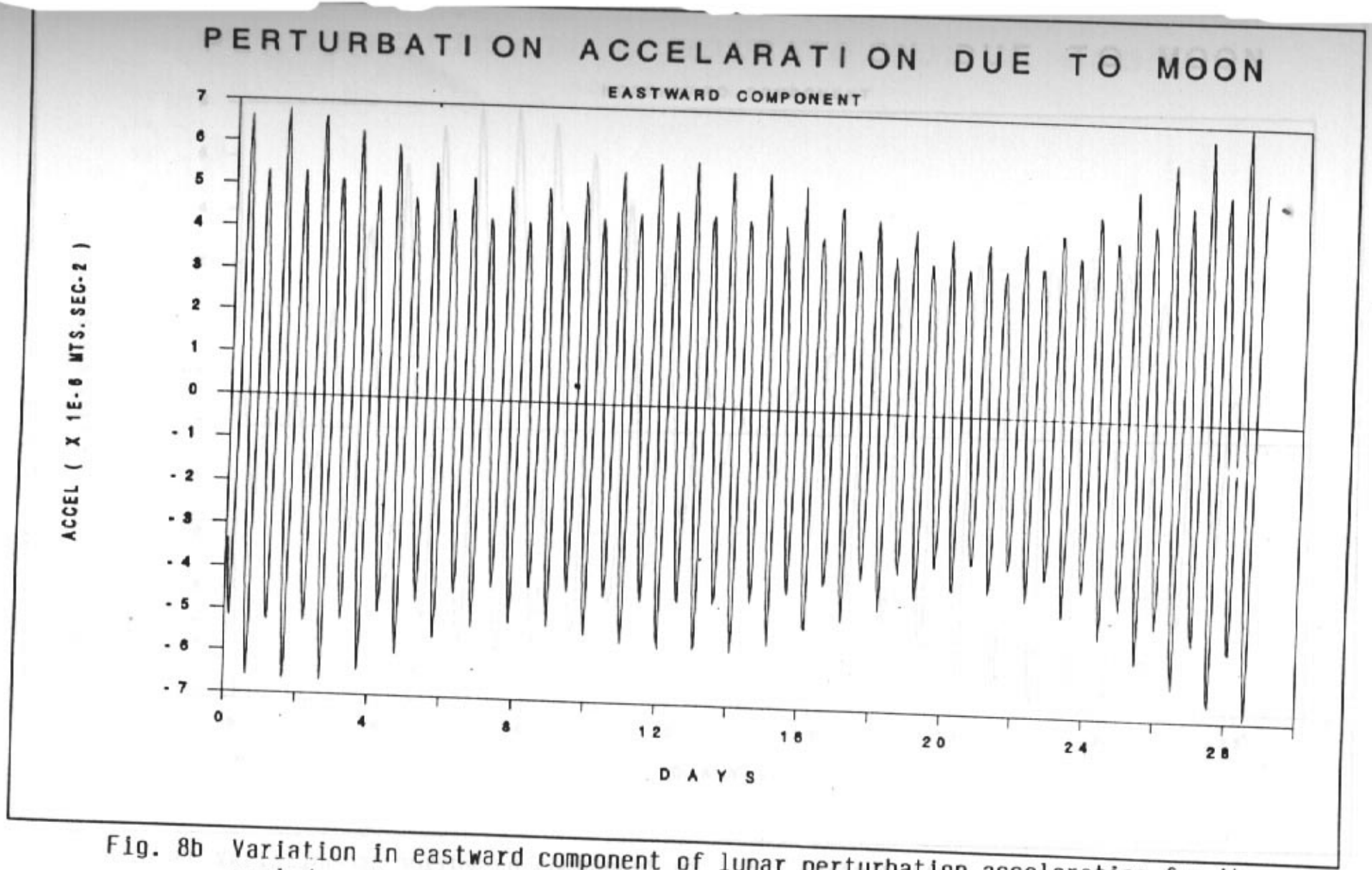

Fig. 8b Variation in eastward component of lunar perturbation acceleration for the same period as in Fig.7.

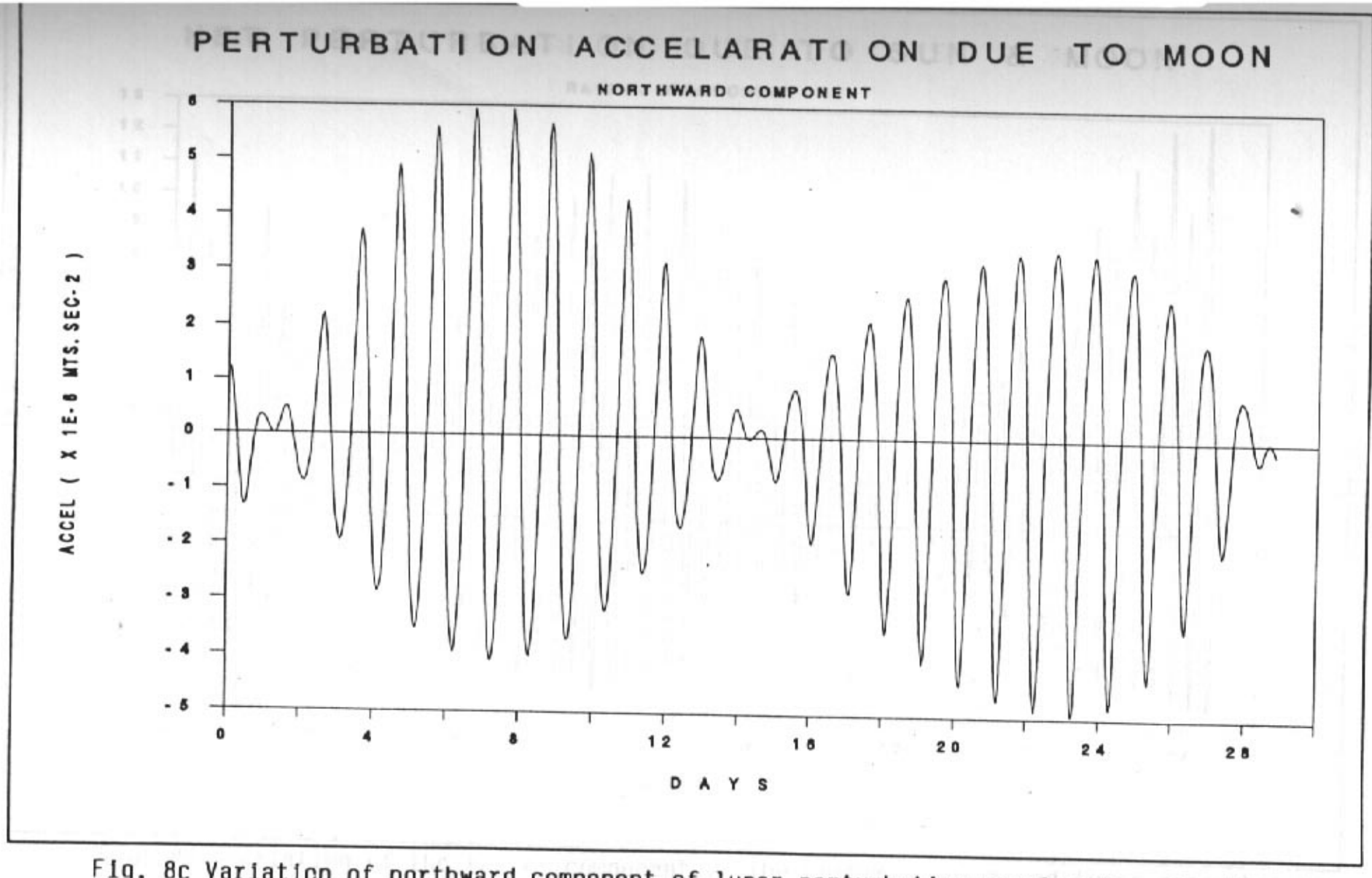

Fig. 8c Variation of northward component of lunar perturbation acceleration for the same period as in Fig.7.

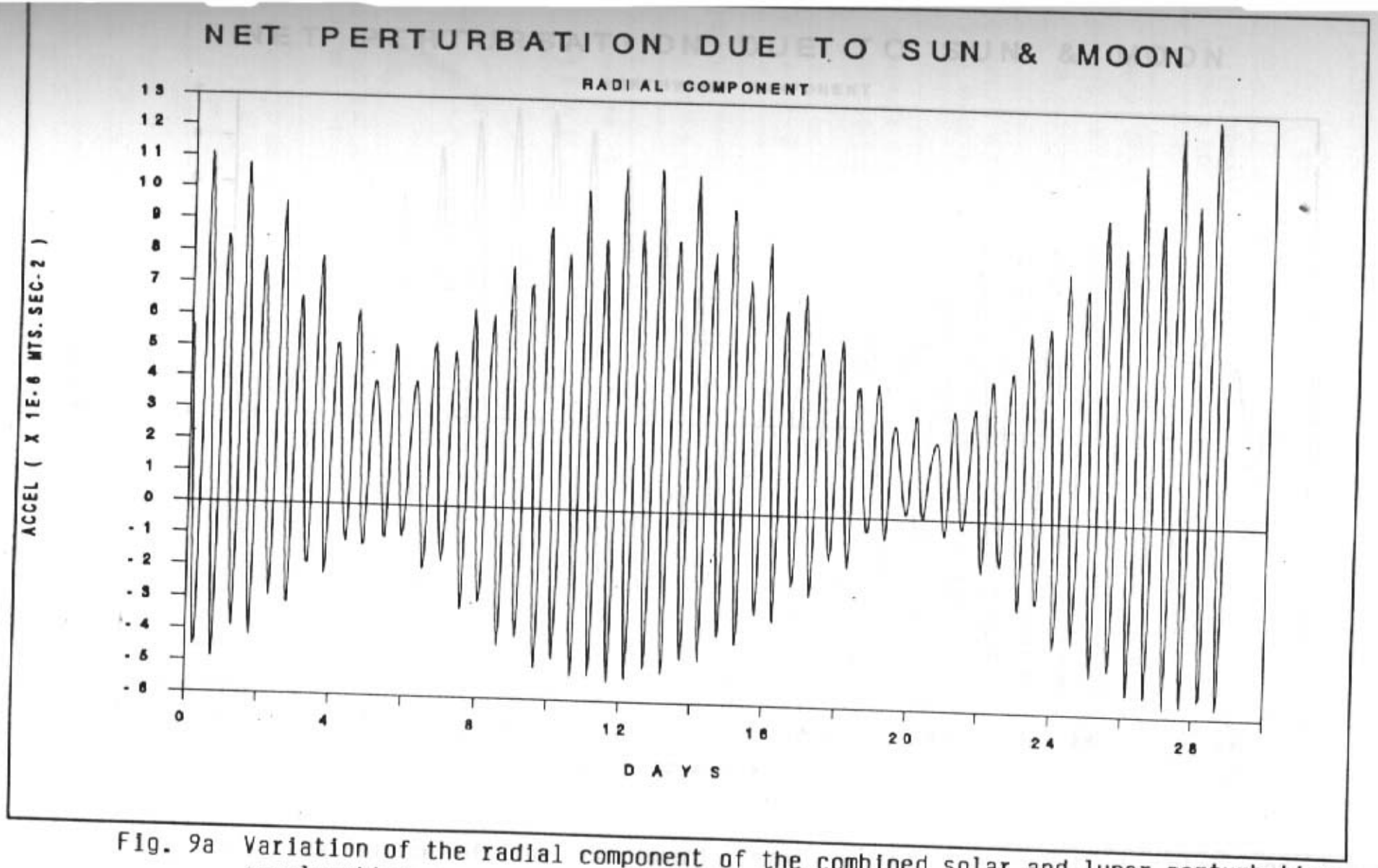

Fig. 9a Variation of the radial component of the combined solar and lunar perturbation acceleration.

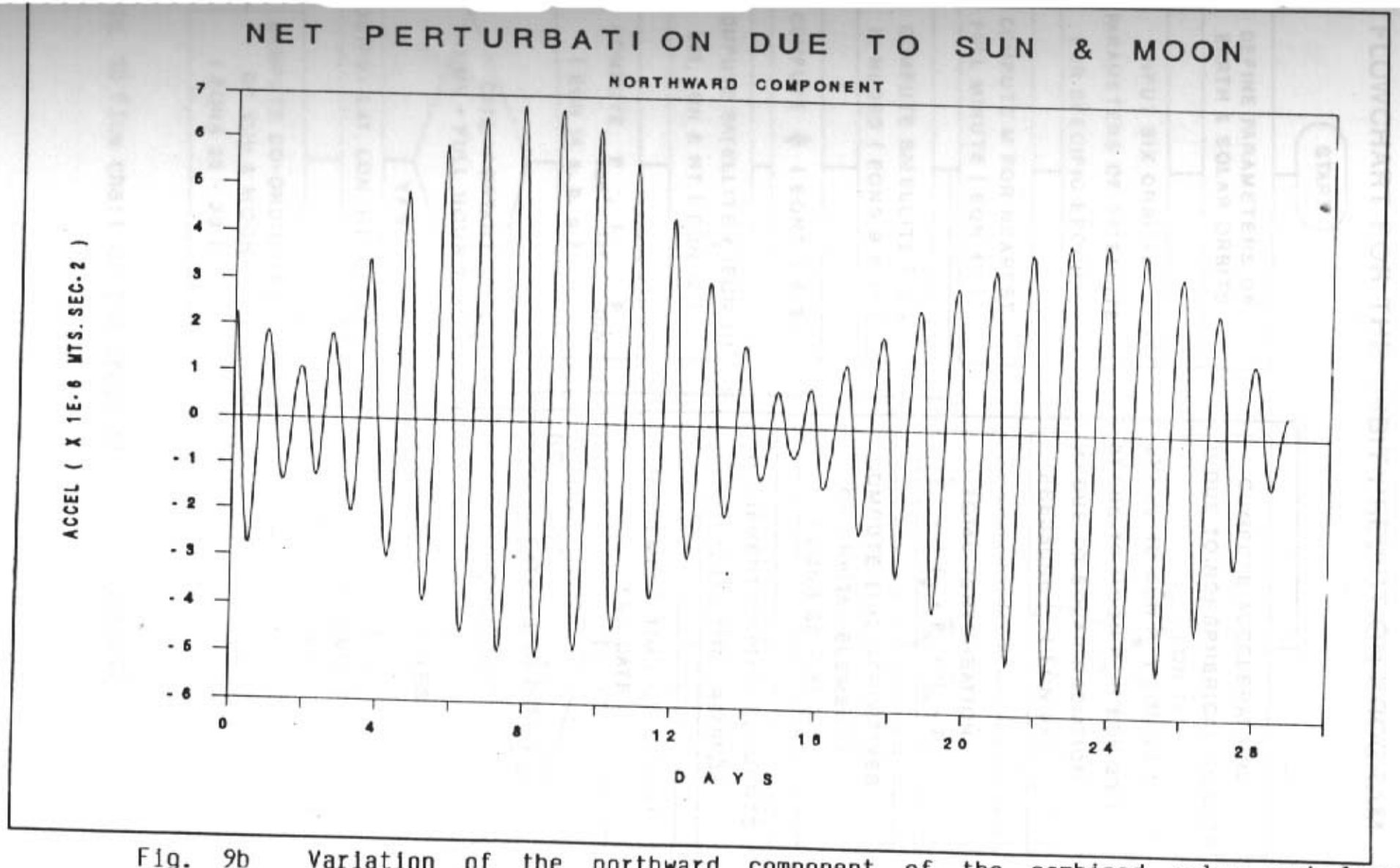

Fig. 9b Variation of the northward component of the combined solar and lunar perturbation acceleration.

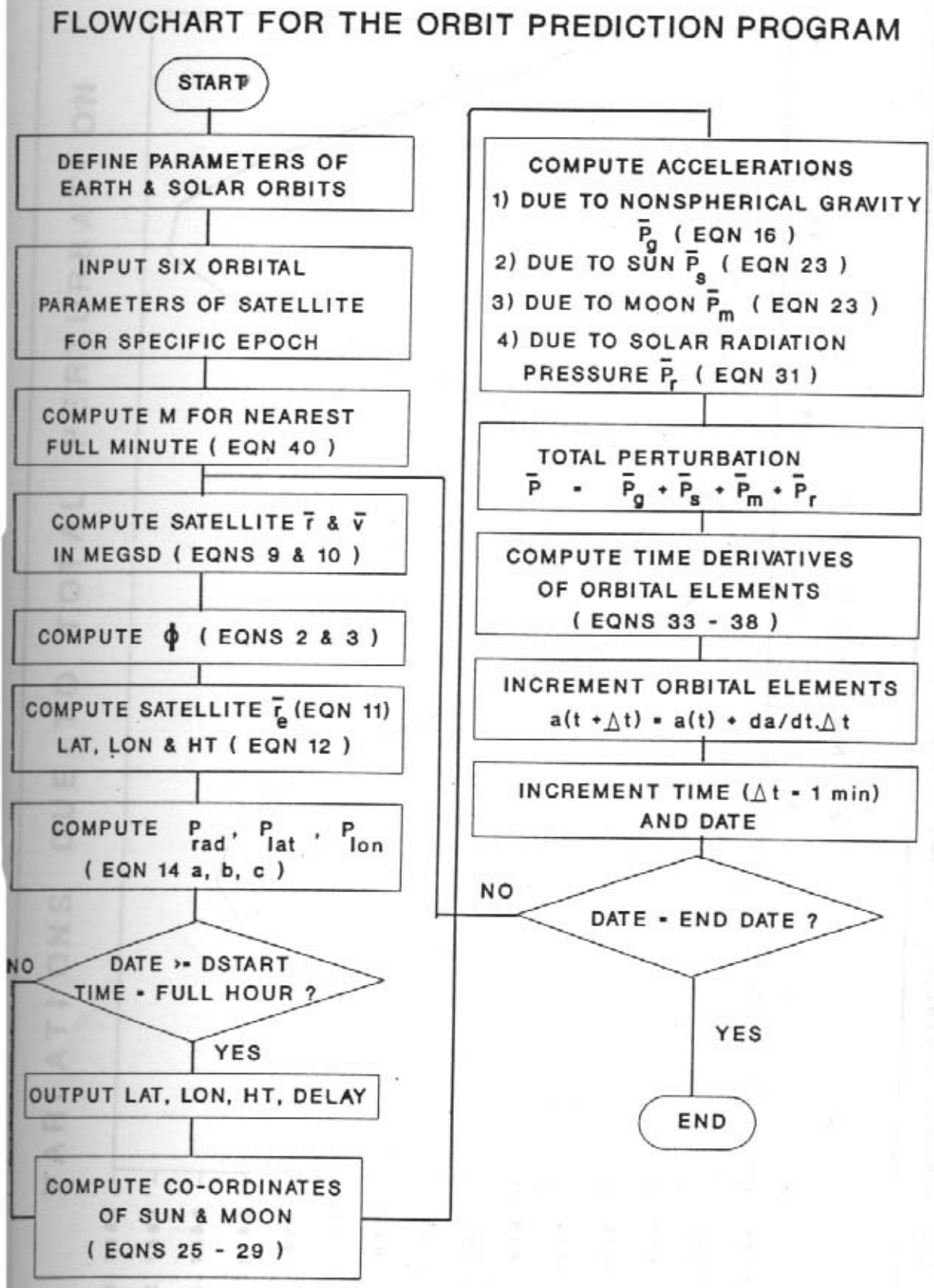

Fig. 10 Flow chart of the orbit prediction program.

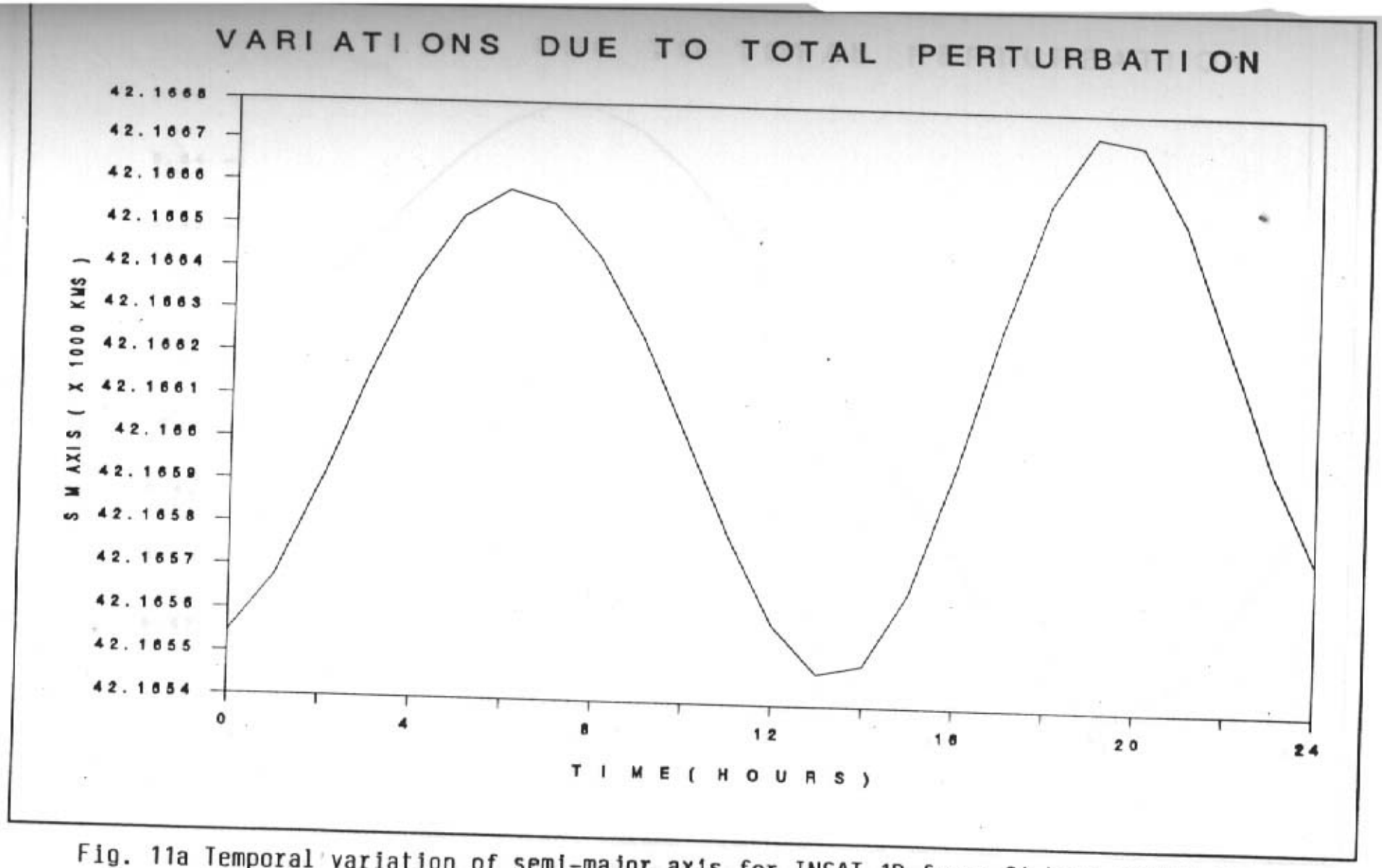

Fig. 11a Temporal variation of semi-major axis for INSAT 1B for a 24 hour period on Feb 3, 1990. All the perturbations have been taken into account.

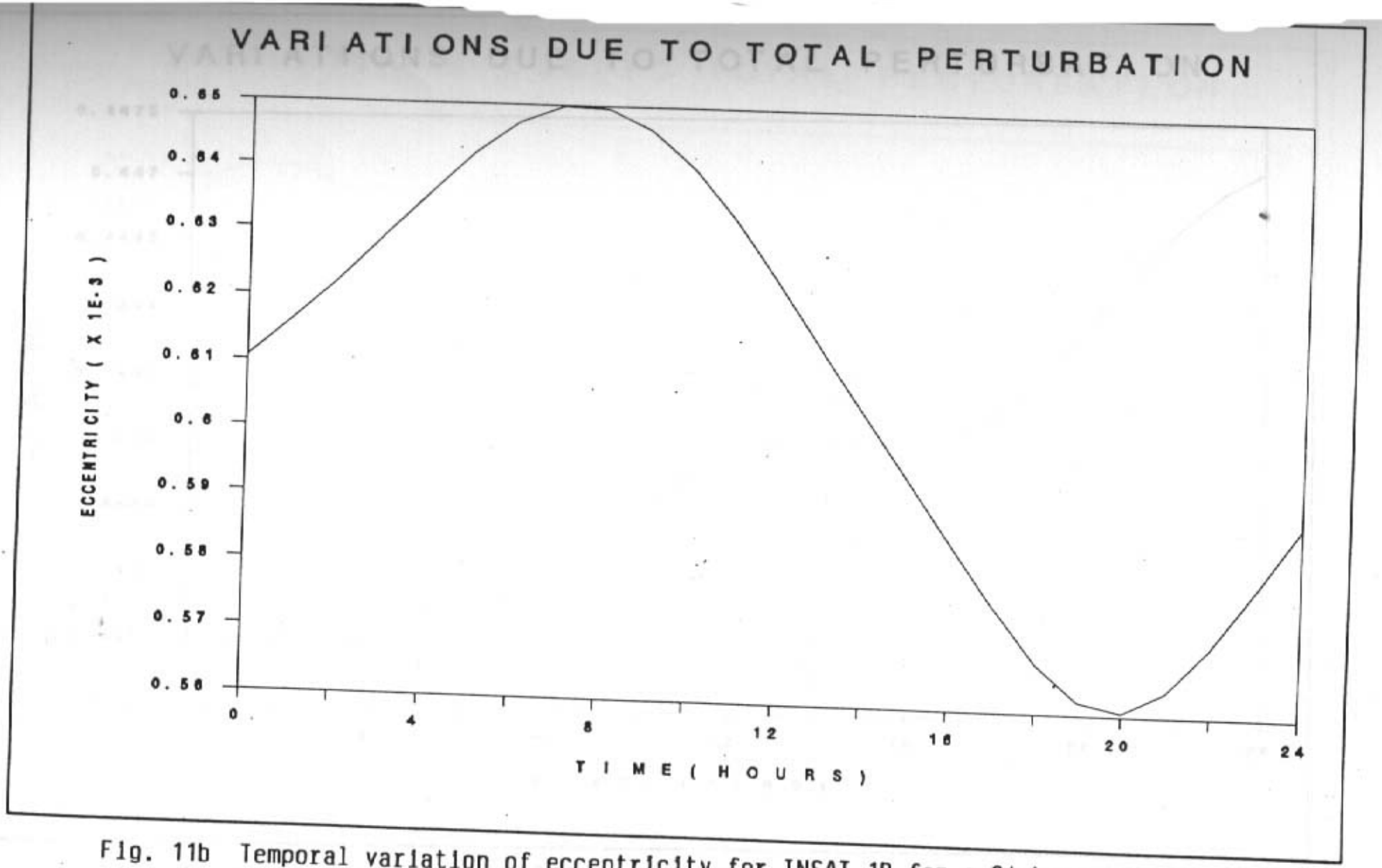

Fig. 11b Temporal variation of eccentricity for INSAT 1B for a 24 hour period on Feb 3, 1990. All the perturbations have been taken into account.

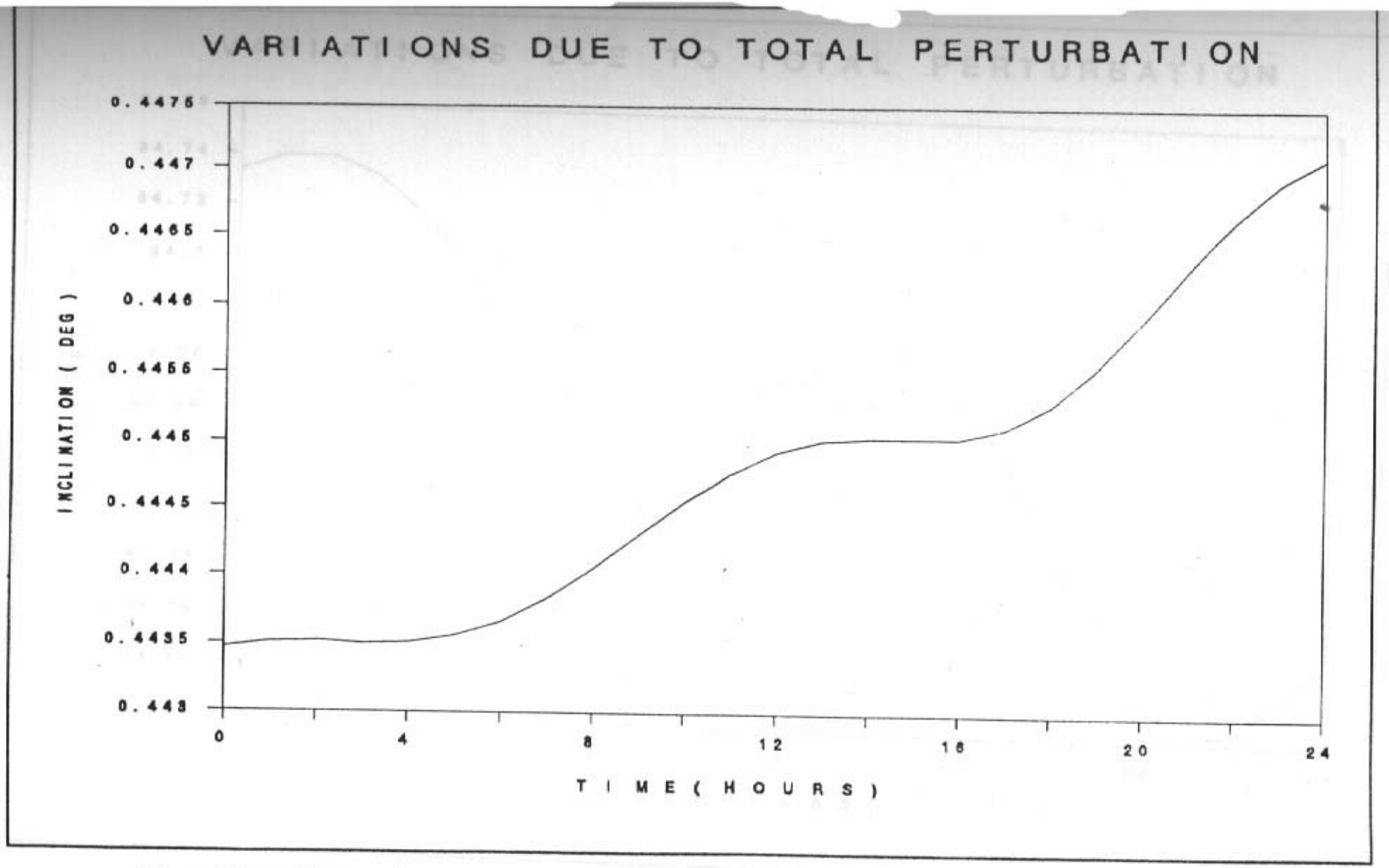

Fig. 11c Temporal variation of inclination for INSAT 1B for a 24 hour period on Feb 3, 1990. All the perturbations have been taken into account.

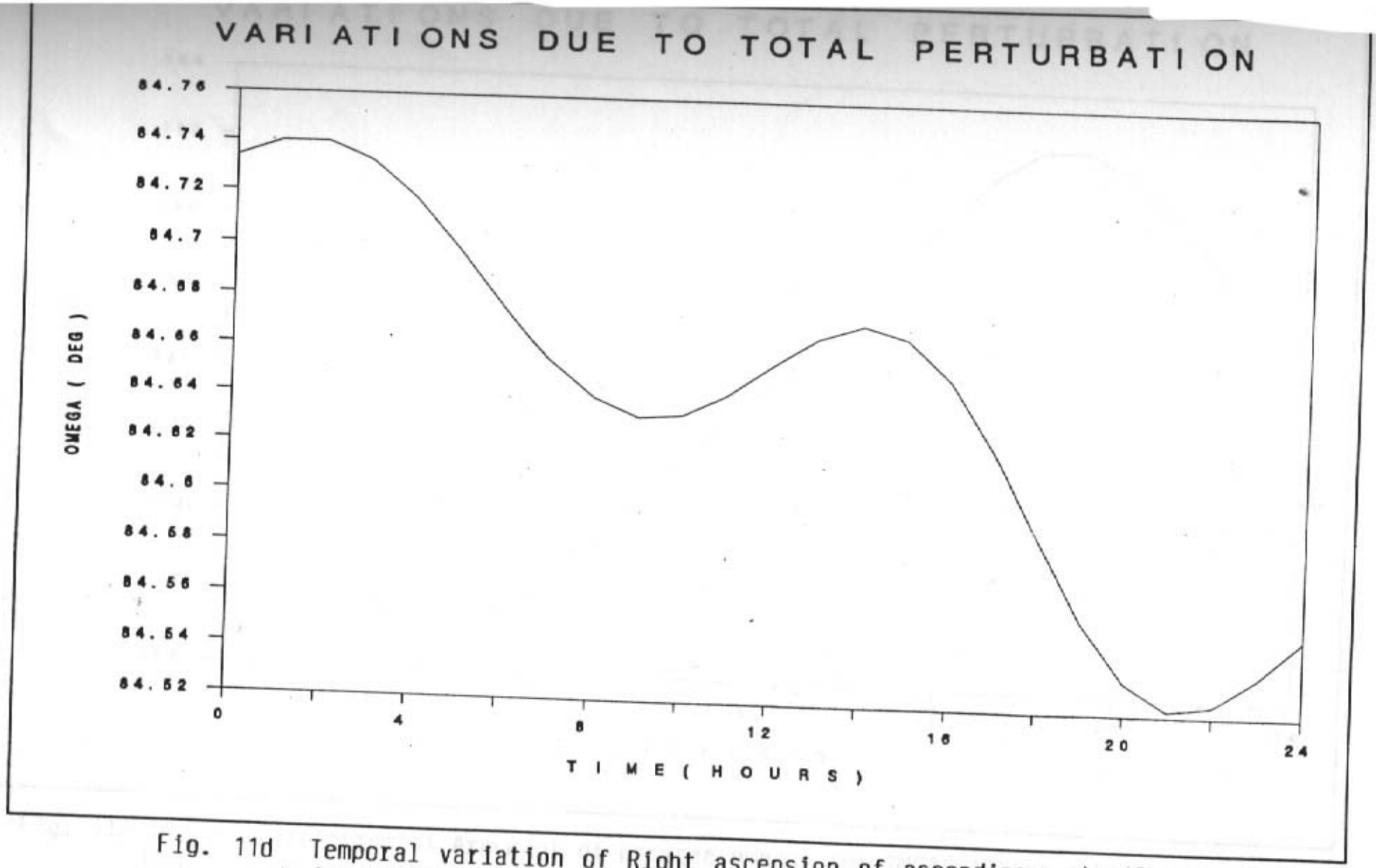

Fig. 11d Temporal variation of Right ascension of ascending node (OMEGA) for INSAT 1B for a 24 hour period on Feb 3,1990. All the perturbations have been

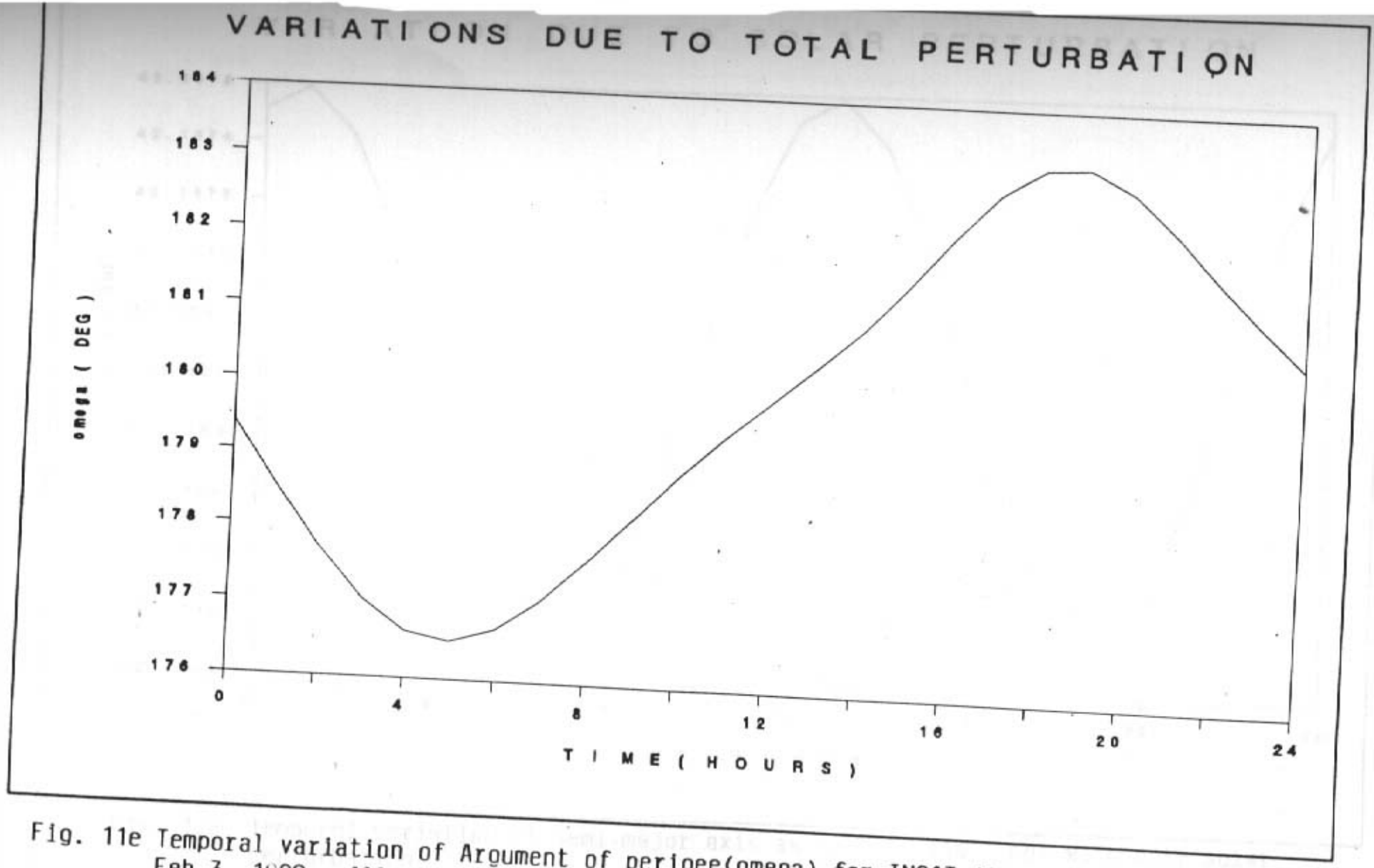

Fig. 11e Temporal variation of Argument of perigee(omega) for INSAT-1B for a 24 hour period on Feb 3, 1990. All the perturbations have been taken into account

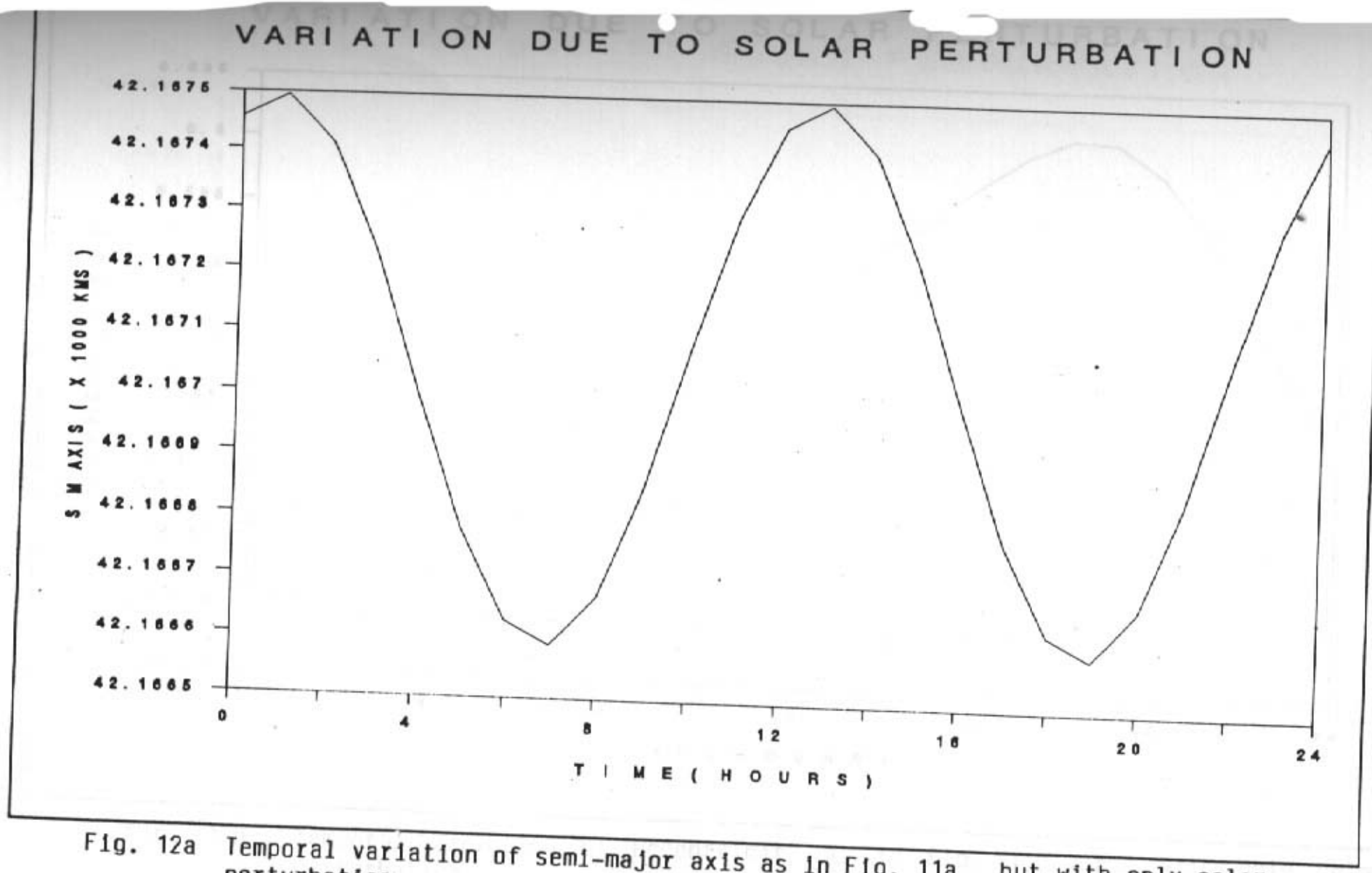

Fig. 12a Temporal variation of semi-major axis as in Fig. 11a but with only solar perturbation.

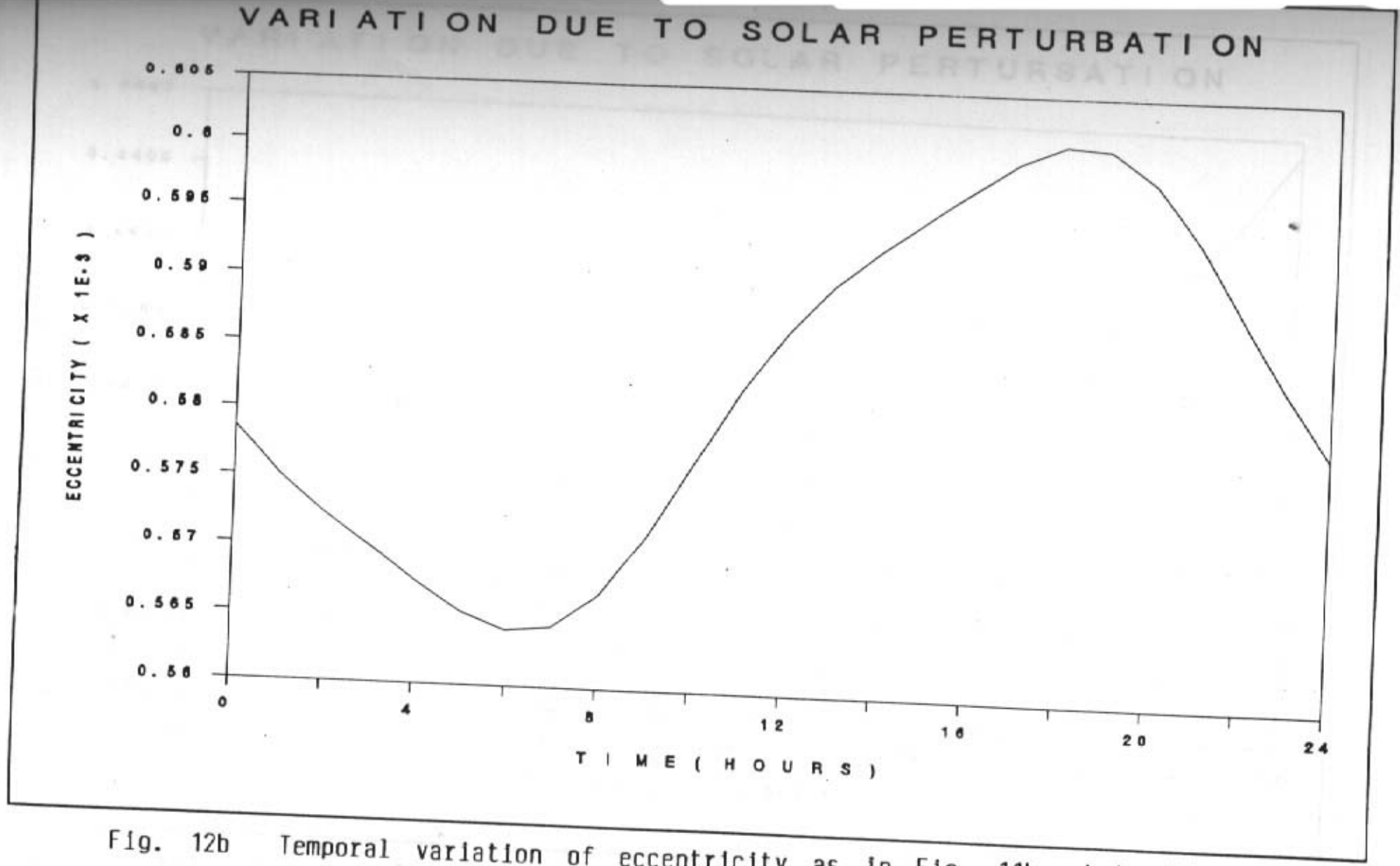

Fig. 12b Temporal variation of eccentricity as in Fig. 11b but with only solar perturbation.

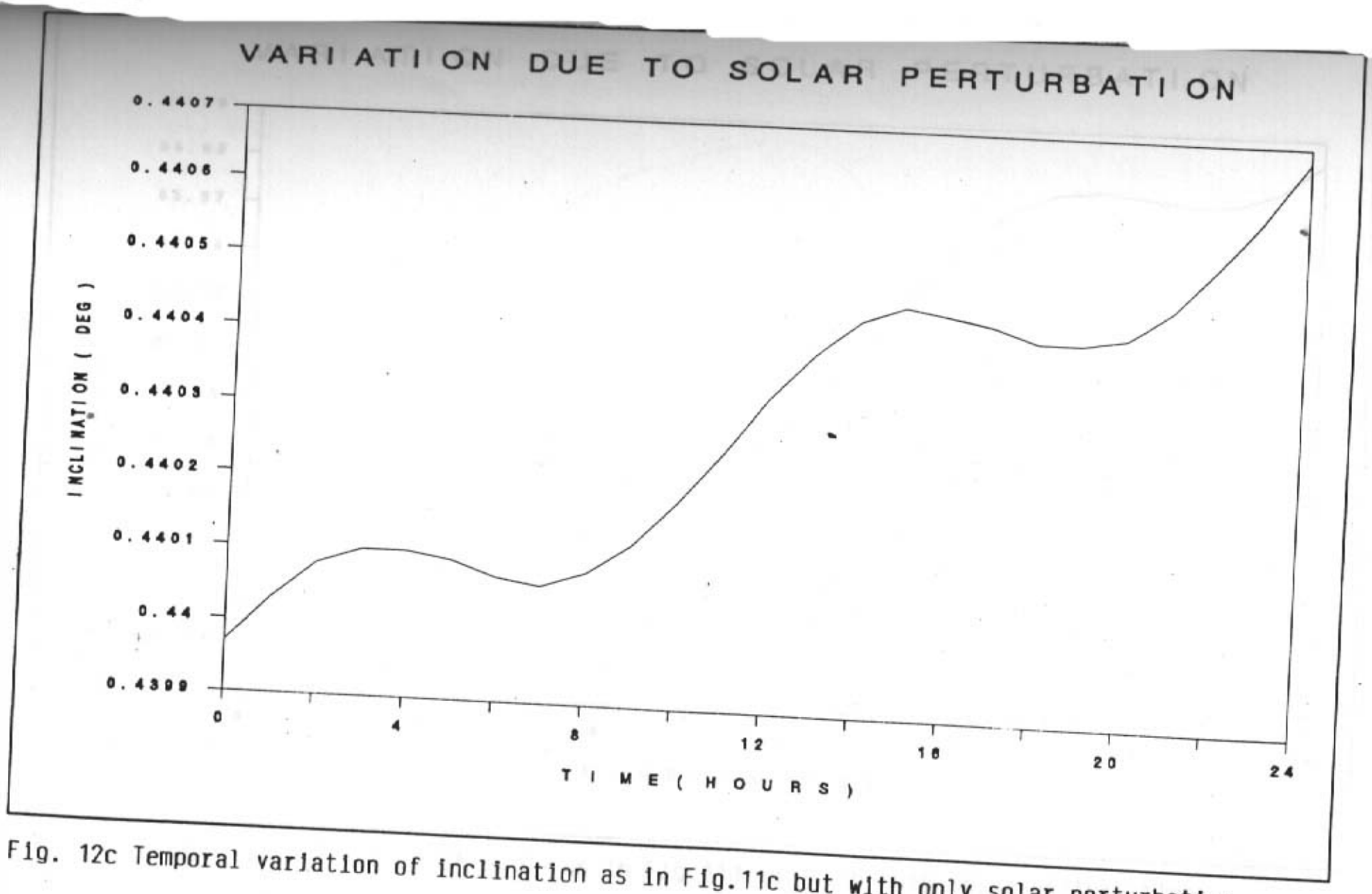

Fig. 12c Temporal variation of inclination as in Fig.11c but with only solar perturbation.

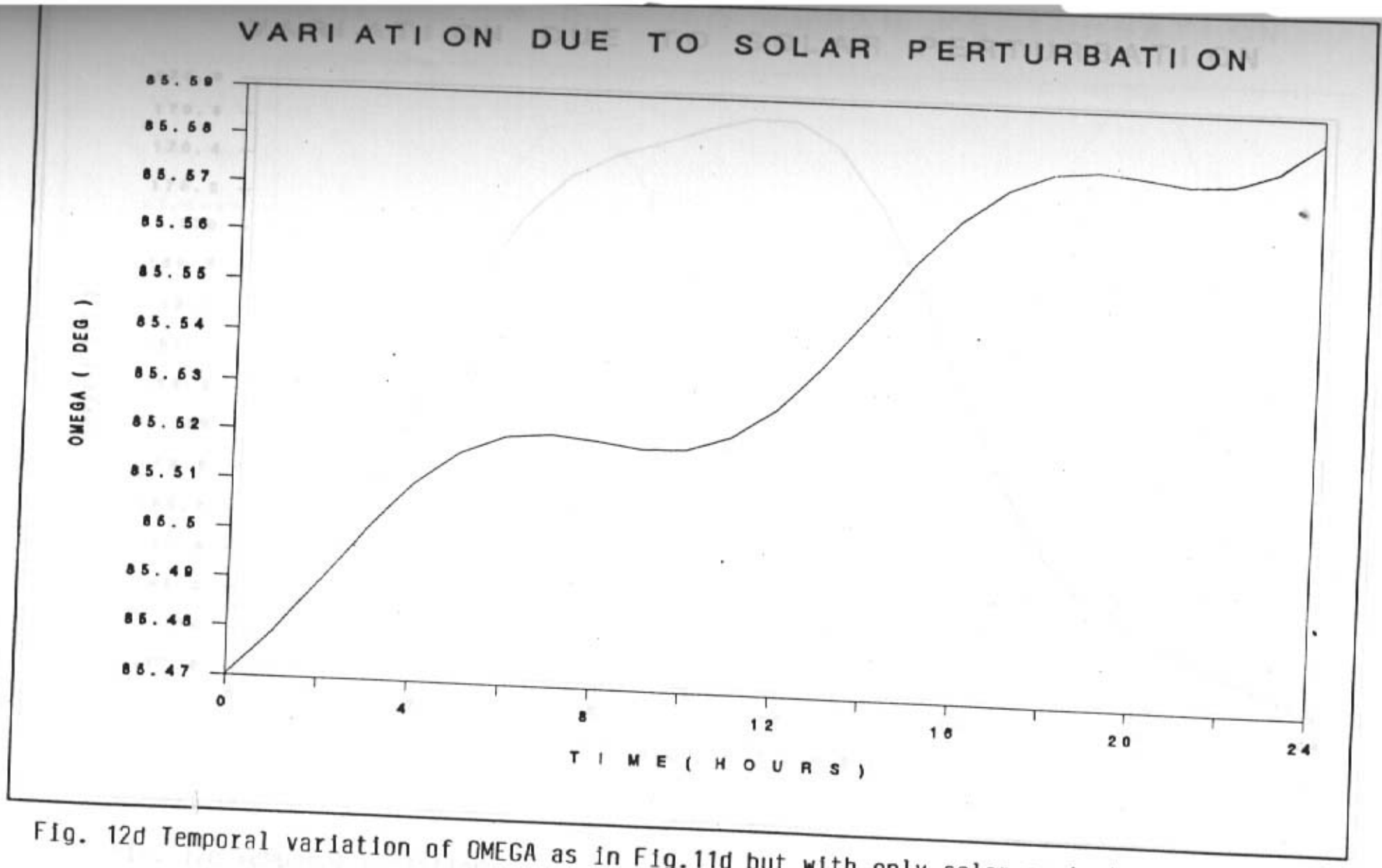

Fig. 12d Temporal variation of OMEGA as in Fig.11d but with only solar perturbation.

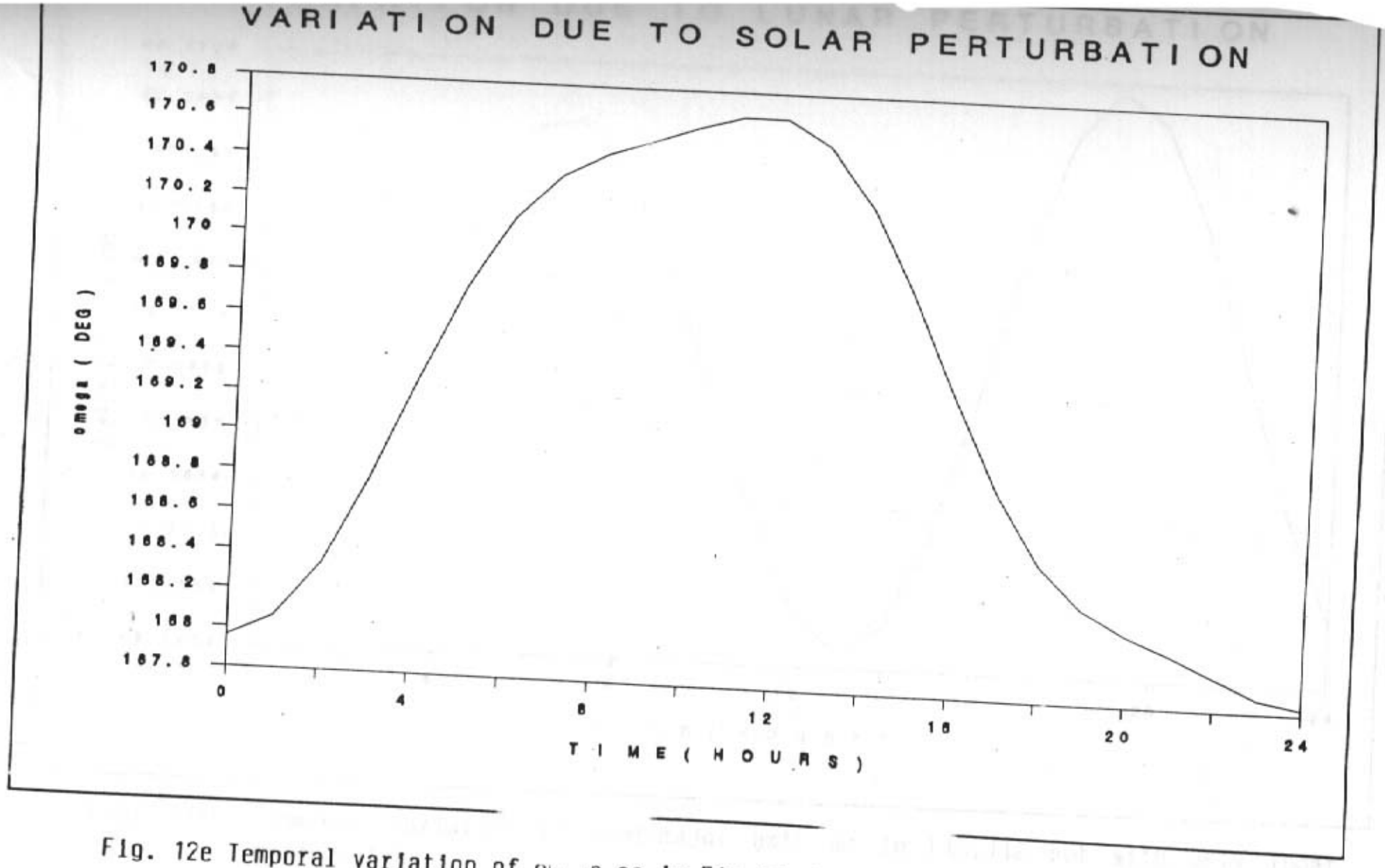

Fig. 12e Temporal variation of Omega as in Fig.11e but with only solar perturbation.

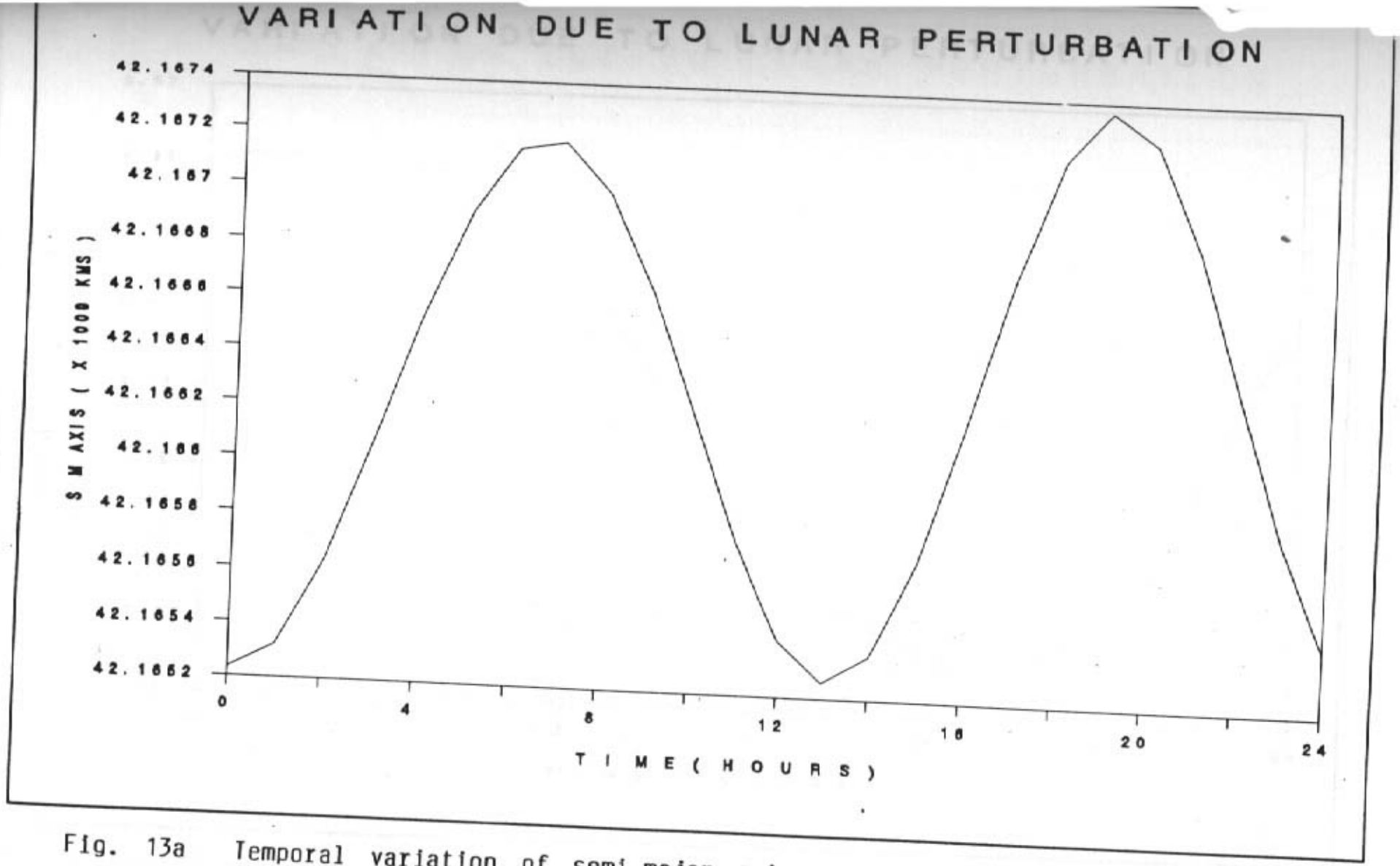

Fig. 13a Temporal variation of semi-major axis as in Fig.11a but with only lunar perturbation.

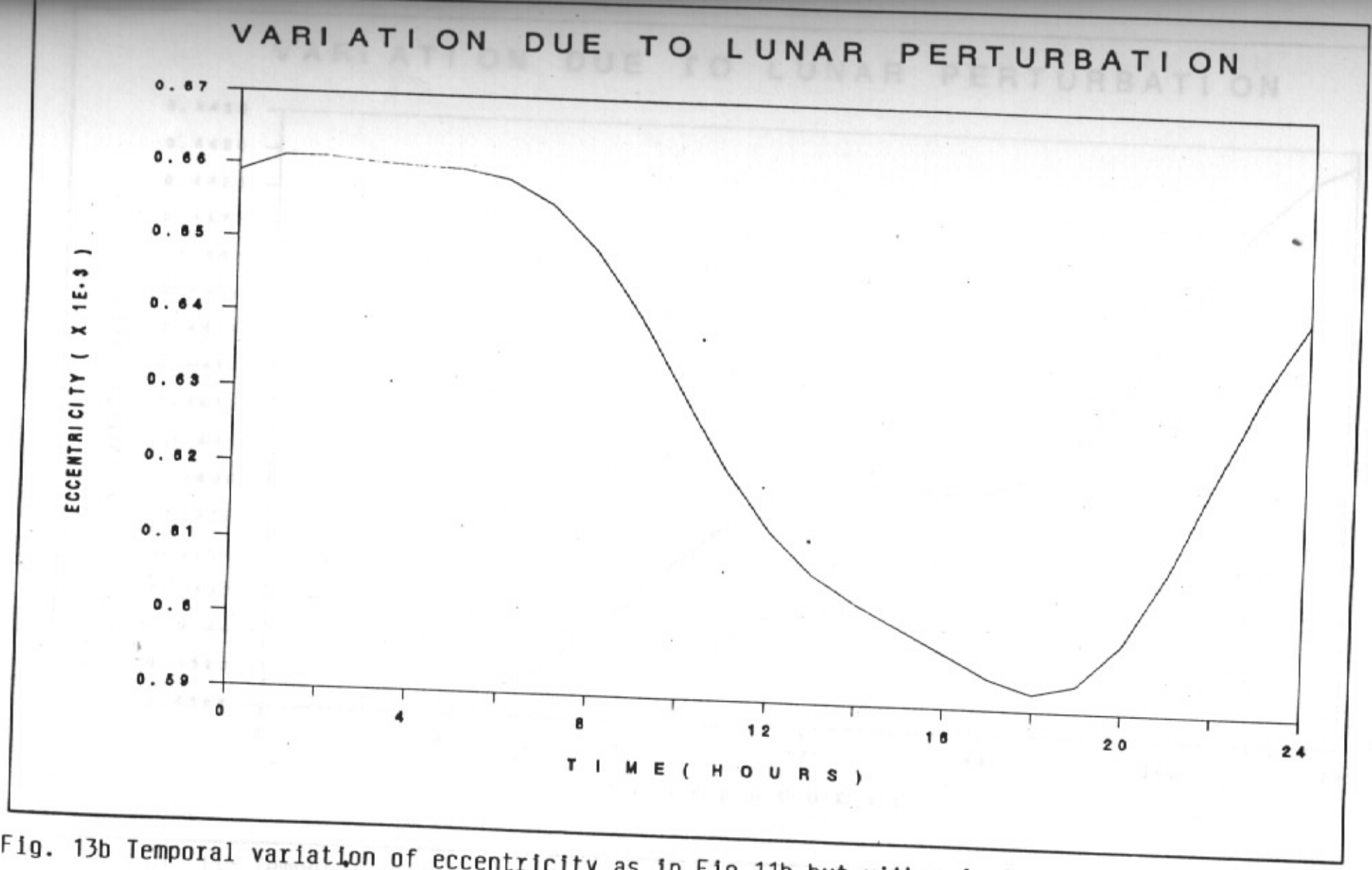

Fig. 13b Temporal variation of eccentricity as in Fig.11b but with only lunar perturbation.

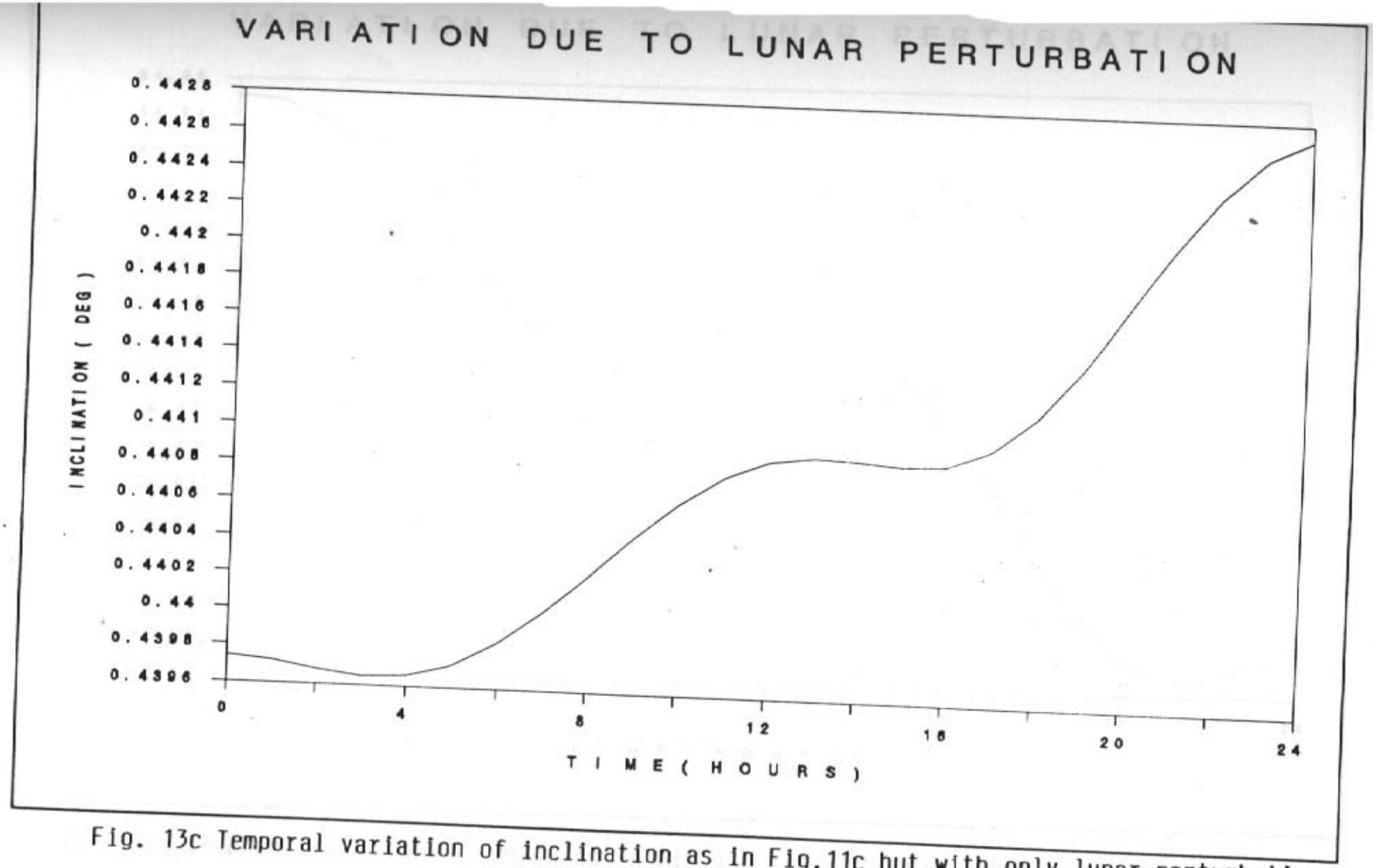

Fig. 13c Temporal variation of inclination as in Fig.11c but with only lunar perturbation.

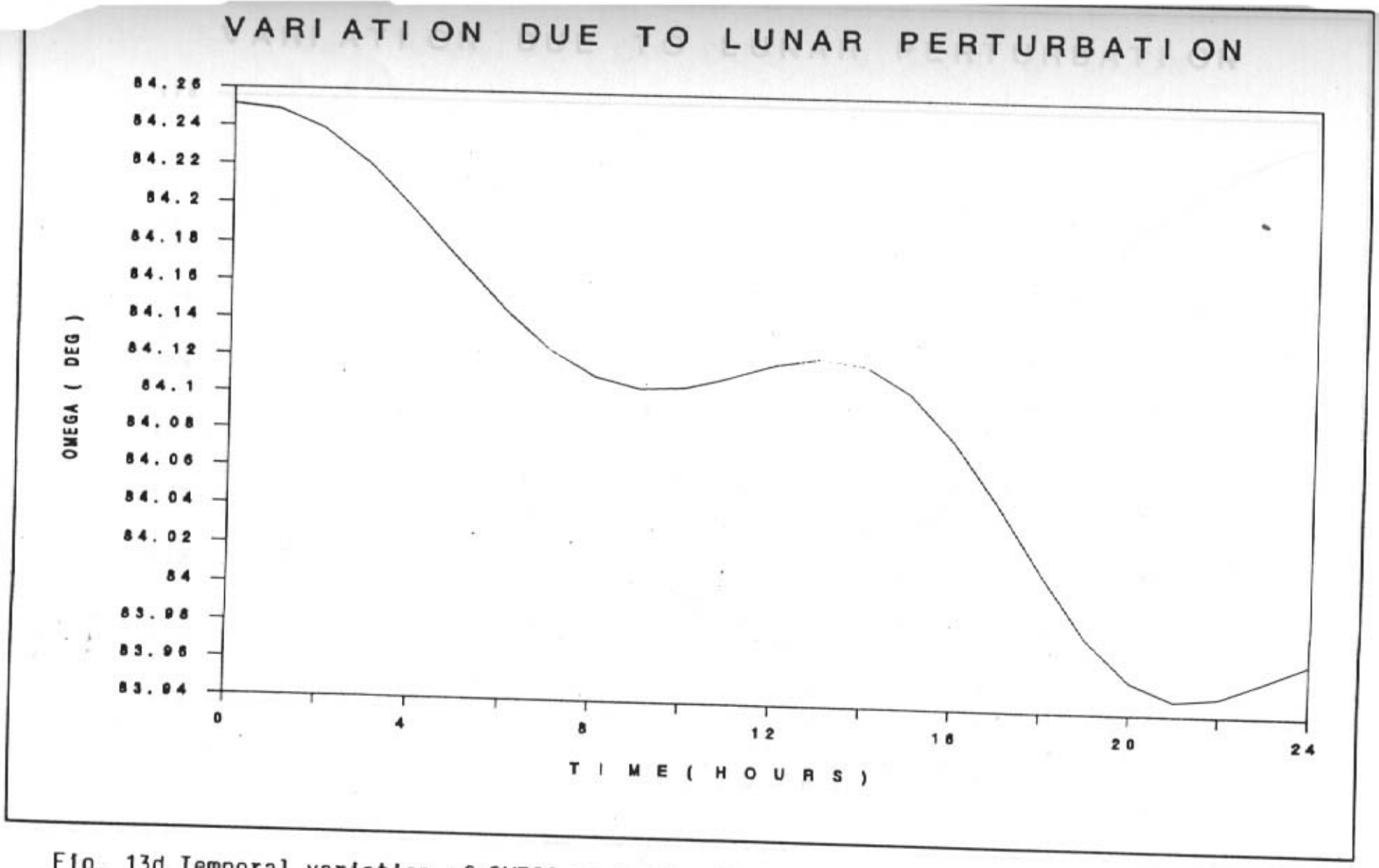

Fig. 13d Temporal variation of OMEGA as in Fig.11d but with only lunar perturbation.

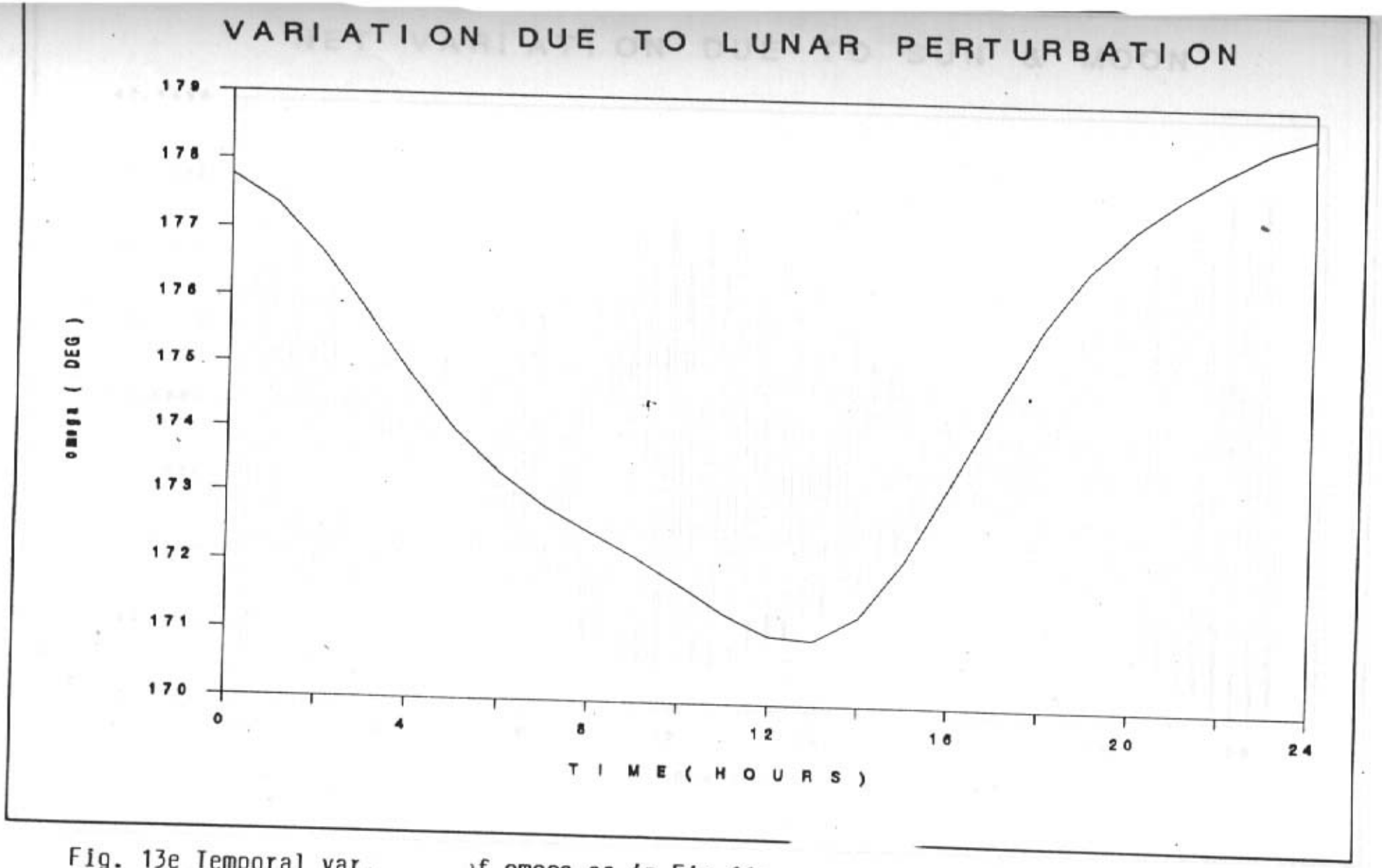

Fig. 13e Temporal var. of omega as in Fig.11c .n only lunar perturbation.

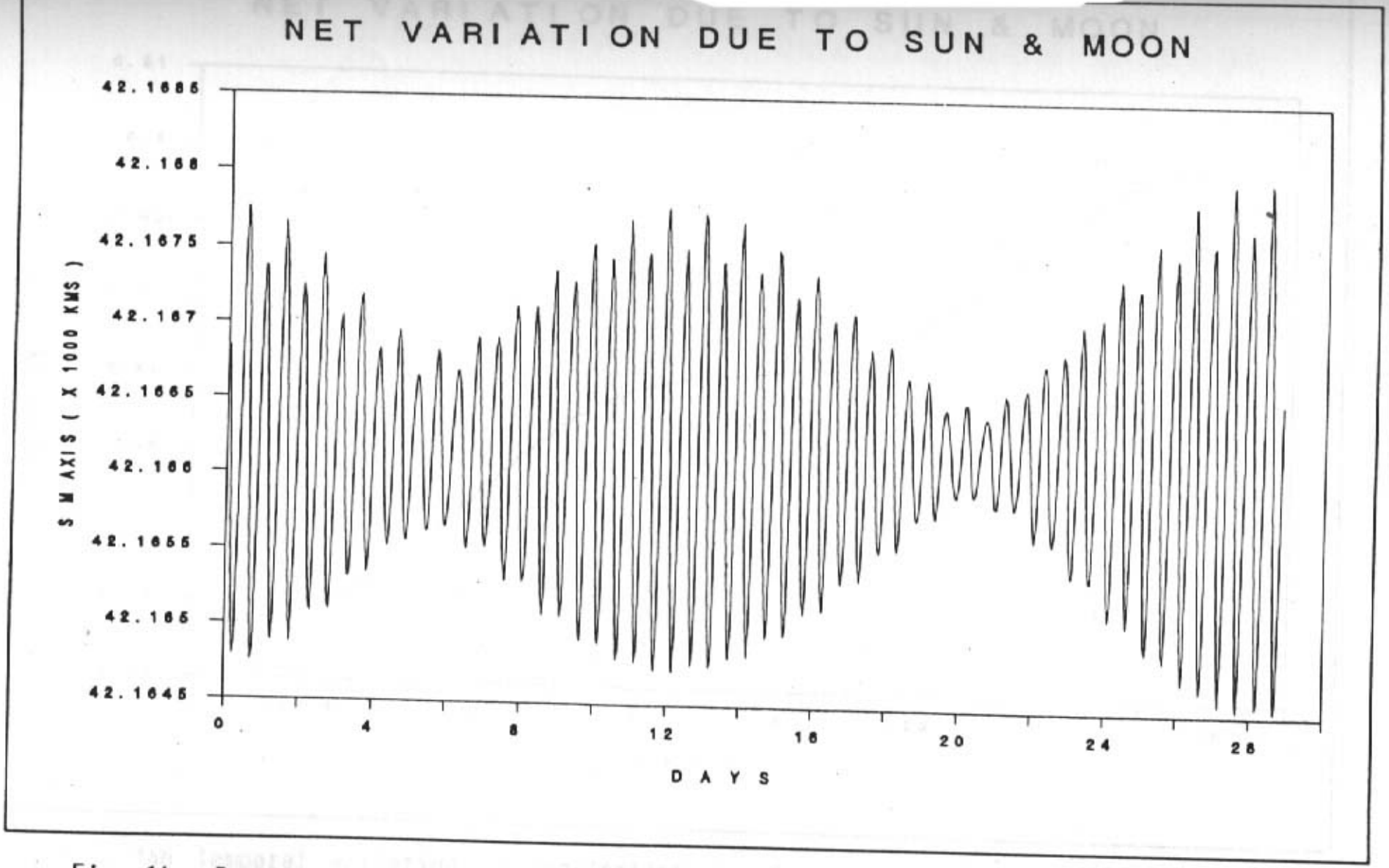

Fig. 14a Temporal variation of semi-major axis due to combined luni-solar effect for the period Jan 29 through Feb 26.

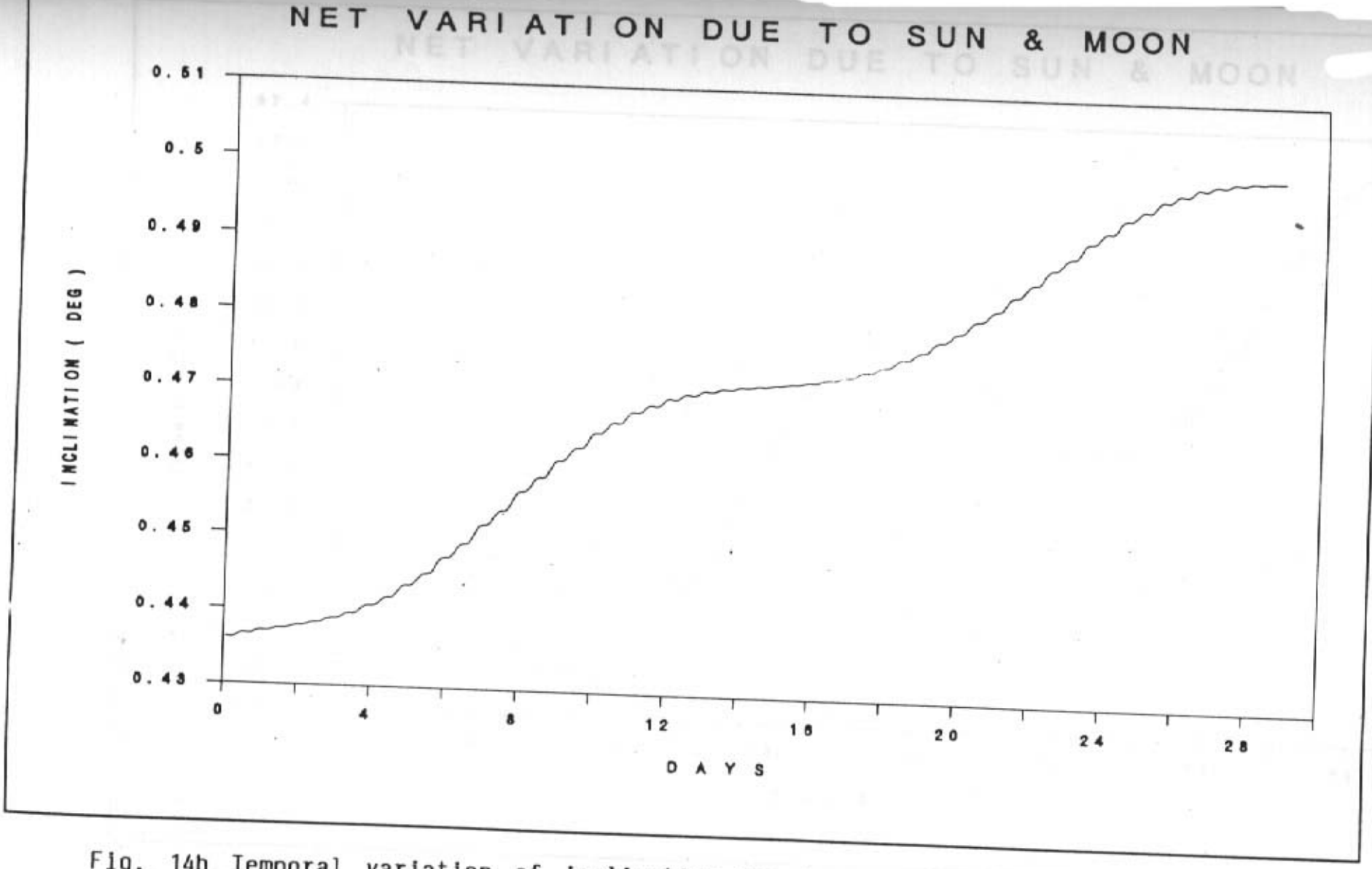

Fig. 14b Temporal variation of inclination due to combined luni-solar effect for the period Jan 29 through Feb 26.

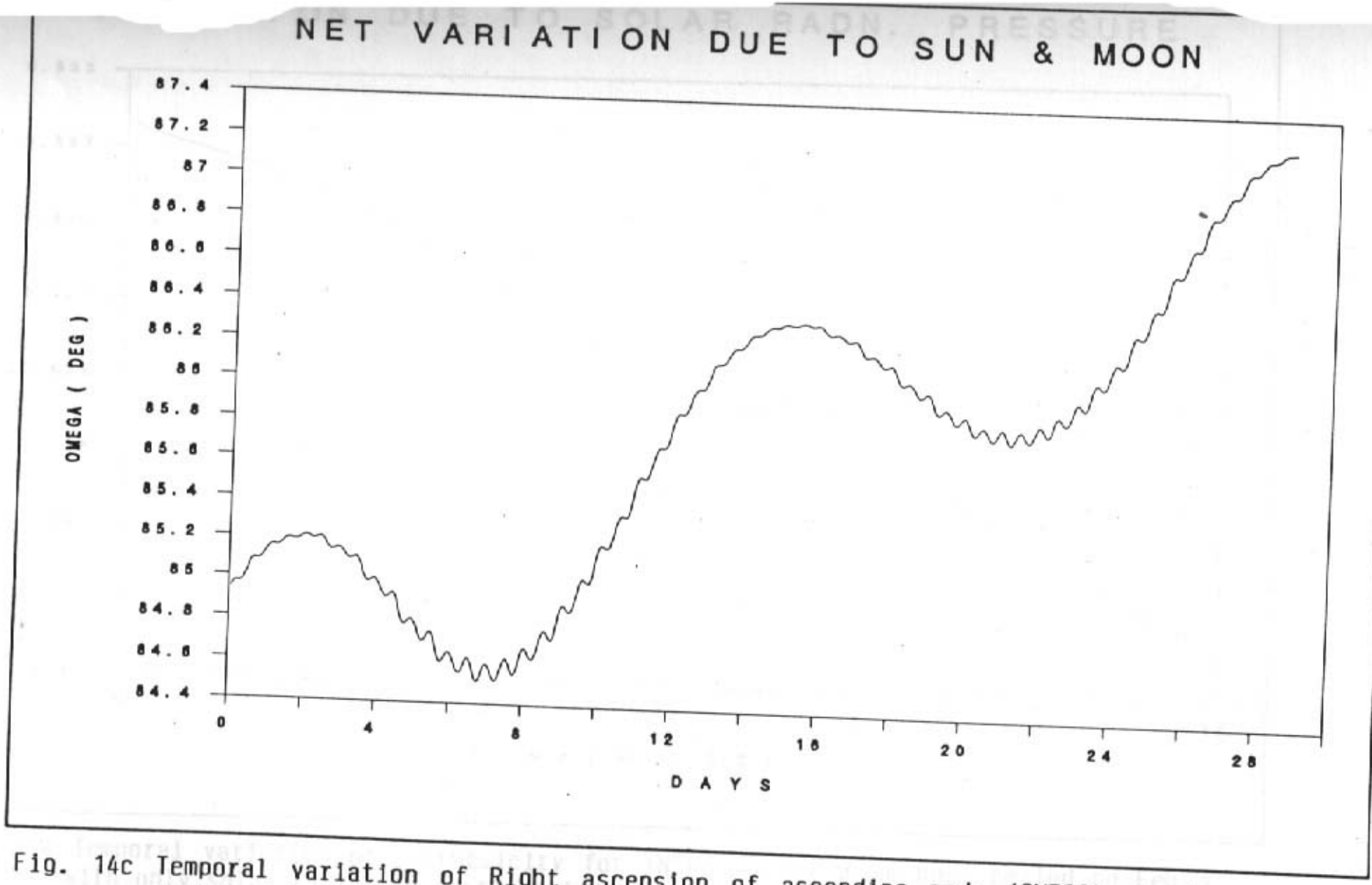

Fig. 14c Temporal variation of Right ascension of ascending node (OMEGA) due to combined luni-solar effect for the period Jan 29 through Feb 26.

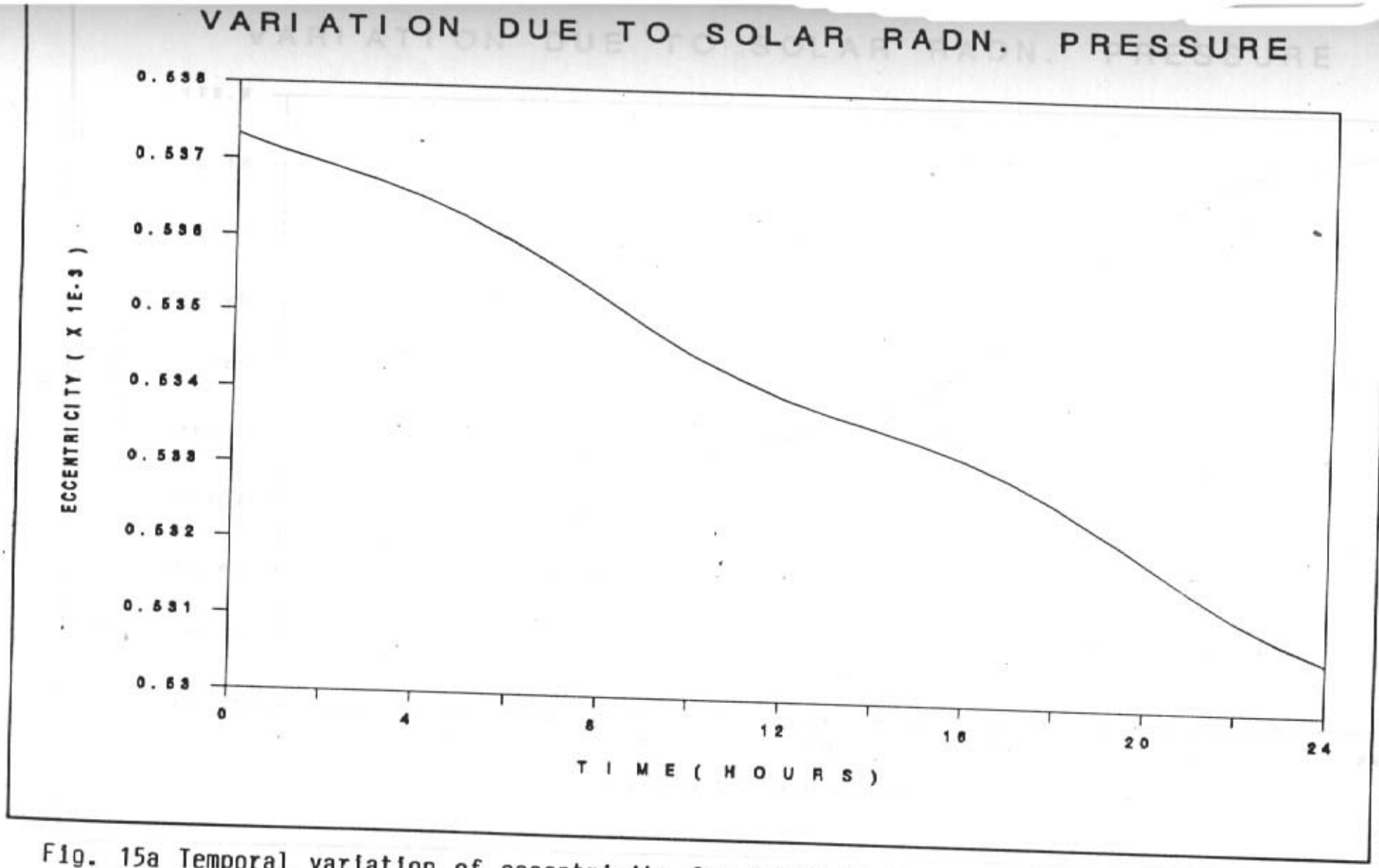

Fig. 15a Temporal variation of eccentricity for INSAT 1B for a 24 hour period on Feb 3 with only solar radiation perturbation.

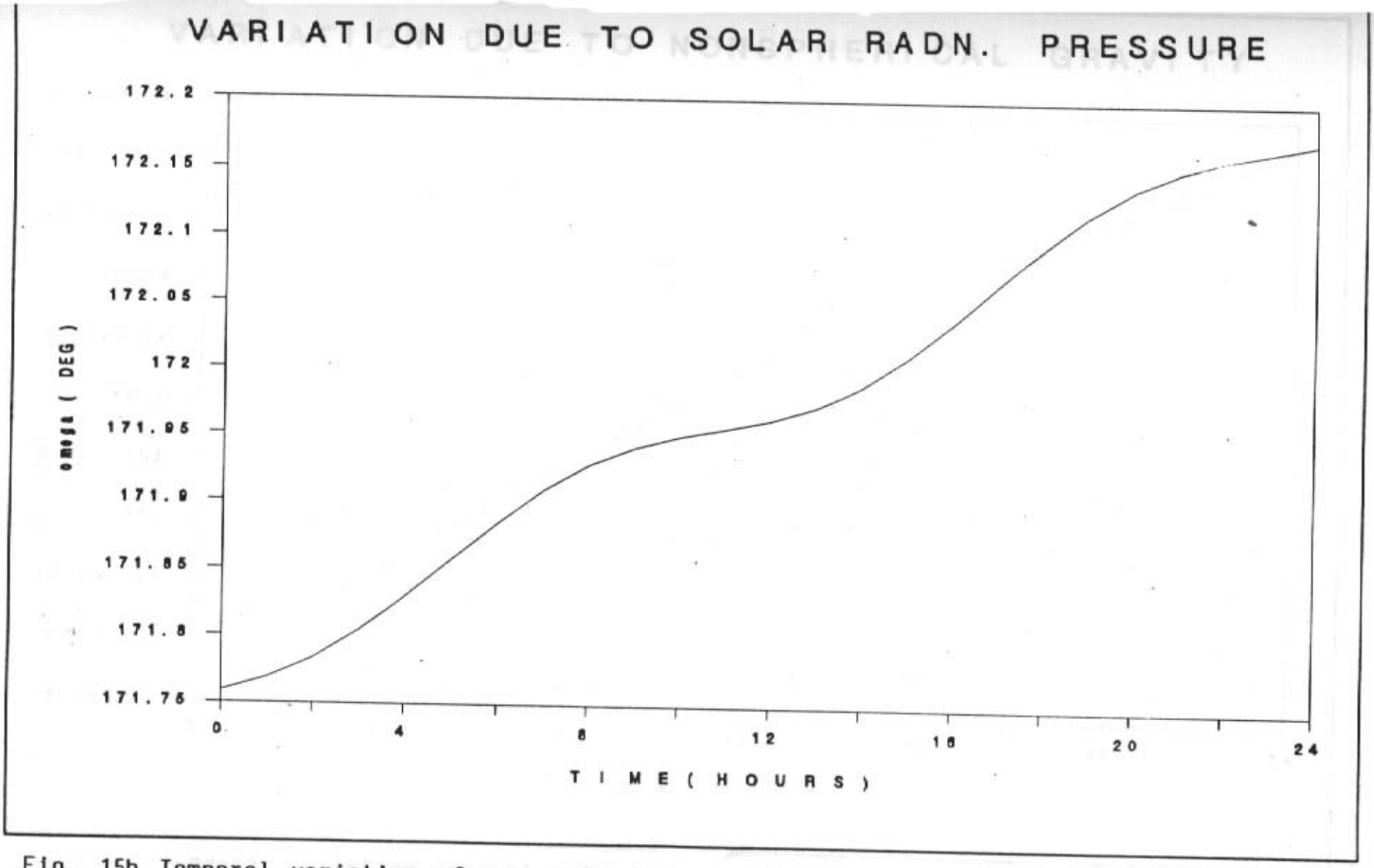

Fig. 15b Temporal variation of argument of perigee (omega) for INSAT 1b for a 24 hour period on Feb 3 with only solar radiation perturbation.

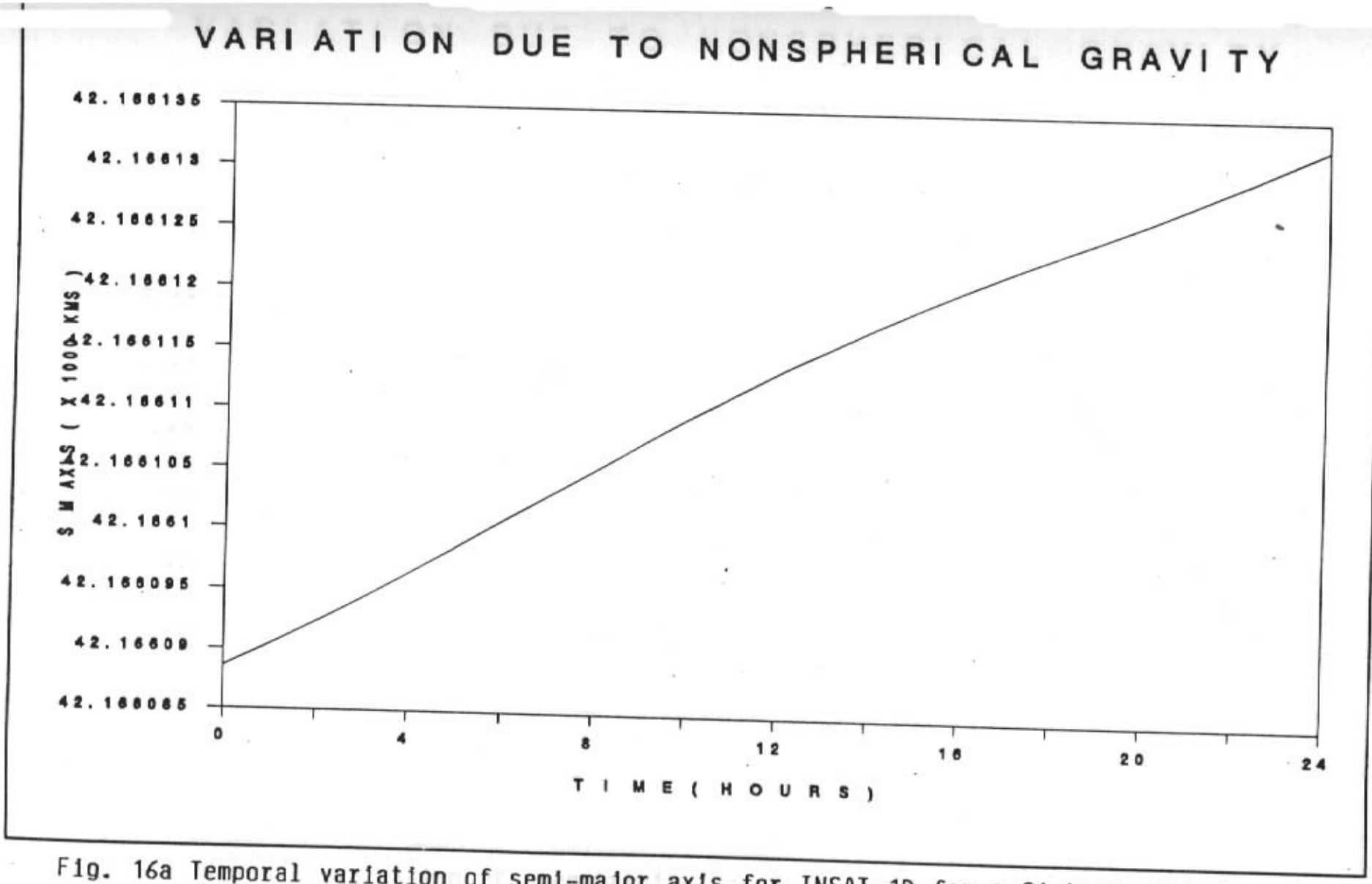

Fig. 16a Temporal variation of semi-major axis for INSAT 1D for a 24 hour period on Sep 23 with only nonspherical gravity effect.

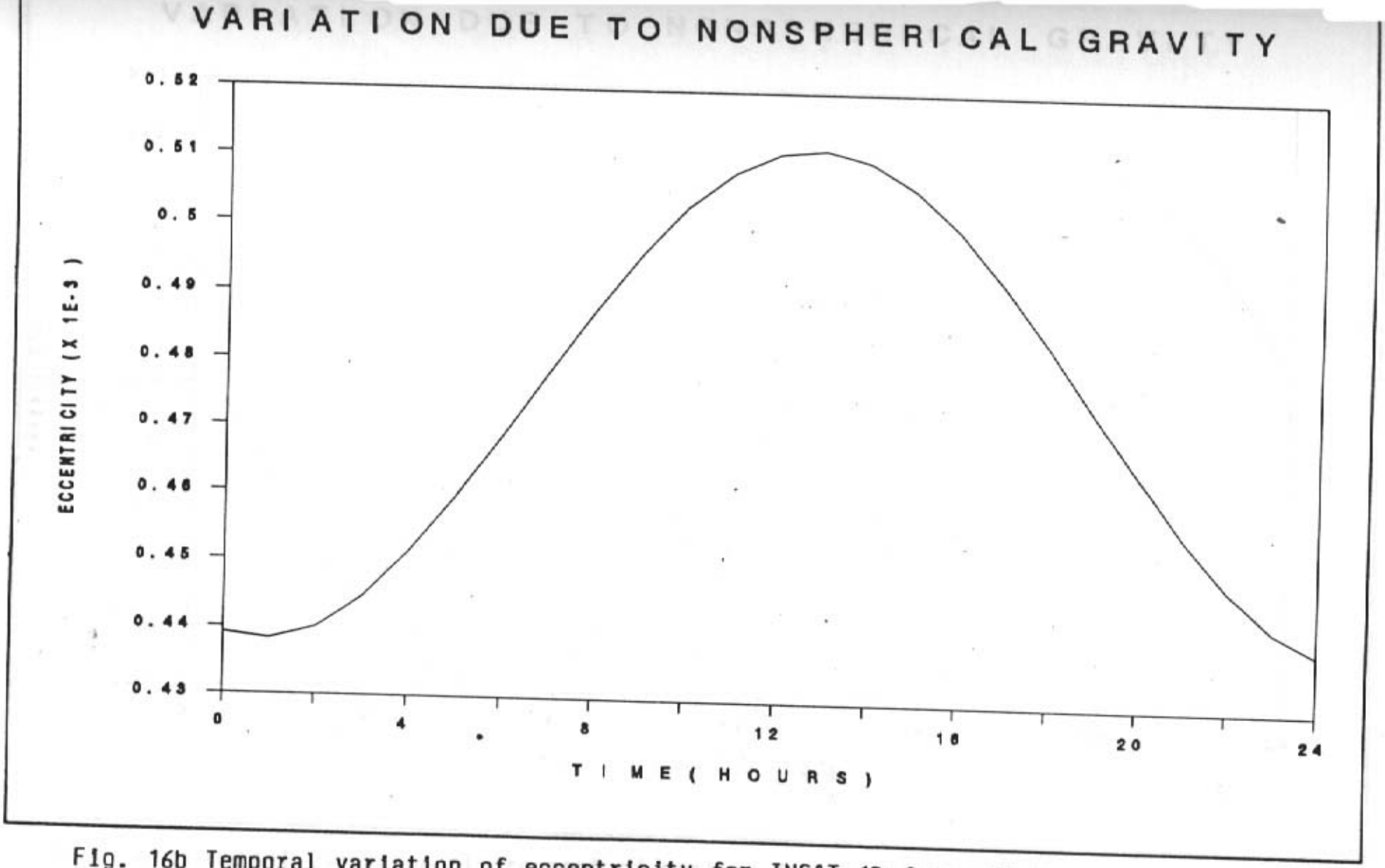

Fig. 16b Temporal variation of eccentricity for INSAT 1D for a 24 hour period on Sep 23 with only nonspherical gravity effect.

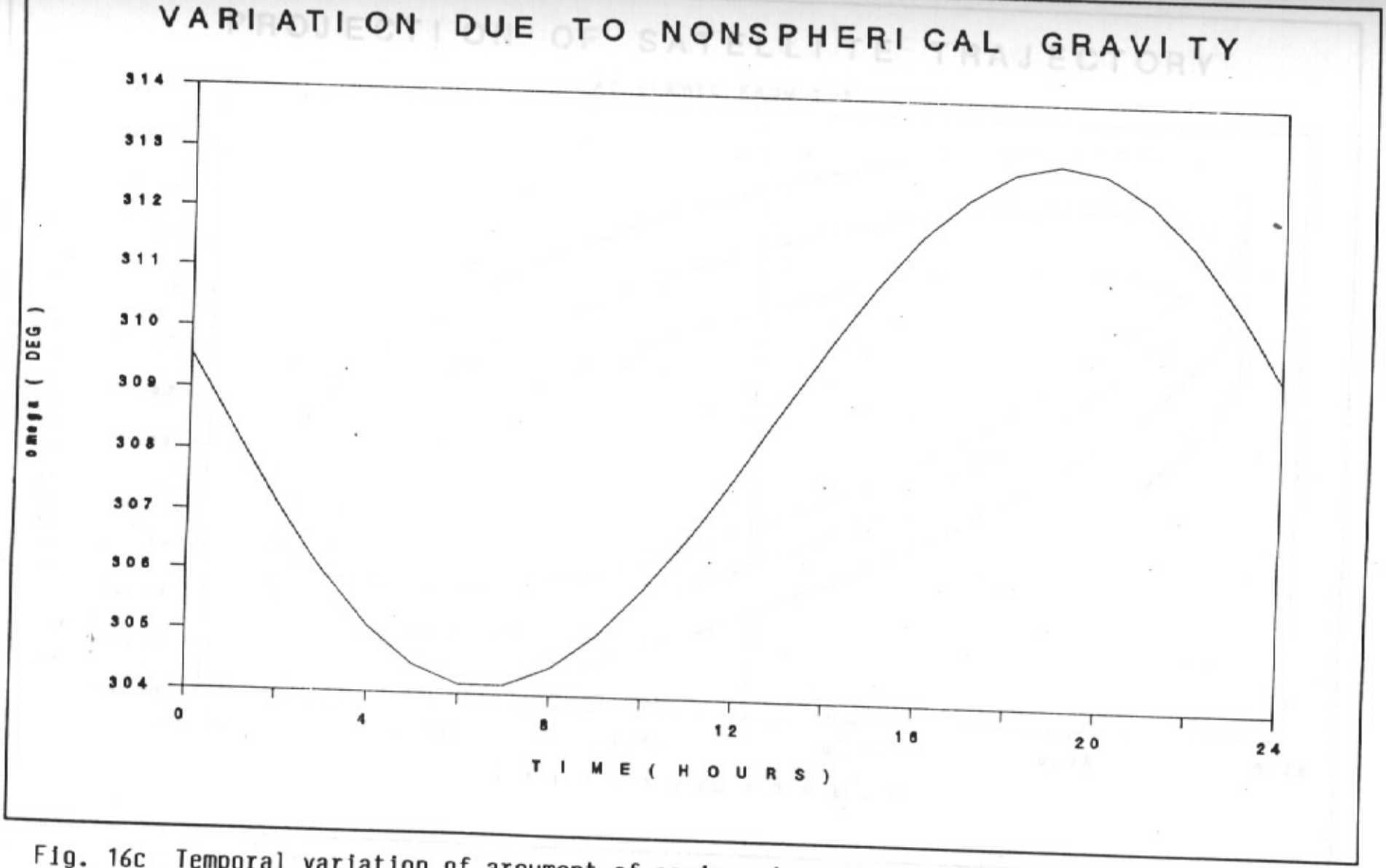

Fig. 16c Temporal variation of argument of perigee (omega) for INSAT 1D for a 24 hour period on Sep 23 with only nonspherical gravity effect.

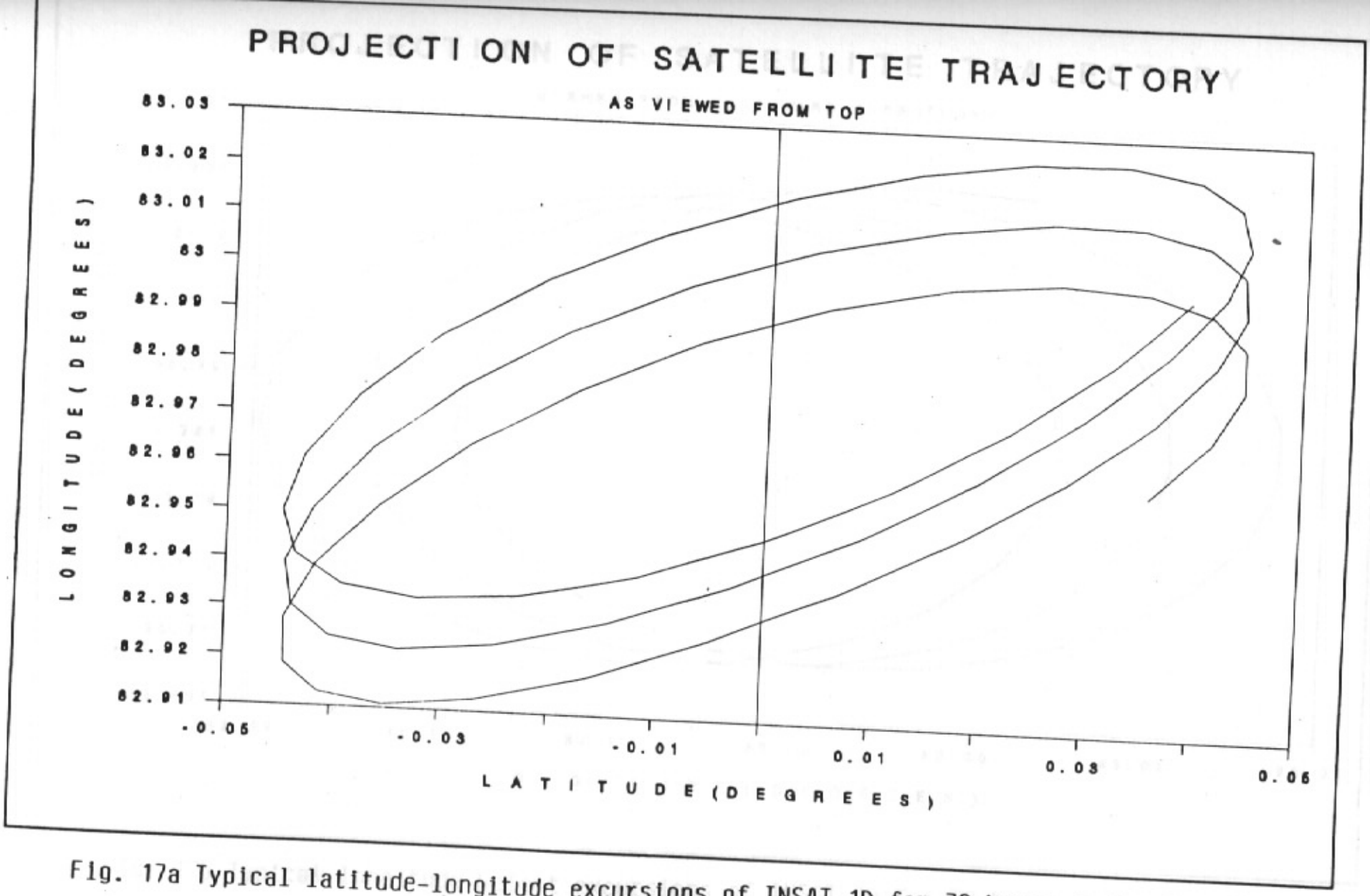

Fig. 17a Typical latitude-longitude excursions of INSAT 1D for 72 hours during Sep 23-25.

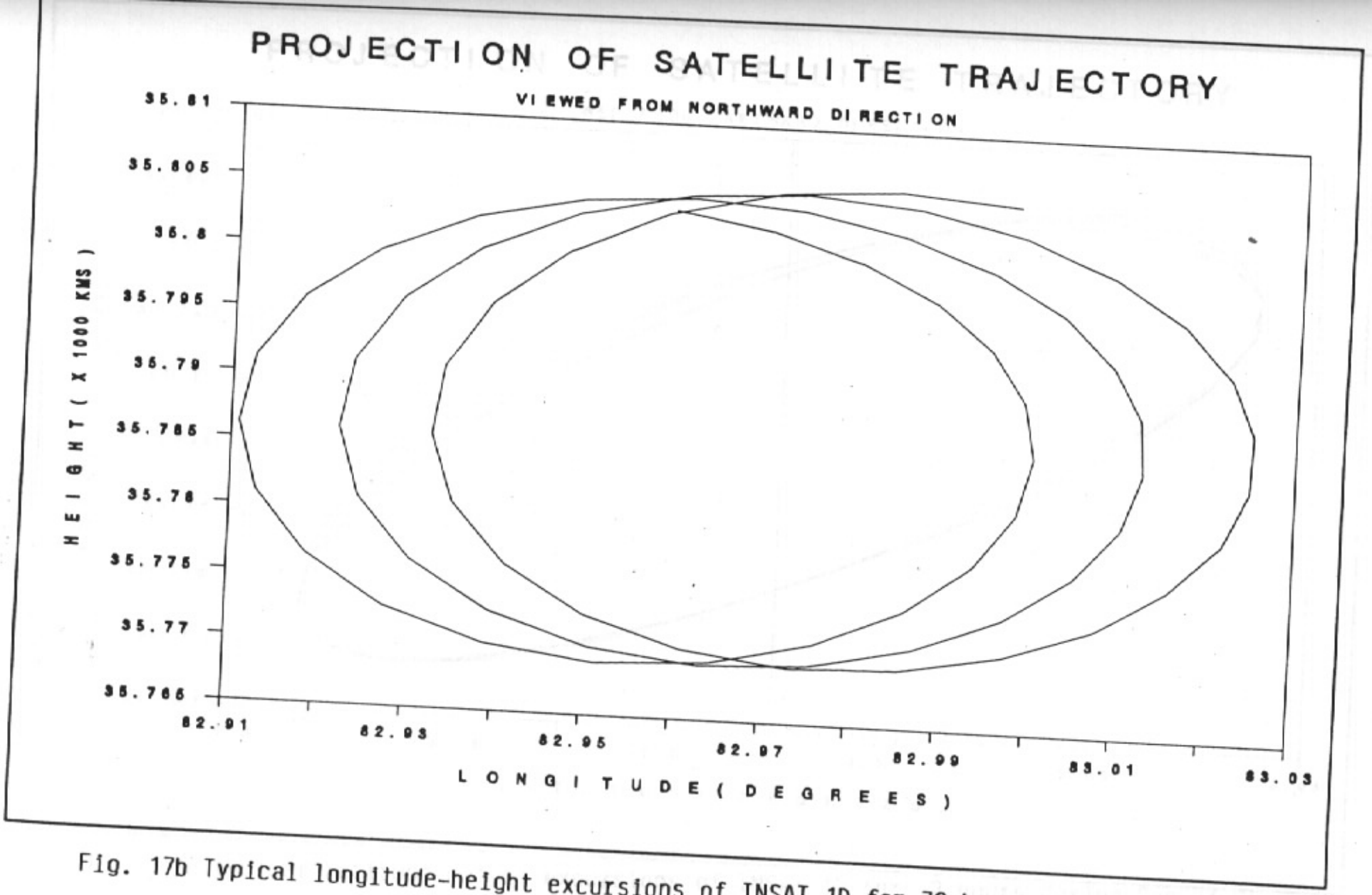

Fig. 17b Typical longitude-height excursions of INSAT 1D for 72 hours during Sep 23-25.

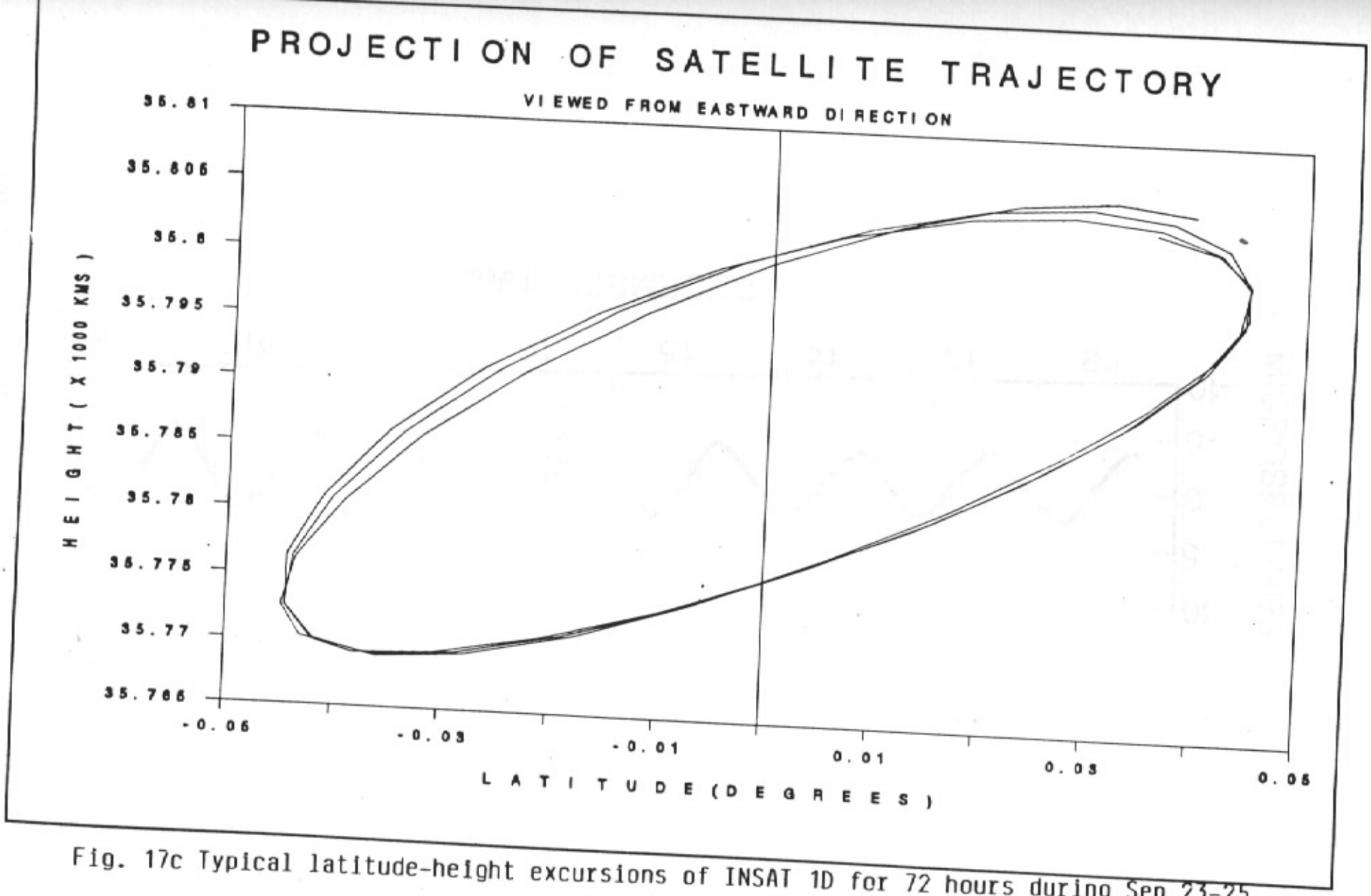

Fig. 17c Typical latitude-height excursions of INSAT 1D for 72 hours during Sep 23-25.

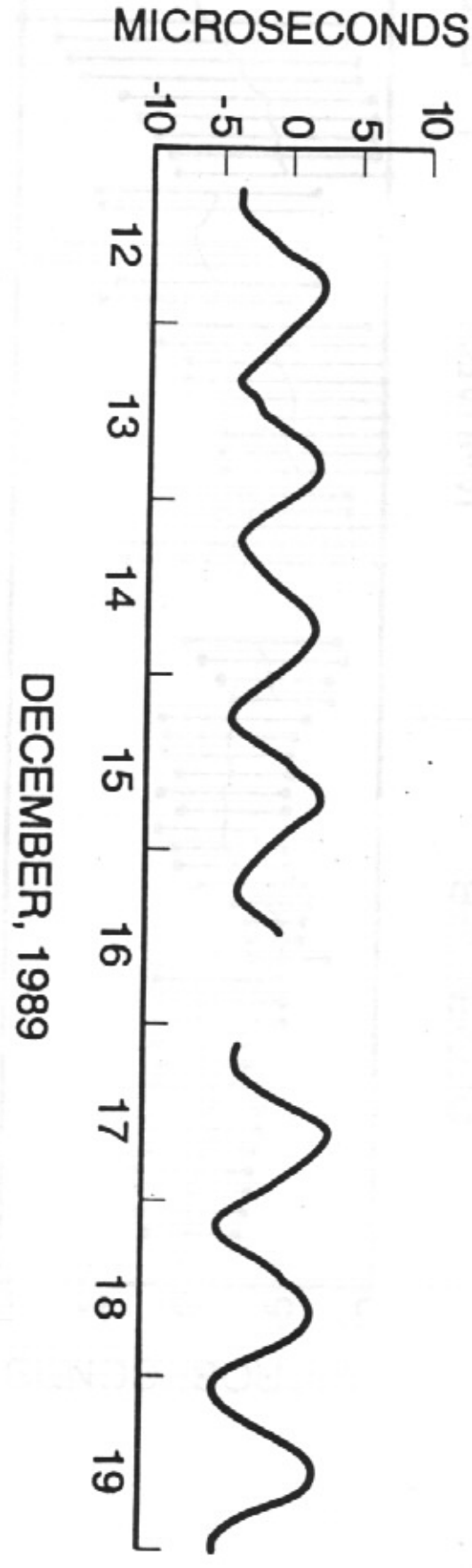

Fig. 18 UTC(NPL)-INSAT 1B residuals: data for Dec 12-19, 1989.

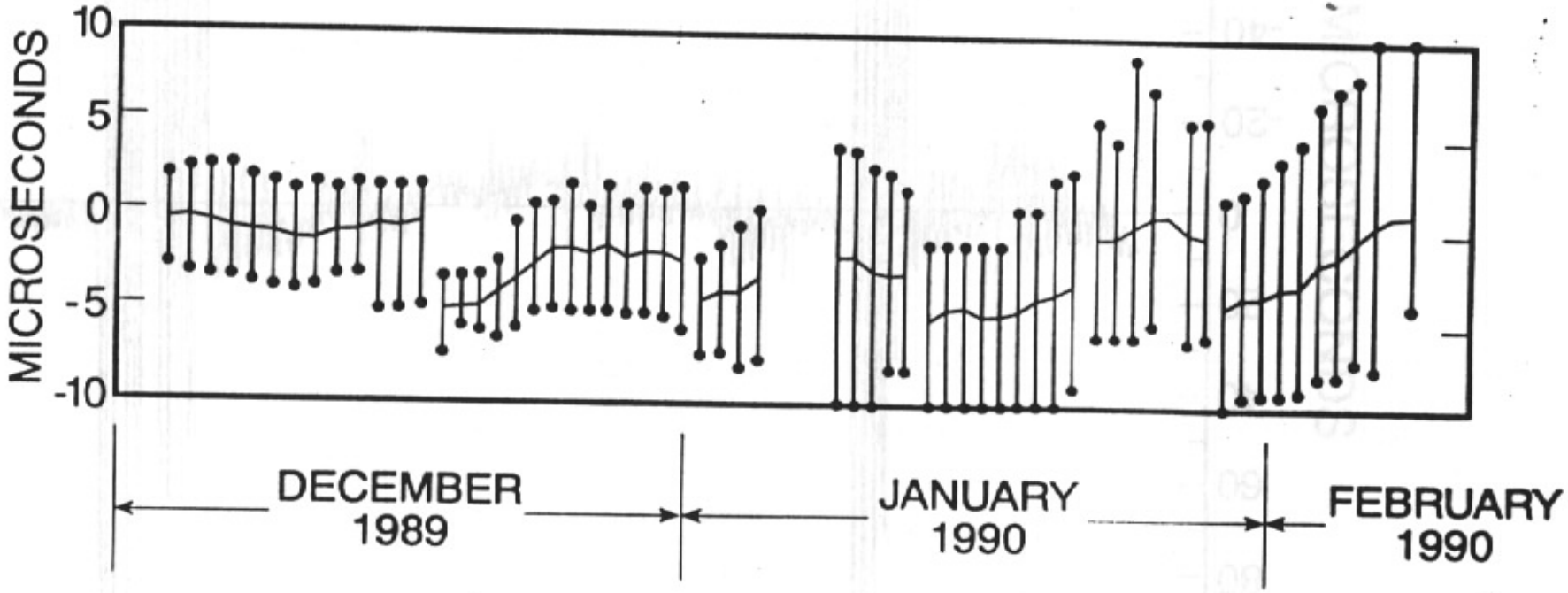

Fig. 19 UTC (NPL)-INSAT 1B residuals: data for Dec,89 - Feb, 90.

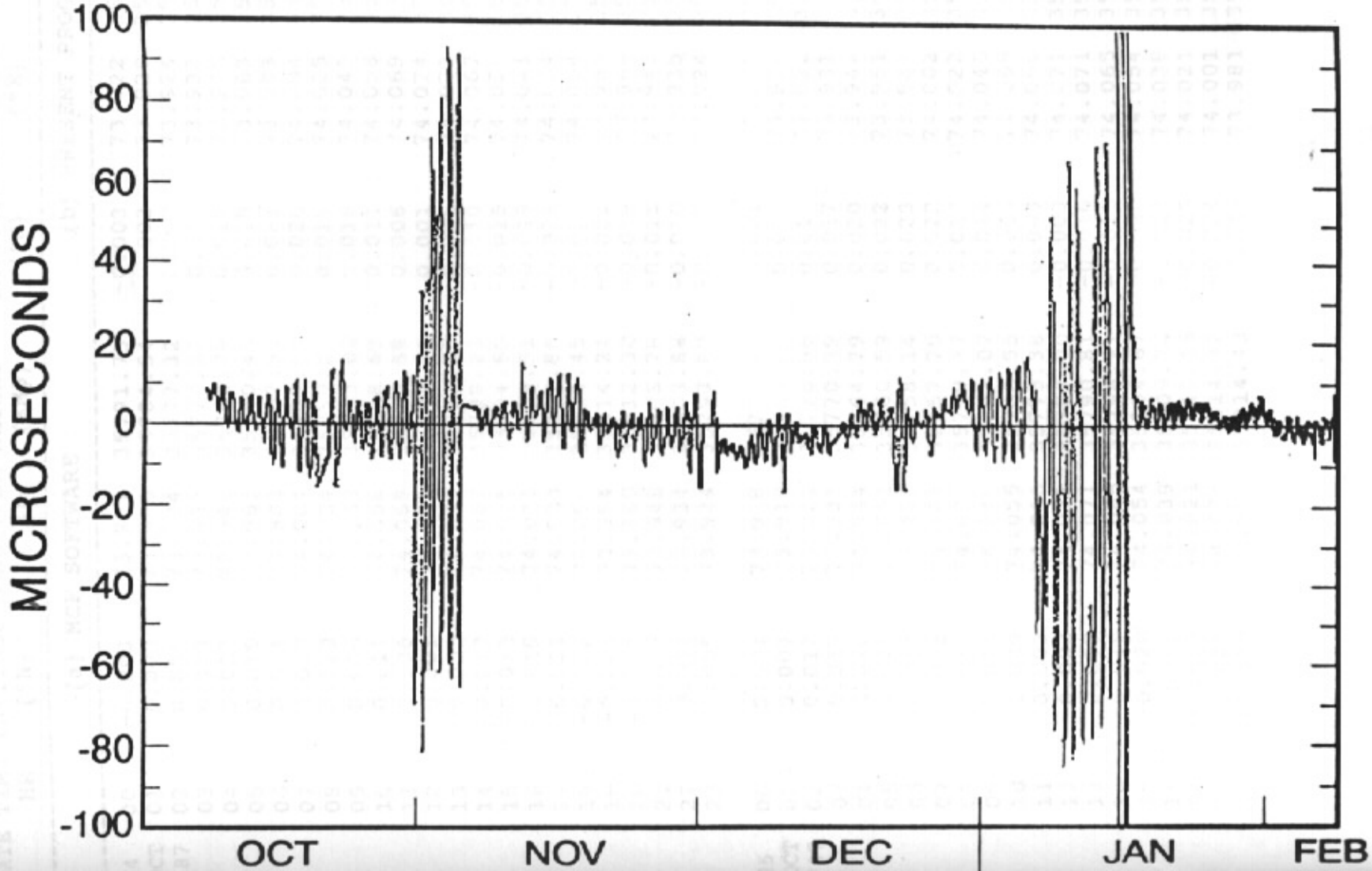
MICROSECONDS
100
80
60
40
20
0
-20
-40
-60
-80
-100
OCT
NOV
DEC
JAN
FEB

TABLE 1 Predicted positions of INSAT 1B using (a) the MCF software; (b) the present program for the period Oct 24 - 27, 1987.

DATE	TIME HR	(a) MCF SOFTWARE LATITUDE (°N)	LONGITUDE (°E)	HEIGHT (KMS)	(b) PRESENT PROGRAM LATITUDE (°N)	LONGITUDE (°E)	HEIGHT (KMS)
24 OCT 87	00	-0.003	73.921	35791.73	-0.003	73.922	35791.74
	01	0.003	73.920	35784.54	0.003	73.920	35784.55
	02	0.008	73.924	35777.32	0.008	73.924	35777.33
	03	0.013	73.933	35770.57	0.013	73.933	35770.57
	04	0.017	73.946	35764.79	0.017	73.946	35764.79
	05	0.019	73.963	35760.45	0.019	73.963	35760.43
	06	0.021	73.983	35757.93	0.021	73.983	35757.91
	07	0.020	74.004	35757.50	0.020	74.004	35757.48
	08	0.019	74.024	35759.27	0.019	74.025	35759.23
	09	0.016	74.043	35763.09	0.016	74.043	35763.07
	10	0.011	74.058	35768.69	0.011	74.058	35768.66
	11	0.006	74.068	35775.59	0.006	74.069	35775.56
	12	0.001	74.073	35783.21	0.001	74.074	35783.19
	13	-0.005	74.073	35790.95	-0.005	74.073	35790.93
	14	-0.010	74.067	35798.23	-0.010	74.067	35798.21
	15	-0.015	74.056	35804.55	-0.015	74.056	35804.54
	16	-0.019	74.041	35809.51	-0.019	74.041	35809.50
	17	-0.021	74.023	35812.86	-0.021	74.024	35812.86
	18	-0.022	74.004	35814.45	-0.022	74.004	35814.45
	19	-0.021	73.984	35814.24	-0.021	73.985	35814.24
	20	-0.019	73.965	35812.30	-0.019	73.966	35812.30
	21	-0.015	73.948	35808.78	-0.015	73.949	35808.78
	22	-0.010	73.934	35803.88	-0.010	73.935	35803.88
	23	-0.005	73.924	35797.89	-0.005	73.924	35797.89
25 OCT 87	00	0.001	73.918	35791.15	0.001	73.919	35791.14
	01	0.007	73.918	35784.02	0.007	73.918	35784.01
	02	0.012	73.922	35776.96	0.012	73.922	35776.94
	03	0.017	73.931	35770.39	0.017	73.931	35770.37
	04	0.020	73.944	35764.79	0.020	73.944	35764.77
	05	0.022	73.961	35760.59	0.022	73.961	35760.57
	06	0.023	73.981	35758.14	0.023	73.981	35758.12
	07	0.022	74.001	35757.70	0.022	74.002	35757.68
	08	0.019	74.022	35759.37	0.019	74.022	35759.35
	09	0.014	74.040	35763.07	0.014	74.040	35763.06
	10	0.009	74.055	35760.55	0.009	74.055	35768.54
	11	0.003	74.066	35775.38	0.003	74.066	35775.37
	12	-0.003	74.071	35783.00	-0.003	74.071	35783.00
	13	-0.009	74.071	35790.81	-0.010	74.071	35790.82
	14	-0.015	74.065	35798.21	-0.015	74.065	35798.22
	15	-0.020	74.054	35804.67	-0.020	74.054	35804.67
	16	-0.023	74.039	35809.74	-0.023	74.039	35809.75
	17	-0.024	74.021	35813.15	-0.025	74.021	35813.16
	18	-0.024	74.001	35814.72	-0.024	74.001	35814.73
	19	-0.022	73.982	35814.43	-0.023	73.981	35814.43

DATE	TIME HR	LATITUDE (°N)	LONGITUDE (°E)	HEIGHT (KMS)	LATITUDE (°N)	LONGITUDE (°E)	HEIGHT (KMS)
		(a) MCF SOFTWARE			(b) PRESENT PROGRAM		
	20	-0.019	73.962	35812.34	-0.019	73.962	35812.34
	21	-0.014	73.946	35808.64	-0.014	73.945	35808.63
	22	-0.008	73.932	35803.59	-0.008	73.932	35803.56
	23	-0.002	73.922	35797.45	-0.002	73.922	35797.43
26	00	0.005	73.916	35790.64	0.005	73.916	35790.62
OCT	01	0.011	73.916	35783.54	0.012	73.916	35783.51
'87	02	0.017	73.921	35776.58	0.017	73.920	35776.54
	03	0.022	73.930	35770.18	0.022	73.930	35770.15
	04	0.025	73.943	35764.78	0.025	73.943	35764.75
	05	0.026	73.960	35760.76	0.026	73.960	35760.73
	06	0.026	73.980	35758.44	0.026	73.979	35758.41
	07	0.024	74.000	35758.04	0.024	74.000	35758.02
	08	0.019	74.020	35759.65	0.020	74.020	35759.65
	09	0.014	74.038	35763.23	0.014	74.038	35763.23
	10	0.008	74.053	35768.54	0.008	74.053	35768.55
	11	0.000	74.064	35775.21	0.000	74.064	35775.23
	12	-0.007	74.069	35782.74	-0.007	74.069	35782.76
	13	-0.014	74.069	35790.54	-0.014	74.069	35790.56
	14	-0.020	74.064	35798.00	-0.020	74.063	35798.03
	15	-0.025	74.053	35804.57	-0.025	74.053	35804.59
	16	-0.028	74.038	35809.78	-0.028	74.038	35809.80
	17	-0.029	74.020	35813.29	-0.029	74.019	35813.32
	18	-0.028	74.000	35814.93	-0.028	74.000	35814.95
	19	-0.025	73.980	35814.63	-0.025	73.979	35814.63
	20	-0.020	73.961	35812.48	-0.020	73.960	35812.46
	21	-0.014	73.944	35808.64	-0.014	73.943	35808.62
	22	-0.007	73.930	35803.42	-0.007	73.929	35803.39
	23	0.001	73.920	35797.16	0.001	73.920	35797.11
27	00	0.008	73.915	35790.24	0.008	73.915	35790.19
OCT							

APPENDIX - I

```
C     ********************************************
C     PROGRAM TO COMPUTE SATELLITE COORDINATES
C     BY  A. SENGUPTA, N.P.L., NEW DELHI
C     ********************************************
C     THE INPUT PARAMETERS ARE STORED IN A FILE CALLED 'SAT.DAT'
C               IN THE FOLLOWING FORM
C     ********************************************
C      DD MM YY         DAY,MONTH,YEAR OF THE EPOCH DATE (FORMAT 3I3)
C      HH MM SS.SS      HOUR,MIN SEC OF THE EPOCH TIME (FORMAT 2I3,F6.2)
C      DS MS YS         DAY,MONTH,YEAR OF THE PRINTOUT START (FORMAT 3I3)
C      DC               NUMBER OF DAYS TO COMPUTE & PRINT (FORMAT I3)
C     AAAAA.AAAAAAAA    SEMIMAJOR AXIS (FORMAT  F14.8)
C          .EEEEEEEE    ECCENTRICITY (FORMAT F14.8)
C          .IIIIIIII    INCLINATION (FORMAT F14.8)
C       ΩΩΩ.ΩΩΩΩΩΩΩΩ   RT. ASCEN. OF ASCENDING NODE Ω (FORMAT F14.8)
C       ωωω.ωωωωωωωω   ARGUMENT OF PERIGEE ω (FORMAT F14.8)
C       MMM.MMMMMMMM   MEAN ANOMALY (FORMAT F14.8)
C     S.LR D-PP        EFFECTIVE CROSS SECTION/MASS m2/KG (FORMAT D9.3)
C     ********************************************
C     THE OUTPUT IS PRINTED ON THE MONITOR AS WELL AS STORED IN A
C     FILE CALLED 'RESULT.DAT'. THE PARAMETERS PRINTED OUT ARE
C     MJD, HOUR, LATITUDE, LONGITUDE, HEIGHT, PROPAGN. DELAY
C     WHERE, PROPAGN. DELAY = TRANSMITTER-SATELLITE-RECEIVER DELAY
C     ********************************************
      IMPLICIT REAL*8(A-H,O-Z)
      DIMENSION C(15,6)
C     THIS PART DEFINES ALL CONSTANTS--------------------
      RPD=3.1415926D0/180.D0
      PI=3.1415926D0
C     NON SPHERICAL GRAVITY COEFFICIENTS
C     THE FOLLOWING ARE C - TERMS
      C(2,1)=-0.108265D-02
      C(2,2)=-0.132673D-08
      C(2,3)=0.1566511D-05
      C(3,1)=0.254503D-05
      C(3,2)=0.2161875D-05
      C(3,3)=0.3172142D-06
      C(3,4)=0.1025055D-06
      C(4,1)=0.167150D-05
      C(4,2)=-0.5052256D-06
      C(4,3)=0.7739965D-07
      C(4,4)=0.5901404D-07
      C(4,5)=-0.3608512D-08
C     THE FOLLOWING ARE S - TERMS
      C(7,1)=0.D0
      C(7,2)=-0.1374346D-07
      C(7,3)=-0.8869932D-06
      C(8,1)=0.D0
      C(8,2)=0.2571596D-06
      C(8,3)=-0.2078203D-06
      C(8,4)=0.1949036D-06
      C(9,1)=0.D0
      C(9,2)=-0.4199062D-06
      C(9,3)=0.1515418D-06
      C(9,4)=-0.1275373D-07
      C(9,5)=0.6386659D-08
C     SUNS PARAMETERS-----------------------------------
      AMUS=1.327D11
      AS=149600000.D0
      ES=0.0167268D0
      AISD=23.440583D0
```

```
      WWS=0.D0
      WOS=281.2208333D0
C     MOONS PARAMETERS-----------------------------------
      AMUM=4.903D3
C     DATE & TIME----------------------------------------
      OPEN(1,FILE='SAT.DAT')
      OPEN(2,FILE='RESULT.DAT')
      READ(1,1)KDAY,KAMTH,KYR
      READ(1,6)KHR,KMNT,SEC
      READ(1,1)KDDAY,KDMTH,KDYR
      READ(1,7)KDC
      DC=KDC
      DAY=KDAY
      AMNTH=KAMTH
      YR=KYR
      HR=KHR
      AMNT=KMNT
      DDAY=KDDAY
      DMNTH=KDMTH
      DYR=KDYR
      READ(1,2)AP
      READ(1,2)EP
      READ(1,2)AIP
      READ(1,2)WWP
      READ(1,2)WP
      READ(1,2)AMP
      READ(1,5)SLRP
      WRITE(*,3)KDAY,KAMTH,KYR
      WRITE(*,8)KHR,KMNT,SEC
      WRITE(*,3)KDDAY,KDMTH,KDYR
      WRITE(*,4)AP
      WRITE(*,4)EP
      WRITE(*,4)AIP
      WRITE(*,4)WWP
      WRITE(*,4)WP
      WRITE(*,4)AMP
      FORMAT(3I3)
      FORMAT(F14.8)
      FORMAT(6X,3I3)
      FORMAT(6X,F15.9)
      FORMAT(D9.3)
      FORMAT(2I3,F6.2)
      FORMAT(I3)
      FORMAT(6X,2I3,F6.2)
      X, Y, Z CO-ORDINATES OF TRANSMITTER AND RECEIVER IN KMS-------
      (TRANSMITTER IS AT DELHI EARTH STATION AND RECEIVER IS AT NPL)
      (FOR OTHER TRANSMITTER, RECEIVER LOCATIONS ENTER CORRESP VALUES)
      TRX=1194.37
      TRY=5481.923
      TRZ=3023.516
      RCX=1243.916
      RCY=5462.553
      RCZ=3038.751
      EARTH(AMU=G.Me IN km3/sec2)------------
      AMU=398601.8D0
      RE=6378.144D0
      GET TIME TO THE PREVIOUS FULL MINUTE UTC-----------
      FMNT=AMNT
      DIFF=SEC/3600.D0
      T=HR+FMNT/60.D0
      AP3=AP**3
      AMP=AMP-130224906.0396D0*DIFF/DSQRT(AP3)
      COMPUTE DAYS SINCE 1 JAN 1900(J.D.-2415020)---------
      AA=0.51D0+1.D0/AMNTH
```

```
      I1=AA
      Y1=YR-I1
      AM1=AMNTH+(I1*12.D0)-3.D0
      AY=365.25D0*Y1
      I2=AY
      AM2=30.6D0*AM1+0.41D0
      I3=AM2
      D=I2+I3+DAY+58,5D0
C     COMPUTE MJD FOR EPOCH ----------
      IDAY=DAY
      MJD=I2+I3+IDAY-24922
C     COMPUTE MJD FOR DATA STARTING DAY -------
      DA=0.51D0+1.D0/DMNTH
      J1=DA
      DY1=DYR-J1
      DM1=DMNTH+(J1*12.D0)-3.D0
      DY=365.25D0*DY1
      J2=DY
      DM2=30.6D0*DM1+0.41D0
      J3=DM2
      JDAY=DDAY
      JDSTRT=J2+J3+JDAY-24922
      KEND=JDSTRT+DC
C     COMPUTE SATELLITE COORDINATES IN INERTIAL FRAME RX,RY,RZ---
      AIP=AIP*RPD
      AMP=AMP*RPD
      WWP=WWP*RPD
      WP=WP*RPD
9     TE=(D+T/24.D0)/36525.D0
C     EAP IS THE ECCENTRIC ANOMALY  (M=E-e.SIN(E) )-------
      AMP2=2.D0*AMP
      AMP3=3.D0*AMP
      AMP4=4.D0*AMP
      AMP5=5.D0*AMP
      EAP=AMP+(EP-(EP**3)/8.D0+(EP**5)/192.D0)*DSIN(AMP)+((EP**2)/2.D0-(
     1EP**4)/6.D0)*DSIN(AMP2)+((EP**3)/2.666D0-(EP**5)/4.7407D0)*DSIN(AM
     2P3)+(EP**4)*DSIN(AMP4)/3.D0+(EP**5)*DSIN(AMP5)/3D0
      DC = DCOS(AIP)
      DS = DSIN(AIP)
      DCS= DSIN(WP)
      DCC= DCOS(WP)
      ECC= DCOS(WWP)
      ECS= DSIN(WWP)
     .R11= ECC*DCC-DC*ECS*DCS
      R21=-ECC*DCS-ECS*DC*DCC
      R12= ECS*DCC+ECC*DC*DCS
      R22=-ECS*DCS+ECC*DC*DCC
      R13=DS*DCS
      R23=DS*DCC
      CEP=DCOS(EAP)-EP
      EP1=1.D0-EP*EP
      SEP=DSIN(EAP)*DSQRT(EP1)
      RX=AP*(CEP*R11+SEP*R21)
      RY=AP*(CEP*R12+SEP*R22)
      RZ=AP*(CEP*R13+SEP*R23)
      COMPUTE SATELLITE VELOCITY COORDINATES VX,VY,VZ-----
      AMUP=AMU/AP
      VO=DSQRT(AMUP)/(1.D0-EP*DCOS(EAP))
      SEV=DSIN(EAP)
      CEV=DCOS(EAP)*DSQRT(EP1)
      VX=VO*(-SEV*R11+CEV*R21)
      VY=VO*(-SEV*R12+CEV*R22)
      VZ=VO*(-SEV*R13+CEV*R23)
      COMPUTE SATELLITE COORDINATES RXE,RYE,RZE IN EARTH ROTATING FRAME
```

```
      PHID=99.69098D0+0.985647335D0*D+15.041068639D0*T
      PHI=PHID*RPD
      CPHI=DCOS(PHI)
      SPHI=DSIN(PHI)
      RXE=(RX*CPHI+RY*SPHI)
      RYE=(-RX*SPHI+RY*CPHI)
      RZE=RZ
C     COMPUTE SATELLITE LAT.,LONG. AND HEIGHT -------
      RYX=RYE/RXE
      IF(RYE.LT.0.D0)GO TO 303
      IF(RXE.LT.0.D0)GO TO 302
301   SLOR=DATAN(RYX)
      GO TO 304
302   SLOR=DATAN(RYX)+PI
      GO TO 304
303   IF(RXE.GT.0.D0) GO TO 301
      SLOR=DATAN(RYX)-PI
304   SLON=SLOR/RPD
      DXY2=RXE*RXE+RYE*RYE
      DXY=DSQRT(DXY2)
      RZD=RZE/DXY
      SLAR=DATAN(RZD)
      SLAT=SLAR/RPD
      DRE2=DXY2+RZE*RZE
      HITE=DSQRT(DRE2)-RE
      DRE=DSQRT(DRE2)
C     COMPUTATION OF LEGENDRE POLYNOMIALS C(N+10,M)
      C(10,1)=1.D0
      C(11,1)=DSIN(SLAR)
      C(11,2)=DCOS(SLAR)
      DO 200 N=2,4
      AN=N
      M=1
      AN21=2.D0*AN-1.D0
      N1=N-1
      AN1=N1
      N2=N-2
      C(N+10,1)=(AN21*DSIN(SLAR)*C(N1+10,1)-AN1*C(N2+10,1))/AN
      C(N+10,N+1)=AN21*DCOS(SLAR)*C(N1+10,N1+1)
40    IF(N1.EQ.M)GO TO 50
      C(N+10,M+1)=C(N2+10,M+1)+(2.D0*AN-1.D0)*DCOS(SLAR)*C(N+9,M)
      GO TO 60
50    C(N+10,M+1)=(2.D0*AN-1.D0)*DCOS(SLAR)*C(N1+10,M)
60    M=M+1
      IF(M.LT.N)GO TO 40
200   CONTINUE
      DO 99 I=2,4
99    C(I+10,I+2)=0.D0
C     COMPUTATION OF NONSPHERICAL GRAVITY ACCELERATIONS
101   PLON=0.D0
      PRAD=0.D0
      PLAT=0.D0
      DO 102 N=2,4
      PLN1=0.D0
      PRD1=0.D0
      PLA1=0.D0
      DO 202 M=1,N+1
      AM=M
      SLRM=(AM-1.D0)*SLOR
      DPL1=C(N+5,M)*DCOS(SLRM)-C(N,M)*DSIN(SLRM)
      DPR1=C(N,M)*DCOS(SLRM)+C(N+5,M)*DSIN(SLRM)
      PLN1=PLN1+DPL1*(AM-1.D0)*C(N+10,M)
      PRD1=PRD1+DPR1*C(N+10,M)
202   PLA1=PLA1+DPR1*(C(N+10,M+1)-(AM-1.D0)*DTAN(SLAR)*C(N+10,M))
```

```
      AN=N
      DPLN=((RE/DRE)**AN)*AMU*PLN1/(DRE*DRE)
      DPRD=-((RE/DRE)**AN)*AMU*PRD1*(AN+1.D0)/(DRE*DRE)
      DPAL=((RE/DRE)**AN)*AMU*PLA1/(DRE*DRE)
      PLON=PLON+DPLN
      PRAD=PRAD+DPRD
02    PLAT=PLAT+DPAL
      IF(MJD.LT.JDSTRT)GO TO 10
      IF(KMNT.NE.0)GO TO 10
      DELU=DSQRT((RXE-TRX)**2+(RYE-TRY)**2+(RZE-TRZ)**2)
      DELD=DSQRT((RXE-RCX)**2+(RYE-RCY)**2+(RZE-RCZ)**2)
      DELAY=(DELU+DELD)/299.7925D0+0.025D0
      AIPD=AIP/RPD
      WWPD=WWP/RPD
      WPD=WP/RPD
      WRITE(*,11)MJD,KHR,SLAT,SLON,HITE,DELAY
      WRITE(2,11)MJD,KHR,SLAT,SLON,HITE,DELAY
1     FORMAT(2X,2I4,4F15.4)
      COMPUTE SUN'S COORDINATES SX,SY,SZ-----------------
0     AIS=AISD*RPD
      WS=(WOS+1.719175D0*TE+0.004527778D0*TE*TE)*RPD
      AMS=0.985600267*(D+T/24.D0-32509.671D0)*RPD
      EAS IS ECCENTRIC ANOMALY OF THE SUN----------------
      EAS=AMS+(ES-(ES**3)/8D0+(ES**5)/192.D0)*DSIN(AMS)+((ES**2)/2D0-(ES
     1**4)/6D0)*DSIN(2.D0*AMS)+((ES**3)/2.66D0-(ES**5)/4.74D0)*DSIN(3.D0
     2*AMS)+(ES**4)*DSIN(4.D0*AMS)/3.D0+(ES**5)*DSIN(5.D0*AMS)/3.1D0
      S11=DCOS(WS)
      S12=DSIN(WS)
      CAIS=DCOS(AIS)
      SAIS=DSIN(AIS)
      S21=CAIS*S12
      S22=-CAIS*S11
      S31=SAIS*S12
      S32=SAIS*S11
      CES=DCOS(EAS)-ES
      SES=DSIN(EAS)*DSQRT(1.D0-ES*ES)
      SX=AS*(CES*S11-SES*S12)
      SY=AS*(CES*S21-SES*S22)
      SZ=AS*(CES*S31+SES*S32)
      COMPUTE MOON'S COORDINATES XM,YM,ZM-----------------
      TEM=TE-1.D0
      ECLIPTIC LONGITUDE OF THE MOON----------------------
      AL0=218.32D0+481267.883D0*TEM
      AL1=6.29D0*DSIN((134.9D0+477198.85D0*TEM)*RPD)
      AL2=1.27D0*DSIN((259.2D0-413335.38D0*TEM)*RPD)
      AL3=0.66D0*DSIN((235.7D0+890534.23D0*TEM)*RPD)
      AL4=0.21D0*DSIN((269.9D0+954397.70D0*TEM)*RPD)
      AL5=0.19D0*DSIN((357.5D0+35999.05D0*TEM)*RPD)
      AL6=0.11D0*DSIN((186.6D0+966404.05D0*TEM)*RPD)
      AL=(AL0+AL1-AL2+AL3+AL4-AL5-AL6)*RPD
      ECLIPTIC LATITUDE OF THE MOON-----------------------
      BE1=5.13D0*DSIN((93.3D0+483202.03D0*TEM)*RPD)
      BE2=0.28D0*DSIN((228.2D0+960400.87D0*TEM)*RPD)
      BE3=0.28D0*DSIN((318.3D0+6003.18D0*TEM)*RPD)
      BE4=0.17D0*DSIN((217.6D0-407332.2D0*TEM)*RPD)
      BE=(BE1+BE2-BE3-BE4)*RPD
      HORIZONTAL PARALLAX OF THE MOON---------------------
      PA1=0.0518D0*DCOS((134.9D0+477198.85D0*TEM)*RPD)
      PA2=0.0095D0*DCOS((259.2D0-413335.38D0*TEM)*RPD)
      PA3=0.0078D0*DCOS((235.7D0+890534.23D0*TEM)*RPD)
      PA4=0.0028D0*DCOS((269.9D0+954397.70D0*TEM)*RPD)
      PA=(0.9508D0+PA1+PA2+PA3+PA4)*RPD
      DISTANCE TO THE MOON--------------------------------
      RM=6378.144D0/DSIN(PA)
```

```
C      LUNAR CO-ORDINATES
       XM=RM*(DCOS(BE)*DCOS(AL))
       YM=RM*(CAIS*DCOS(BE)*DSIN(AL)-SAIS*DSIN(BE))
       ZM=RM*(SAIS*DCOS(BE)*DSIN(AL)+CAIS*DSIN(BE))
C      COMPUTE PERTURBATION ACCELERATIONS-----------------
C      (A) DUE TO THE SUN--------------------------------
       DSS=DSQRT((SX-RX)*(SX-RX)+(SY-RY)*(SY-RY)+(SZ-RZ)*(SZ-RZ))
       DS=DSQRT(SX*SX+SY*SY+SZ*SZ)
       PSX=AMUS*((SX-RX)/(DSS*DSS*DSS)-SX/(DS*DS*DS))
       PSY=AMUS*((SY-RY)/(DSS*DSS*DSS)-SY/(DS*DS*DS))
       PSZ=AMUS*((SZ-RZ)/(DSS*DSS*DSS)-SZ/(DS*DS*DS))
C      (B) DUE TO THE MOON-------------------------------
       DMS=DSQRT((XM-RX)*(XM-RX)+(YM-RY)*(YM-RY)+(ZM-RZ)*(ZM-RZ))
       DM=DSQRT(XM*XM+YM*YM+ZM*ZM)
       PMX=AMUM*((XM-RX)/(DMS*DMS*DMS)-XM/(DM*DM*DM))
       PMY=AMUM*((YM-RY)/(DMS*DMS*DMS)-YM/(DM*DM*DM))
       PMZ=AMUM*((ZM-RZ)/(DMS*DMS*DMS)-ZM/(DM*DM*DM))
C      (C)RADIAL & NORTHWARD COMPONENTS DUE TO NONSPHERICAL EARTH POTENTIAL
       DSAT=DSQRT(RX*RX+RY*RY+RZ*RZ)
       PZX=(PRAD*DCOS(SLAR)+PLAT*DSIN(SLAR))*RX/DSAT
       PZY=(PRAD*DCOS(SLAR)+PLAT*DSIN(SLAR))*RY/DSAT
       PZZ=PRAD*DSIN(SLAR)+PLAT*DCOS(SLAR)
C      (D)TANGENTIAL COMPONENT DUE TO NONSPHERICAL EARTH POTENTIAL
       PTX=-PLON*RY/DSAT
       PTY=PLON*RX/DSAT
       PTZ=0.D0
C      (E) SOLAR RADIATION PRESSURE
       DSP=DSQRT((SX-RX)*(SX-RX)+(SY-RY)*(SY-RY)+(SZ-RZ)*(SZ-RZ))
       PRX=-SLRP*4.5D-09*(SX-RX)/DSP
       PRY=-SLRP*4.5D-09*(SY-RY)/DSP
       PRZ=-SLRP*4.5D-09*(SZ-RZ)/DSP
C      TOTAL ACCELERATION--------------------------------
       PX=PSX+PMX+PZX+PTX+PRX
       PY=PSY+PMY+PZY+PTY+PRY
       PZ=PSZ+PMZ+PZZ+PTZ+PRZ
       COMPUTE VARIATION OF PARAMETERS A,E,I,W,WW,M--------
       AN2=(AMU/(AP*AP*AP))
       COMPUTE DA/DT-------------------------------------
       DADT=2.D0*(VX*PX+VY*PY+VZ*PZ)/(AN2*AP)
       --------------------------------------------------
       DE1=DSQRT(1.D0-EP*EP)/(DSQRT(AN2)*AP*EP)
       DE2=DSQRT(1.D0-EP*EP)/(AP*DSQRT(AN2))
       DE11=SEP*R11-CEP*R21+DE2*VX
       DE12=SEP*R12-CEP*R22+DE2*VY
       DE13=SEP*R13-CEP*R23+DE2*VZ
       COMPUTE DE/DT-------------------------------------
       DEDT=DE1*(DE11*PX+DE12*PY+DE13*PZ)
       --------------------------------------------------
       DI1=DSQRT(AN2)*AP*AP*DSQRT(1.D0-EP*EP)*DSIN(AIP)
       DI2=AP*DCOS(AIP)*SEP
       DI3=AP*DCOS(AIP)*CEP
       DI11=DI2*R11-DI3*R21-RY
       DI12=DI2*R12-DI3*R22+RX
       DI13=DI2*R13-DI3*R23
       COMPUTE DI/DT-------------------------------------
       DIDT=-(DI11*PX+DI12*PY+DI13*PZ)/DI1
       --------------------------------------------------
       DWW1=RZ*DSIN(WWP)
       DWW2=-RZ*DCOS(WWP)
       DWW3=AP*(CEP*DSIN(WP)+SEP*DCOS(WP))*DCOS(AIP)
       COMPUTE DWW/DT------------------------------------
       DWWDT=(DWW1*PX+DWW2*PY+DWW3*PZ)/DI1
       --------------------------------------------------
       ALL=AP*AP*(EP*DCOS(EAP)-1.D0-DSIN(EAP)*DSIN(EAP))/DSAT
```

```
      ANN=AP*AP*DSIN(EAP)*CEP/(DSAT*DSQRT(1.D0-EP*EP))
      DW1=DE1/AP
      DW2=-DCOS(AIP)/DI1
      DW11=DW1*(ALL*R11+ANN*R21)+DW2*DWW1
      DW12=DW1*(ALL*R12+ANN*R22)+DW2*DWW2
      DW13=DW1*(ALL*R13+ANN*R23)+DW2*DWW3
C     COMPUTE DW/DT----------------------------------------
      DWDT=DW11*PX+DW12*PY+DW13*PZ
C     ---------------------------------------------------
      DM1=2.D0/(DSQRT(AN2)*AP*AP)
      DM2=DSQRT(1.D0-EP*EP)*DW1
      DM11=DM1*RX+DM2*(ALL*R11+ANN*R21)
      DM12=DM1*RY+DM2*(ALL*R12+ANN*R22)
      DM13=DM1*RZ+DM2*(ALL*R13+ANN*R23)
C     COMPUTE DM/DT----------------------------------------
      DMDT=DSQRT(AN2)-(DM11*PX+DM12*PY+DM13*PZ)
C     THE INCREMENTED VALUES OF ORBITAL PARAMETERS
      AP=AP+DADT*60.D0
      EP=EP+DEDT*60.D0
      AIP=AIP+DIDT*60.D0
      WWP=WWP+DWWDT*60.D0
      WP=WP+DWDT*60.D0
      AMP=AMP+DMDT*60.D0
      INCREMENTED TIME
      T=T+1.D0/60.D0
      KMNT=KMNT+1
      IF(KMNT.LT.60)GO TO 14
      KMNT=KMNT-60
      KHR=KHR+1
      IF(KHR.LT.24)GO TO 14
      KHR=KHR-24
      MJD=MJD+1
      IF(MJD.NE.KEND+1)GO TO 9
      STOP
      END
```

APPENDIX - 2

COMMENTS ON GOES DATA PLOTS

Each of the 3 plots shows the hourly measurements of GOES/East and GOES/West time codes as received in Boulder vs. UTC(NIST). The data with the larger diurnal variation are from GOES/West in each plot.

GOES/East is the GOES-7 satellite at 112° West longitude with an orbit inclination of about 0.1°. GOES/West is the GOES-2 satellite at about 137° West longitude with an orbit inclination of about 10°.

All data are from our newest True-Time Model 468DC Mark III receivers which fully correct for path delay variations. These receivers are as received from the manufacturer and currently do not have proper compensation settings for internal receiver delays. As a result, the absolute measurements in microseconds on the plots include a constant offset error of about 30-70 μs, depending on the particular receiver. However, the comparisons between the GTDS and GOESTRAK output data are still valid.

Each plot compares two (or three) consecutive time periods of a few days each where the transmitted GOES position data in one period are generated from the normal GTDS orbit prediction program run on a large mainframe computer, while the data in the other period are generated from Dr. Sen Gupta's PC-based position prediction program, called GOESTRAK here at NIST. Whether generated from GTDS or GOESTRAK, the position predictions are based on the same set of orbital elements within a given plot. Each plot has a notation of the epoch date for the orbital element sets used and a subtitle giving the range of dates included in the plot.

UTC-GOES E&W (Corrected for Delay): BAK

Hr Meas: 11/07-11/12/92

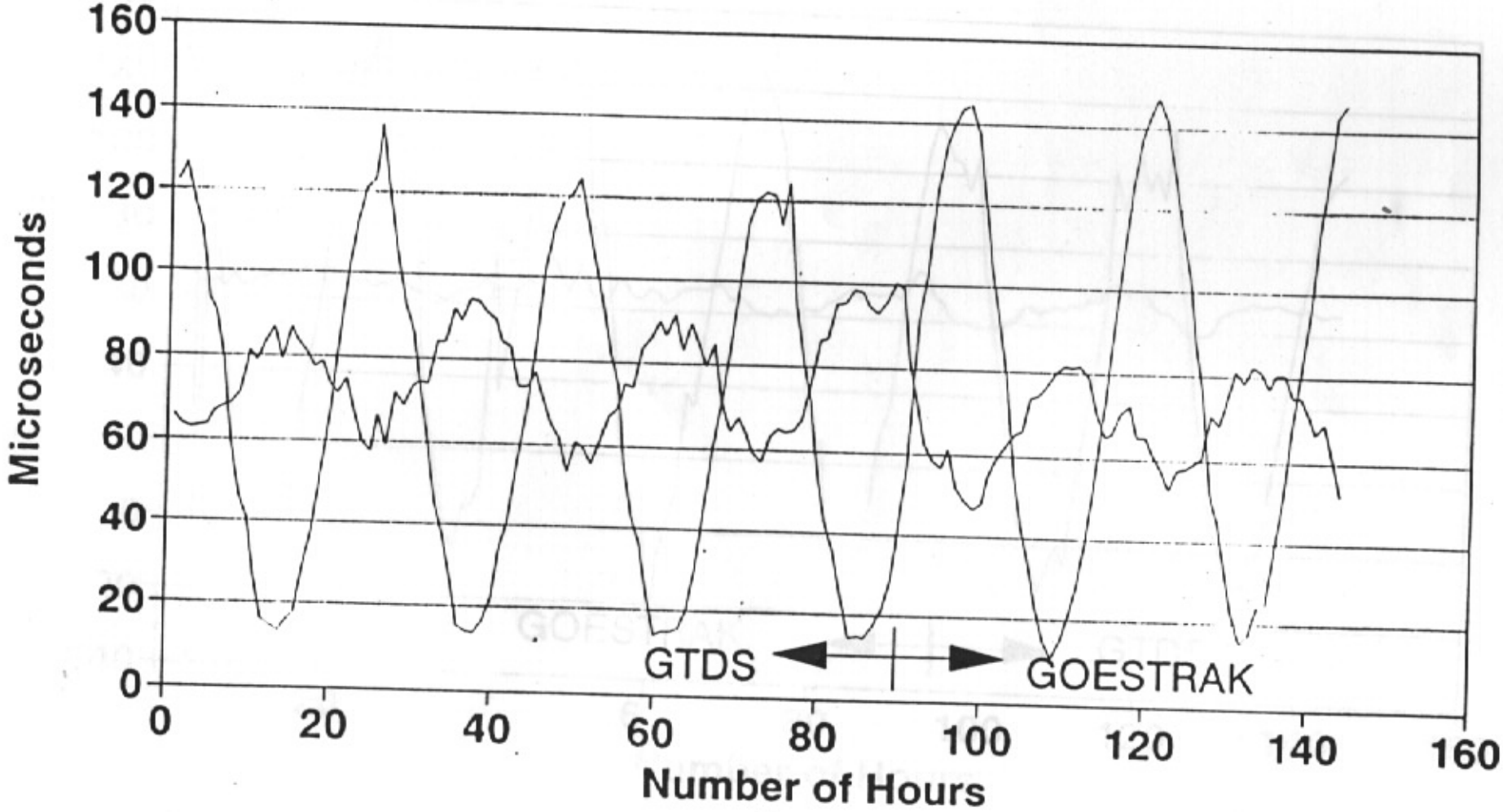

East — West

ORB EL/E=10/18/92

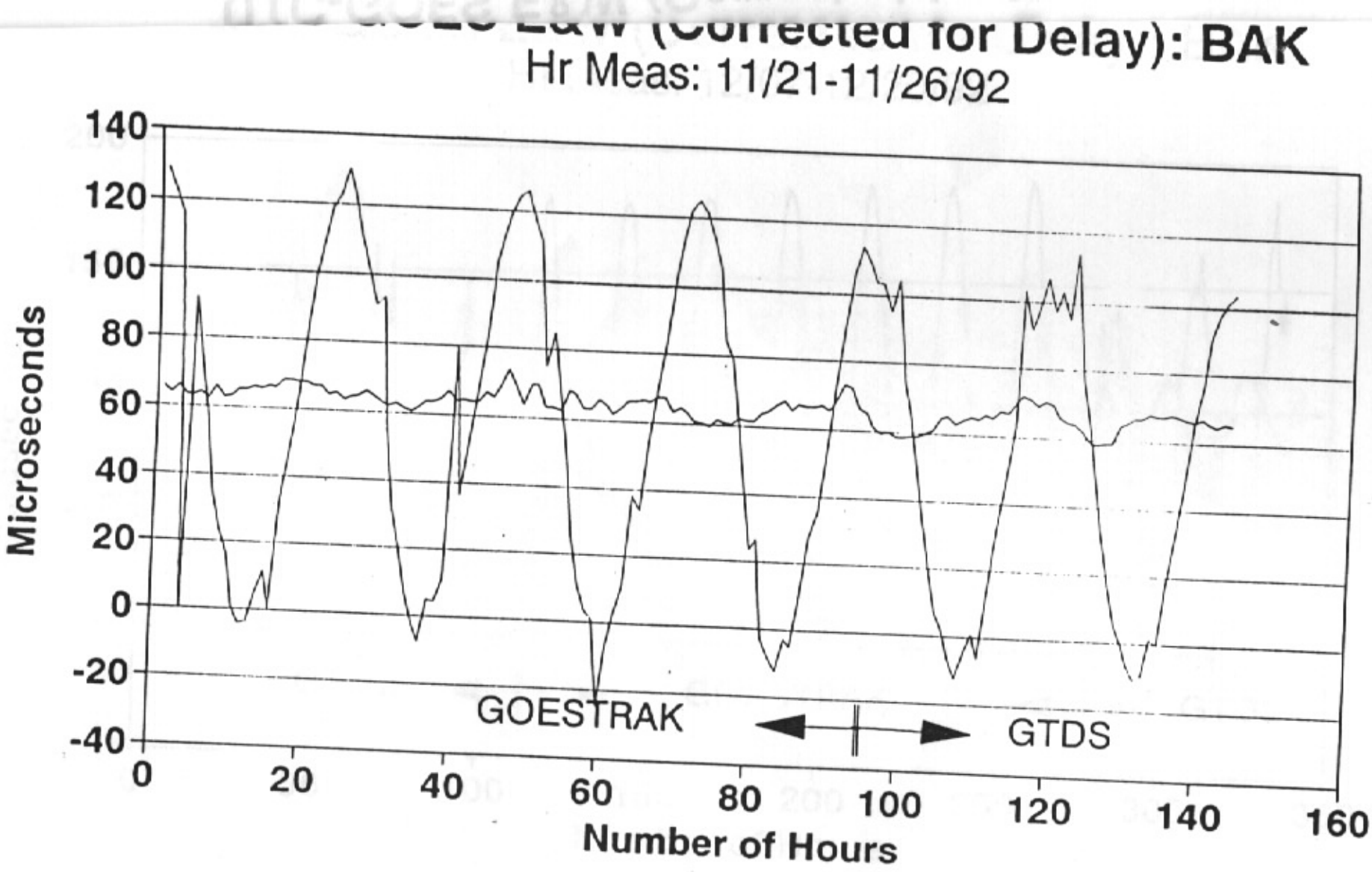

East — West

ORB EL/E=11/19/92

GTS-GOES E&W (Corrected for Delay): BAK

Hr Meas: 12/07-12/20/92

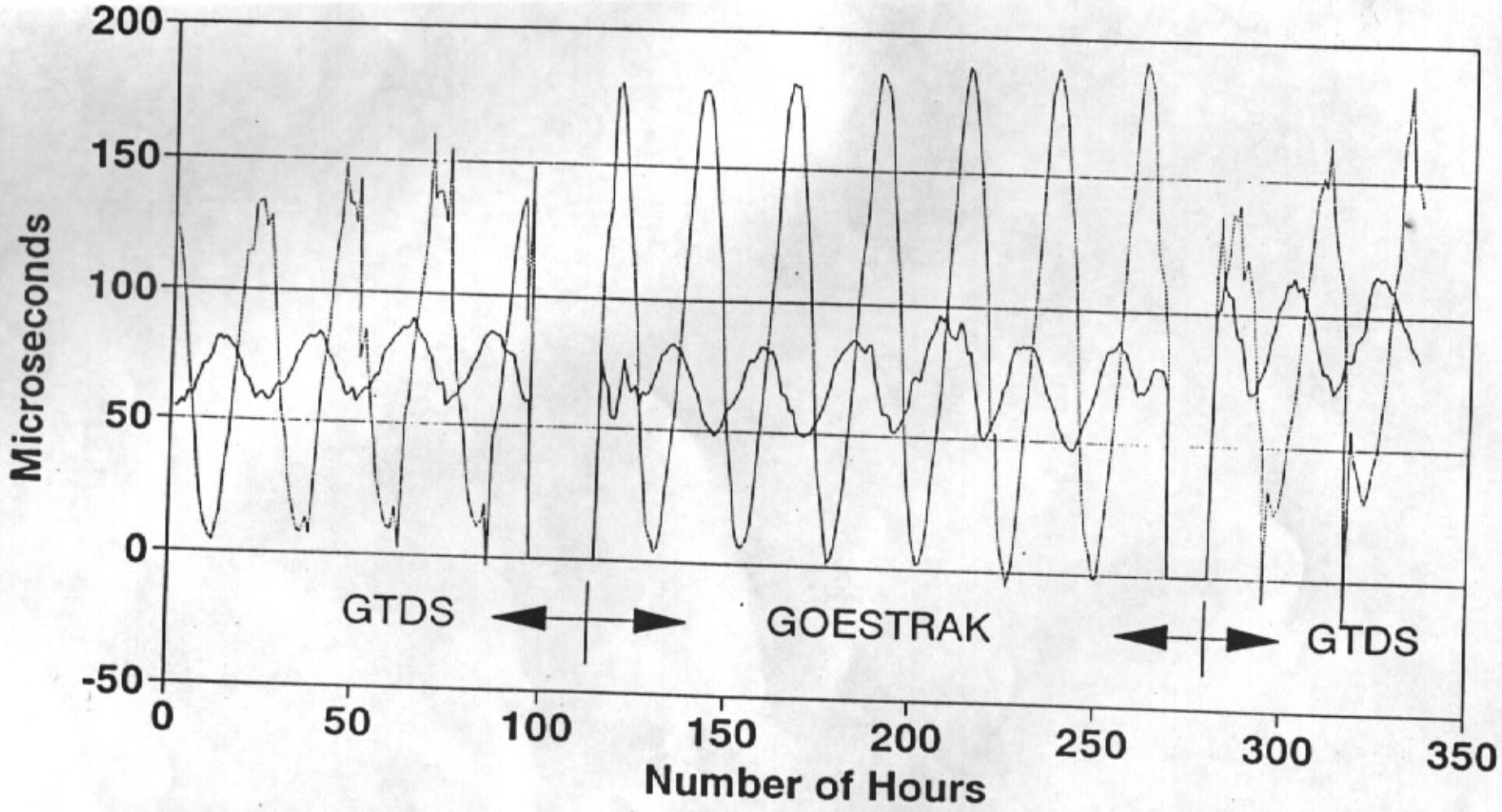

East West

ORB EL/E=11/19/92